भू-जल न्यूज़

Bhu-Jal News

Quarterly Journal

Volume 30, No. 1-4
Jan - Dec. 2020

CENTRAL GROUND WATER BOARD
Govt. of India
Ministry of Jal Shakti
Department of Water Resources, River Development and
Ganga Rejuvenation
Faridabad (Haryana)

भू-जल न्यूज़

Quarterly Journal of Central Ground Water Board
Ministry of Jal Shakti
Government of India

Published by Chairman, Central Ground Water Board, Department of Water Resources, River Development & Ganga Rejuvenation, Bhu-Jal Bhawan, NH-IV, Faridabad - 121 001 (Haryana)

All Editorial correspondence in future may be addressed to the Editors, "Bhu-Jal News", RGNGWTRI, Naya Raipur-492 016 (C.G.) • E-mail : bhujal@nic.in

CONTENTS

Volume - 30 **Number 1 - 4** **2020**

Chairman's Page

India is a vast country having different hydrogeological terrains. Each terrain has its unique characteristics with quantity as well as quality problems. For example, the Gangetic and Brahmputra alluvial tracts have immense ground water potential, but shallow aquifers suffer from Arsenic, Fluoride and Iron contamination. Similar is the case with southern India in hard rock terrains.

From water well drilling perspectives, the exploratory drilling in different terrains require different types of understanding and different types of drilling rigs. In hard rock terrains of southern and central India, aquifers are limited in extent and drilling needs a lot of expertise. Deccan basalts of central India has its unique problems in ground water exploration.

I expect our Officers from different Regions to document their field experiences and contribute to Bhujal News for publication. Engineers have a feeling that writing papers is not their prerogative. In fact, they are the best people to highlight the drilling problems faced in the country and offer solutions to them or seek solutions to solve those problems. I request that they become more participative in communicating their engineering vents.

Publication of Bhujal News has now been shifted to Rajiv Gandhi National Ground Water Training and Research Institute (RGNGWTRI), Raipur. They have done a wonderful job in bringing out this publication with some quality papers. I hope that they will have good number of contributions from our Officers to carry forward this publication in the future too on regular basis. I congratulate all authors to have seen their papers published. I expect active participation from them in the future issues of the periodical too.

Last but not the least, I congratulate RGNGWTRI to have been able to bring out this issue of the Bhujal News during the pandemic.

G.C. Pati

Chairman, CGWB

EDITORIAL

Central Ground Water Board is the National Apex Agency entrusted with the responsibilities of providing scientific inputs for management, exploration, monitoring, assessment, augmentation and regulation of ground water resources of the country. With a vision for sustainable development and management of ground water resources, it functions with the mandate to develop and disseminate technologies, and monitor and implement National policies for scientific and sustainable development and management of India's ground water resources, including their exploration, assessment, conservation, augmentation, protection from pollution and distribution, based on the principles of economic and ecological efficiency and equity.

As of today, there are 4017 regular employees in CGWB of which 882 belong to scientific stream and 1868 to engineering stream; the rest 1267 manage the administration. Of the 882 employees in scientific stream, 408 belong to Group A and 397 to Group B categories. Similarly, of the 1868 employees in engineering stream, 56 are in Group A and 354 are in Group B categories. With so many Officers who may already be writing reports in official capacities, their contribution towards Bhujal News is almost negligible. We request them to vent their thoughts in whatever way they can and contribute to this very own journal of ours.

Bhujal News started in the year 1985 with an objective to highlight the important news items besides publishing the technical contributions from CGWB's employees in a journal format. It also publishes articles received from outside of CGWB system. But, its publication has not been very regular. For example, there was a hiatus of its publication during the past six years. There are many reasons. One of them is lack of interest in ourselves in publishing our very own work.

The work assignments in CGWB are mostly field-based and the output is measured by submission of reports on the basis of field studies. But, because, the reports have limited circulation, the results of these field studies and ideas developed thereof do not reach to the scientific community. Even CGWB's own Officers are deprived of these information. Bhujal News fulfils this gap and serves as a conduit between CGWB and the outside world by highlighting CGWB's contributions to the general public. Therefore, without hesitation, all workers of CGWB, whether in scientific or engineering stream, should make it a point that after completion of their assignments, whether in field or laboratory, the results are conveyed in a journal format and submitted to Bhujal News.

Historically there has been very minimal representation from engineering stream. We appeal to our engineers to write about the numerous field problems that we face on regular basis in many of our drilling operations. Success stories too are highly welcome.

The publication of Bhujal News has now been shifted to Rajiv Gandhi National Ground Water Training & Research Institute (RGNGWTRI), Raipur for its steady publication. A new editorial committee has been constituted. All it needs is contributions from CGWB's scientists and engineers. We hope that its journey at RGNGWTRI will be smooth without any hiatus.

--Editors

Bhujal News, 30(1-4):1-6

Determination of Hydraulic Conductivity and Transmissivity from Slug Tests in Shillong Proterozoic Basin, Meghalaya, India

T Chakraborty[1], S Kent[1]
[1]Central Ground Water Board, State Unit office, Shillong
*Corresponding author-email-tapan.cgwb@gmail.com

ABSTRACT

A common technique for determining aquifer parameters is to conduct slug tests. A slug test is the addition or extraction of a known volume of fluid to a well while monitoring the response of the aquifer material in order to estimate hydraulic conductivity or transmissivity. Slug tests usually are single-well tests that give estimates of hydraulic conductivity near the bore or screen of the test well. Shillong Proterozoic basin is located in Meghalaya plateau and is mostly underlain by Quartzites. Groundwater occurs mainly in the weathered residuum and in fractures/ joints/ weak planes in Quartzites. In this basin twenty eight exploratory bore holes were drilled by CGWB to know the aquifer characteristics and aquifer geometry. Out of these, three bores drilled are found to be showing very less discharge (<0.2LPS). Slug test were carried out in these bores with less discharges to find hydraulic conductivity and transmissivity. The water level data collected during the tests were analysed by employing different common slug test analysis methods. Hydraulic conductivity was determined by using Hvorslev and Bouwer-Rice methods. While transmissivity was determined from Ferris-Knowles and Cooper-Bredehoeft-Papdopulous methods. A comparison between the results obtained was also analysed.

Key words: Slug Tests, Hydraulic Conductivity, Transmissivity, Proterozoic Basin, Shillong

INTRODUCTION

Slug tests usually are single-well tests that give estimates of hydraulic conductivity near the bore or screen of the test well. The method of slug testing is to instantaneously increase or decrease the water level in a well and monitor the subsequent water level recovery. Analytical solutions can then be applied to hydrographs of water level recovery and to well characteristics to determine hydraulic conductivity of the subsurface rock surrounding the well (Bouwer and Rice, 1976; Cooper and others, 1967). Slug tests generally are conducted in formations that exhibit low K. They may not be appropriate in fractured rock or formations with T greater than 250 m^2/day (Kruseman and de Ridder, 1990). Hydraulic properties determined by slug tests are representative only of the material in the immediate vicinity of the well. However, by performing a series of slug test at discrete vertical intervals and tests in closely spaced wells, important information can be obtained about the vertical and horizontal variations of hydraulic properties for the site (Butler, 1998).

In Shillong Proterozoic basin, twenty eight exploratory bore holes were drilled by CGWB to know the aquifer characteristics and aquifer geometry. Out of these, three bores drilled are found to be showing very less discharge (<0.2LPS). Slug tests were performed in three very low discharge bore holes. Hydraulic properties were determined by using various slug test analysis methods like Hvorslev, Bouwer-Rice, Ferry-Knowles and Cooper-Bredehoeft-Papdopulous.

GEOLOGICAL SETTING OF SHILLONG PROTEROZOIC BASIN

In the eastern and central part of the Meghalaya plateau subsequent to the cratonization of the gneissic complex, a shallow basin was developed in an intra cratonic setting. The meta- sediments deposited unconformably over the basement rocks comprising of the Shillong Group of rocks. It consists of thick arenaceous and argillaceous meta-sediments. The Shillong Group has been affected by two major episode of igneous activity. The first is in the form of basic dykes and sills known as Khasi greenstones. And probably in

the later part of middle Proterozoic a number of discordant granitic plutons like Mylliem granite, South Khasi batholith, Kalang pluton etc.

HYDROGEOLOGY

Hydrogeologically, Quartzite formation of Proterozoic Shillong Group lack primary porosity. The movement and occurrence of ground water are controlled by physiography, zone of weathering and interconnected zones of weakness or secondary porosity like joints, faults etc. Groundwater occurs under unconfined condition in the weathered residuum, and under semi-confined condition in the secondary porosity like fractures, fissures etc. The depth to water level (DTWL) ranges from 2 to 26 m below ground level (bgl).

SITE AND WELL INFORMATION

Slug tests were carried out in three exploratory bore holes located at Laskein, Namdong and Mawshohroh in Khasi and Jaintia Hills and shown in Fig-1.

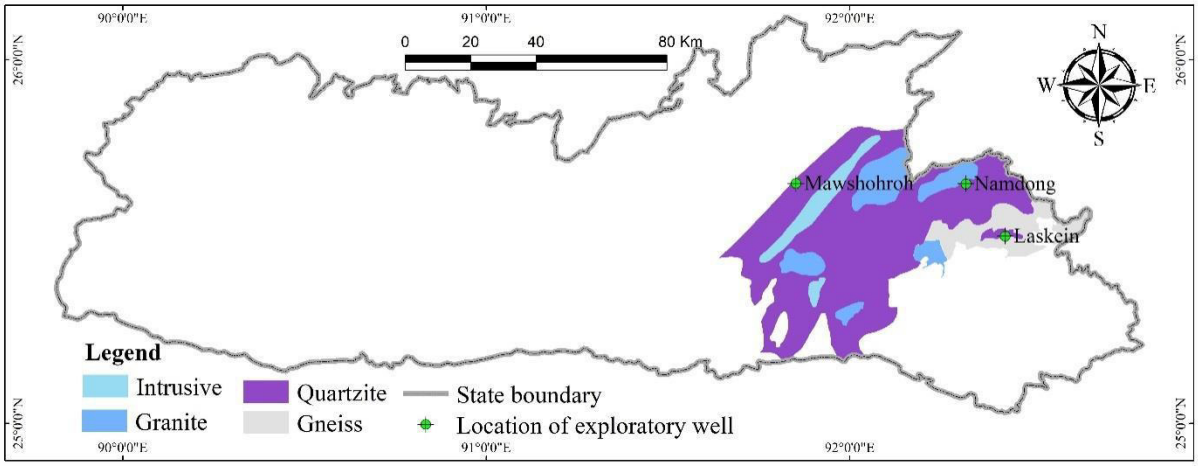

Fig 1: Location Map of Slug Test sites

All the three boreholes are underlain by Quartzite and the fractures encountered during drilling have yielded very less water. Laskein bore hole which is located in an intermontane valley has encountered two fractures at a depth of 22 m and 117 m. Namdong borehole which is located on a small mount encountered one fracture at the contact zone of Quartzite and Amphibolite, which is an intrusive rock. The fracture was encountered at a depth of 96 m. Mawshohroh bore hole encountered three fractures at a depth of 68 m,136 m,191 m and is located on a hill top. Details of the bore holes are given in Table 2 and lithologs are shown in Fig-2.

Table 2: Details of Bore holes

Sl. No.	Location	Easting	Northing	Depth of Bore hole (mbgl)	Radius (m)		Fracture (mbgl)	Piezometric Head (mbgl)	Initial Rise in Water Level (m)
					Casing	Rest of Bore Hole			
1	Laskein	442525	2822141	201.9	0.089	0.083	22 /117	16.23	0.93
2	Namdong	431738	2838132	202.5	0.089	0.083	96	12.99	1.14
3	Mawshohroh	384806	2838572	215.7	0.089	0.083	68/ 136/ 191	27.655	1.205

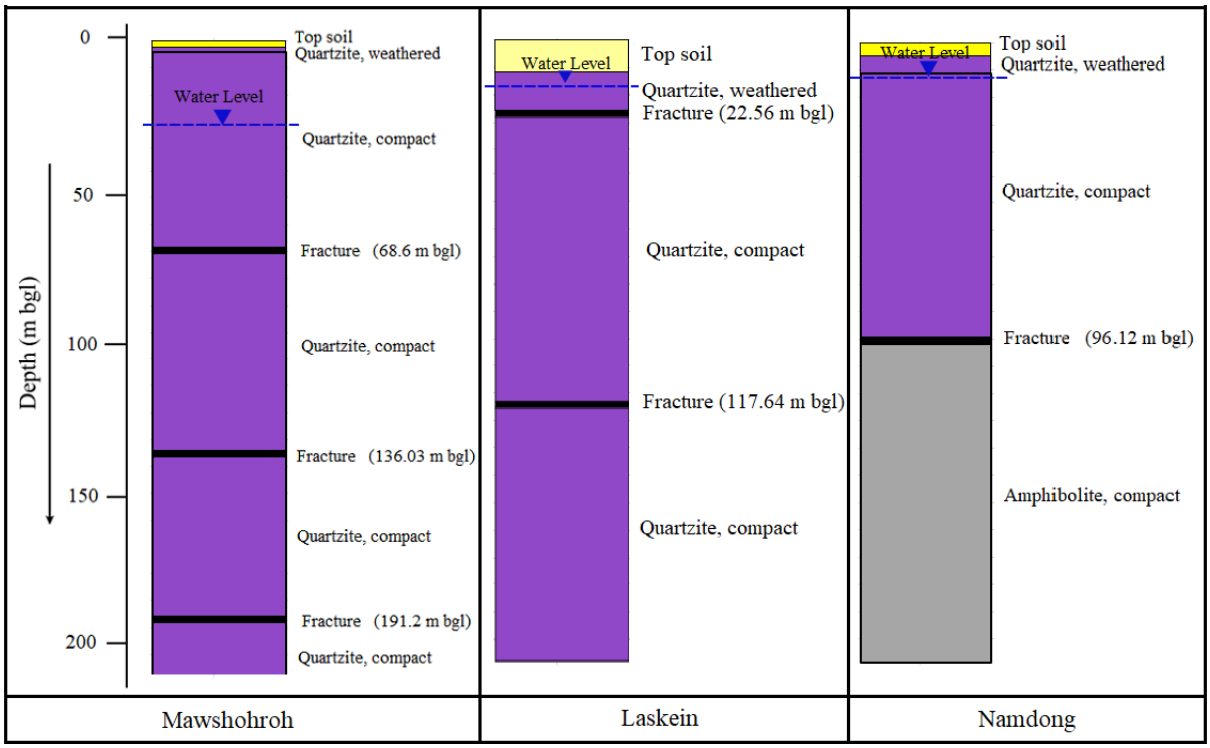

Fig 2: Lithologs of Bore holes

METHODS AND DATA ANALYSIS

Falling-head tests were conducted by rapidly raising the water level in the exploratory bore hole and subsequently measuring the falling water level. Slug tests were performed by quickly pouring 30 liters of water at the bore holes. The test bore holes were not packed off during the test. The water level/ piezometric head was then measured and recorded every 10 seconds for the first several minutes with the measuring frequency decreased during a period of about 140 minutes to once every 10 minutes. Water-level data for the slugged bore holes wells were analyzed for hydraulic conductivity (K) by using the methods of Hvorslev (1951); Bouwer and Rice (1976) in SlugIn 1.0 software developed by Geological Survey of Spain. Transmissivity (T) is calculated by using Ferris-Knowles method (1962) in excel spreadsheet and also by using Cooper-Bredehoeft-Papadopulous method (1967) in SlugIn 1.0 software.

RESULTS & DISCUSSION

Hydraulic conductivity is calculated by using the Hvorslev and Bouwer-Rice methods. While transmissivity is calculated by using the Ferris-Knowles and Cooper-Bredehoeft-Papadopulous methods. Results obtained for K and T from different methods are shown in Table 2.

Table2: Results of Slug Tests

Sl. No.	Location	K (m/day)		Mean K (m/d)	T (m^2/day)		Mean T (m^2/day)
		Hv	B-R		F-K	C-B-P	
1	Laskein	0.78	0.69	0.74	0.32	1.47	0.90
2	Namdong	0.33	0.29	0.32	0.02	0.78	0.4
3	Mawshohroh	0.086	0.09	0.09	0.06	0.26	0.16

*Hv=Hvorslev method; B-R= Bouwer – Rice method; F-K= Ferry-Knowles method; C-B-P= Cooper- Bredehoeft – Papadopulous method

Graphs produced from different methods during slug test data analysis for Laskein, Namdong and Mawshohroh were shown in Fig 3. (a), (b) and (c) respectively. In all three cases, it was found that K values obtained from Bouwer & Rice method is slightly lesser than the values obtained from Hvorslev method. Co-efficient of variation between these methods varies from 3.2 to 9.1%.

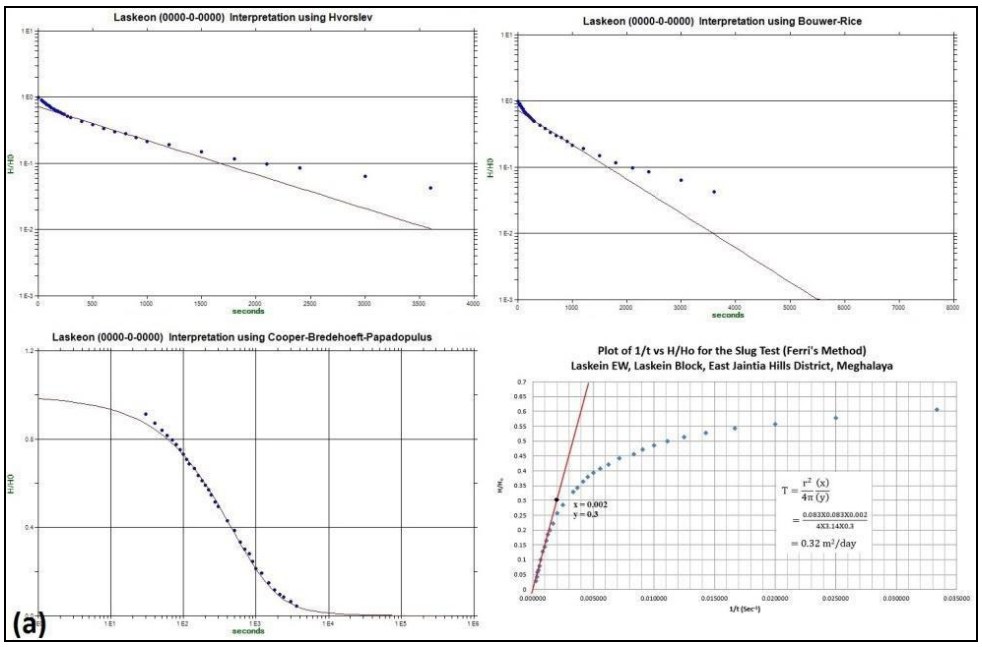
Laskeon (0000-0-0000) Interpretation using Hvorslev
Laskeon (0000-0-0000) Interpretation using Bouwer-Rice
Laskeon (0000-0-0000) Interpretation using Cooper-Bredehoeft-Papadopulus
Plot of 1/t vs H/Ho for the Slug Test (Ferri's Method)
Laskein EW, Laskein Block, East Jaintia Hills District, Meghalaya
x = 0.002
y = 0.3
T = r² (x) / 4π (y)
= 0.083X0.083X0.002 / 4X3.14X0.3
= 0.32 m²/day
(a)

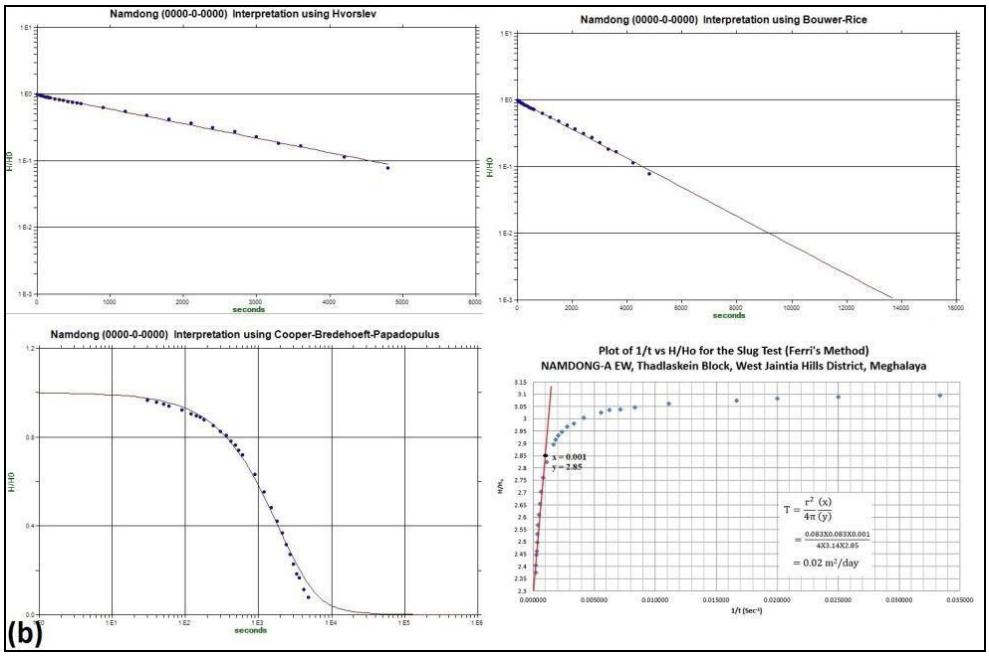
Namdong (0000-0-0000) Interpretation using Hvorslev
Namdong (0000-0-0000) Interpretation using Bouwer-Rice
Namdong (0000-0-0000) Interpretation using Cooper-Bredehoeft-Papadopulus
Plot of 1/t vs H/Ho for the Slug Test (Ferri's Method)
NAMDONG-A EW, Thadlaskein Block, West Jaintia Hills District, Meghalaya
x = 0.001
y = 2.85
T = r² (x) / 4π (y)
= 0.083X0.083X0.001 / 4X3.14X2.85
= 0.02 m²/day
(b)

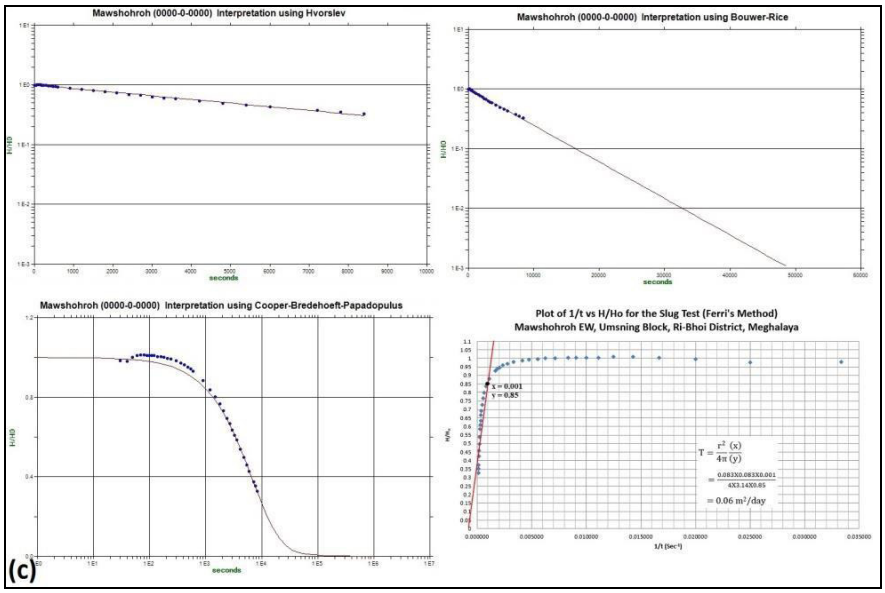

Fig 3: Graphs from different methods for (a) Laskein; (b) Namdong and (c) Mawshohroh

The original Bouwer & Rice (1976) method was developed for unconfined aquifers, but has been shown to apply to confined and leaky confined aquifers as well (Bouwer, 1989). It has more recently been shown that this method tends to underestimate K with errors ranging from 10% to 100%, but still considered to be superior to results from the Hvorslev method.

Transmissivity values obtained from Ferris-Knowles method is much lesser than the values obtained from Cooper et al method. Co-efficient of variation between these methods varies from 88 to 134%. The results obtained for K and T from different methods cannot be compared with any other slug test data from this area, as no slug tests were conducted earlier, in this area.

The Cooper, et al. method has essentially replaced the Ferris and Knowles method. Cooper method is commonly known to be more accurate. Summers et al. (1983) used the Ferris-Knowles method in their study and plotted measured depth to water versus 1/t. toward late times in the test, the plot should produce a straight line as the levels approach zero (0). If this fails to occur then the method will not function on the particular data set. If a straight line occurs then the slope of the line is equal to s/ (1/t) and the equation can be solved for K. While the method gave what appeared to be reasonable results, they were often inconsistent with the results produced by other methods and substantial time was required to conduct the test.

CONCLUSIONS

The results obtained for K and T from different methods cannot be compared with any other slug test data from this area, as no slug tests were conducted earlier, in this area. A quantitative comparison between two different analytical methods of falling head slug tests to determine hydraulic conductivity (K) hardly shows any difference. So, mean hydraulic conductivity value can be considered for the bore holes. However, in case of transmissivity (T), the results obtained between Ferris, et al. method and Cooper et al method is highly variable. Since the Cooper method has essentially replaced the Ferris method and Cooper method is commonly known to be more accurate. Again other studies had already shown that Ferris method is inconsistent. Therefore, T values obtained from Cooper et al method may be considered for any future reference.

ACKNOWLEDGEMENT

The authors are highly thankful to Shri G C Pati, Chairman, Central Ground Water Board, Faridabad for according permission to publish this paper. Thanks are also due to Shri. U Gogoi, Member (East), Shri S Marwah, Member (CGWB) and Shri Biplab Ray, HOO, CGWB, North Eastern Region, Guwahati for their constant encouragement and support in the work

Further, authors are also grateful to the SlugIn 1.0 software team especially Dr. Carolina Guardiola Albert, Spanish Geological Services for providing the software. Authors also express their gratitude to the Scientists of Central Ground Water Board, Shillong, whose field studies have provided invaluable data for preparation of this paper.

REFERENCES

Farooqi, M.A.(2014) Groundwater Exploration in Meghalaya, Central Ground Water Board, North Eastern Region, Guwahati.

Bhatia , A.(2015); Hydrogeological Conditions of Meghalaya State, Central Ground Water Board, North Eastern Region, Guwahati, 2015.

Kent, S. (2017); Aquifer Mapping and Management Plan of Ri Bhoi district, Meghalaya (2016-17), Central Groundwater Board, North Eastern Region, Guwahati.

Kent, S. (2019); Aquifer Mapping and Management Plan of East Jaintia Hills district, Meghalaya (2017-18), Central Groundwater Board, North Eastern Region, Guwahati.

Kent, S. (2019); Aquifer Mapping and Management Plan of West Jaintia Hills district, Meghalaya (2017-18), Central Groundwater Board, North Eastern Region, Guwahati.

Pandey, P. (2019); Aquifer Mapping and Management Plan of East Khasi Hills district, Meghalaya (2017-18), Central Groundwater Board, North Eastern Region, Guwahati.

Kenzi Karasaki (1987), Well Test Analysis in Fractured Media, Earth Sciences Division, University of California, Ph.D Thesis.

Binkhorst, G. A et al. (1994), A review and assessment of factors affecting hydraulic conductivity values determined from Slug test, Environmental Monitoring Systems Laboratory-Las Vegas, Office of Research and Development, U.S. Environmental Protection Agency, EPA/600/R-93/202.

Gonthier, G. J et al. (2003), Slug-test results from a well completed in fractured crystalline rock, U.S. Air Force plant 6, Marietta, Georgia.

Tonderet, G J V et al. (2005), The applicability of slug tests in fractured-rock formations, Institute for groundwater Studies, University of the Free State, Bloemfontein 9300, South Africa, ISSN 0378-4738 = Water SA Vol. 31 No. 2, page- 157-159.

The University of Kansas, Department of Geology and Kansas Geological Survey (2005), Hydraulic Tomography and High-Resolution Slug Testing to Determine Hydraulic Conductivity Distributions – Year, Annual Report SERDP Strategic Environmental Research and Development Program, Project # ER1367.

Olivier Audouin, Jacques Bodin (2008), Cross-borehole slug test analysis in a fractured limestone aquifer, Journal of Hydrology, Elsevier, 348, pp.510-523.

Lewis, M (2013), A Comparative Analysis of Two Slug Test Methods in Puget Lowland Glacio-Fluvial Sediments near Coupeville, WA, University of Washington, MESSAGe Technical Report Number: 004

Alfaifi, Hussain Jaber (2015), Comparing Slug Test Methods for Unconfined Aquifers, Western Michigan University, Dissertations. 511.

Fadugba, O G et al. (2016), Slug Tests for Determination of Hydraulic onductivity of Contaminated Wells, Environment and Natural Resources Research; Vol. 6, No. 2, ISSN 1927-0488 E-ISSN 1927-0496.

Sergio Martos Rosillo (Instituto Geológico y Minero de España), SlugIn 1. 0 User Manual Slug Test Analysis Software.

Todd, D.K. and Mays, L.W. (2004) Groundwater Hydrology (3rd Ed.) John Wiley & Sons, Inc.*Summers, W. K.* (1983). The hydraulic properties of the pierres hale, A comparison of methods.

Bhujal News, 30(1-4):7-16

Delineation of Saturated Fractures using Gradient Profiling and Vertical Electrical Sounding in Hard Rock area of Mirzapur district, Uttar Pradesh, India

Shashi Kant Singh[1] & Anirudh Singh[1]
[1]Central Ground Water Board, Northern Region, Lucknow
*Corresponding Author-email- singhskbhu@gmail.com, asgeo7@gmail.com

ABSTRACT

Surface geophysical surveys comprised of Vertical Electrical Sounding (VES) and Gradient profiling (GP) have been successfully utilized as a preliminary tool to identify fractured zones saturated with groundwater in hard-rock areas at Gosaipur, Chunar-Rajgarh road, Mirzapur district, Uttar Pradesh, India. Conducting vertical electrical sounding at randomly selected places may not provide fruitful results since fractures are sparsely distributed in hard rocks. In gradient profiling, current electrodes with large separation remain fixed. Simultaneously, the potential dipole is moved between the current electrodes in the central one-third portion of the profile at a small station interval of 5m. A GP survey conducted along four profiles having different lengths in a small sector of the study area. Low resistive zones have been identified which correspond to the fractured zones. A few Vertical Electrical Soundings were carried out to investigate the depth and thickness of the fractured zones. A contour map of apparent resistivity was also prepared on basis of gradient profiles. Based on the apparent resistivity contour map and VES results, one site is recommended for test drilling. A test borehole drilled, yielded continuous discharge of freshwater (10,000 L/h). The present study confirms the findings of GP survey is a powerful technique that identifies a fractured zone's presence, especially in a hard-rock area covered with a thin soil layer.

Key Word: Gradient Profiling, Vertical Electrical Sounding, Hard Rock, Fracture, Groundwater.

INTRODUCTION

It is well known that the selection of any geophysical method or combination of techniques for their application in exploration work is based on the contrast between the physical properties of the target and the surrounding medium. Fractures occur in hard rock's up to a few hundred meters. If the fractures are saturated with groundwater, good contrast between fractured rocks and smooth, hard rock's would be observed; fractured rocks show lower resistivity than hard rock's (Karous and Mares 1988). Although direct current (DC) resistivity method is the most suitable method for groundwater investigations in hard rock areas than all other geophysical methods, the delineation of fracture zones in low-permeability hard rock's is still challenging.

Generally, geoelectrical surveys are conducted to find lateral changes of resistivity from place to place to a targeted depth (resistivity profiling) or to find out resistivity variation with depth (resistivity sounding). The profiling is done only for qualitative evaluation, whereas sounding is conducted for quantitative evaluation of thickness and resistivity of different layers at a specific location. Suppose the survey's objective is to determine the depth of aquifer in the thick alluvial covered areas. Resistivity sounding alone is sufficient to provide the required information, however, in the thin soil covered hard rock areas where groundwater occurs in secondary porosity with a limited extent, which is developed due to weathering, fracturing, joints, etc. However, vertical electrical sounding alone may not give fruitful results due to improper site selection. Hence, there is a need for integrated resistivity surveys to identify fracture zones in hard rock areas.

The application of different techniques and their integrated approach in such areas as discussed by Yadav and Singh (2007 & 2008) and successfully applied a GP survey followed by geoelectrical sounding for delineating water-saturated fracture zones in Gurudev Nagar, Mirzapur district, and Robertsganj, Sonebhadra district, Uttar Pradesh, India respectively. The present study area lies to the south-west at a distance of about 3.5 km from Chunar having a similar geological setup.

STUDY AREA AND LOCAL HYDROGEOLOGY

The area under study lies between the latitudes 25^0 4.28'N to 25^0 4.53'N and longitudes 82^0 51.43'E to 82^0 51.78'E situated in 3.5 km southwest from Chunar on the Chunar-Rajgarh road at Campus of Gurukul (Womens College) near Gosaipur, Chunar, Mirzapur (Fig. 1). A thin surface soil covers the part of the area. The terrain is undulating and has several Vindhyan exposures (Krishnan, 1982) in some parts of the study area. A minor seasonal nala flowing southeast to northwest nearby the area under investigation, thereby indicating the slope of the land is towards the northwestern side. The average annual rainfall is about 1090 mm. The primary source for recharging the area is rainfall during the monsoon season. As the area under study is lying in the close vicinity of the Vindhyan exposures, the bedrock (Vindhyan Super Group of rocks) is expected below the surface soil cover (Krishnan, 1982). Groundwater may occur in the weathered, and fractured sandstone provided the zone is connected with recharging sources. These fractures may be present even below the thin bed of semi-compact sandstone rocks. It is well known that fractures play an important and crucial role in fluid flow, especially movement and accumulation of groundwater in hard rock areas. The amount of water that can be taken out from the bedrock-fracture zones depends on the size and location of fractures, the interconnection of the fractures, and the quantity of the material that may be clogging the fractures. Many a time, the minor fractures present in bedrock, if interconnected, can give copious supply of groundwater. The resistivity surveys were conducted only at the locations where the ground surface was suitable for laying out the array. Thus the entire area could not be mapped through the resistivity survey. The locations of the survey points covered through Gradient profile (GP) and Vertical electrical sounding (VES) are presented in Fig. (1).

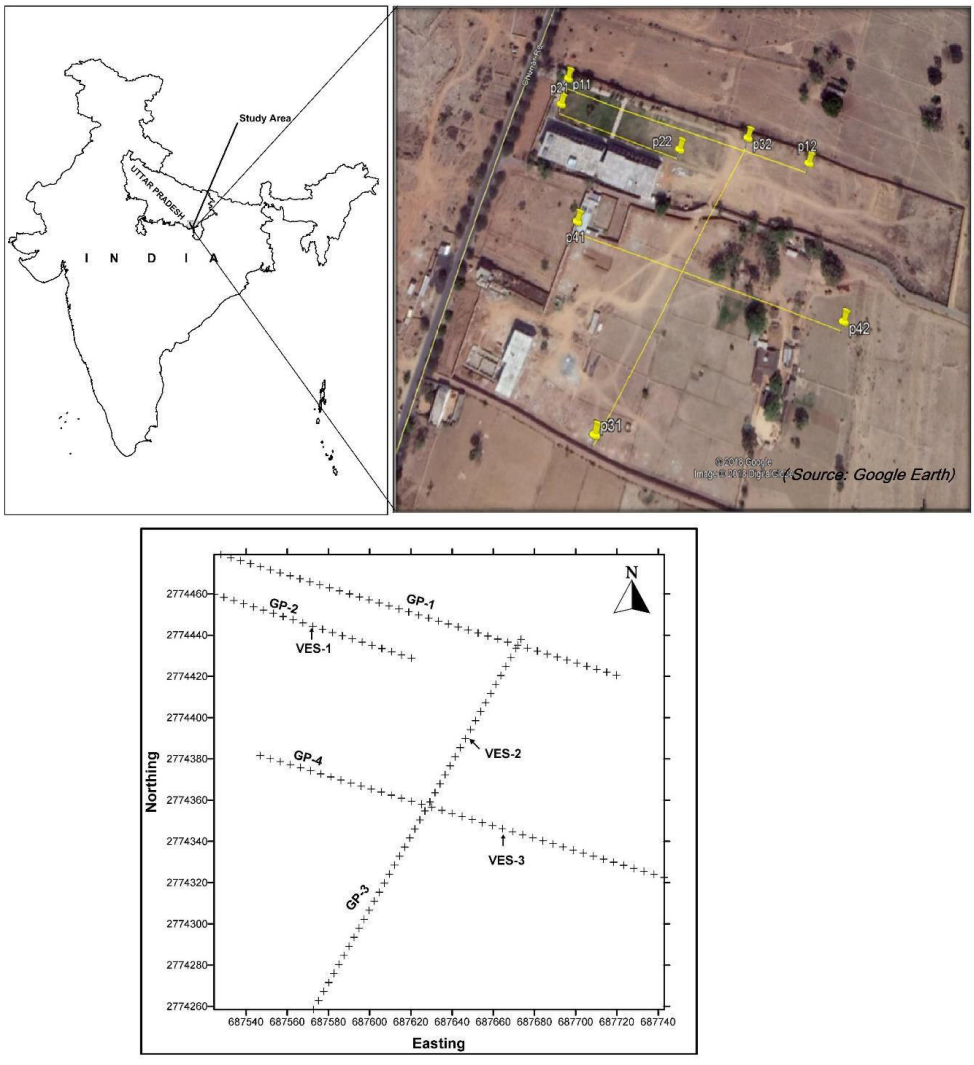

Fig-1-Location map of the study area along with the position of GP and VES

METHODOLOGY AND FIELD PROCEDURES

It is well known that the potential field is governed by the contributions of the distance between source and measuring point. As well as contribution due to the formation resistivity of the material up to which current get penetrated. The gradient profiling array consists of two fixed current electrodes separated by a significant distance and one moving potential dipole with considerably smaller electrode separation. The resistivity measurements can be made with the potential dipole in the central region i.e., 33% between the widely separated current electrodes along the line joining to the current electrodes or parallel to it. The potential field is constant in this region; consequently, a uniform horizontal electric field is generated in the homogeneous earth. Therefore, in principle, any inhomogeneity encountered between these regions gives variation in the response, which can be easily identified. This is the logic behind the joint use of gradient profiling and vertical electrical sounding techniques for groundwater exploration in hard rock areas.

The general layout of the gradient array, along with the variations of potential and potential gradient along a straight line passing through point sources at a surface of the homogeneous earth, is shown in Fig. (2). In the upper portion of the figure (Fig. 2a), a fixed separation of current electrodes A & B is taken as 600 m. The central 1/3rd space between the current electrodes (-100 m to 100 m, both sides of center) can be scanned at regular station intervals of 5 m for the smallest possible spacing of potential electrodes. The smallest spacing of potential electrodes can be taken as 10 m, 20 m, or 30 m which satisfies the condition (L-x) >> 5b to measure the potential gradient (Kunetz, 1966; Summer, 1976; Bertin and Loeb, 1976; Kearey and Brooks, 1984; Sharma, 1997; and Telford et al., 1998). The current electrode separation can be increased or decreased depending on the availability of the space. Accordingly, the observations within the central region may be increased or decreased to fulfill the condition for the measurement of a potential gradient. One can easily derive the formula for the field apparent resistivity as

$$\rho_a = K\frac{\Delta V}{I}$$

where K is the geometrical factor and can be written using Fig. (2a) as

$$K = 2\pi \Big/ \left(\frac{1}{MA} - \frac{1}{MB} - \frac{1}{NA} + \frac{1}{NB}\right) \text{ With}$$

$$MA = \sqrt{(L+x-b)^2 + d^2};\ MB = \sqrt{(L-x+b)^2 + d^2};$$
$$NA = \sqrt{(L+x+b)^2 + d^2};\ \text{and } NB = \sqrt{(L-x-b)^2 + d^2} \qquad \ldots \quad \ldots \quad (1)$$

In the above equation, 2L & 2b are the distances between the current electrodes and the potential electrodes; x is the distance between the centers of the current electrodes and the potential electrodes. (d) is the distance between the main profile and parallel sub-profile, ΔV is the observed potential difference, and 'I' is the input current. The lower portion of the figure (Fig. 2b) shows the theoretical responses of potential (mV) and potential gradient (mV/m) over homogeneous earth for a fixed current electrode separation AB=600m. The computation of theoretical potential gradient is done keeping ($I\rho/2\pi$) = 5000 (I=1000 mA, ρ=31.4 ohm-m). The curve for potential gradient shows almost constant value in the 1/3rd central region, and outside this region, there is a significant change in the potential gradient. Thus, the array can be used to measure the potential gradient within the limit specified as $L \geq |3x| \geq 0$ and $L \geq |3d| \geq 0$. It is worthwhile mentioning here that the field strength and depth of investigation will be nearly constant in the central region bounded by |x|=L/3 and |d|=L/3 in case of homogeneous ground. Under the similar earth condition, if the potential electrodes MN are kept outside the said region, then the depth of investigation decreases, and horizontal electric field deviates due to the influence of either current electrode A or B depending upon its position. The above changes in electric field and depth of investigation in real field conditions would produce a response leading to a false interpretation of inhomogeneity' presence, which are not there.

Gradient profiling aims to locate lateral inhomogeneity. As mentioned above, the array can be used as a *Gradient profiling* for taking observations along the main profile AB when d = 0 and along the parallel sub-profile for a fixed value of d for the same setup of current electrodes, AB. The measurements along parallel sub-profiles are generally done to trace the lateral extents and orientation of anomalous features. In case, the zone of interest exceeds the 1/3rd central region or to increase the coverage the entire profile is shifted along the same line with the same current electrodes spacing so that the latter 1/3rd central region overlaps the former so that the new portion of the zone could be covered.

Apart from the field advantage of gradient profiling, it has a serious limitation also. The depth of investigation varies within the current electrode interval; it is deeper towards the center of AB and shallower closer to A or B. This problem can be minimized, provided the observations are confined to the central one-third of AB. However, the technique is used only for a qualitative interpretation of data to identify the fractured zone's positions. Applying the sounding procedure, the same array can be used as a Schlumberger array for conducting the *vertical electrical sounding* at the desired location while taking L ≥ 5b and d, x = 0.(Fig-2)

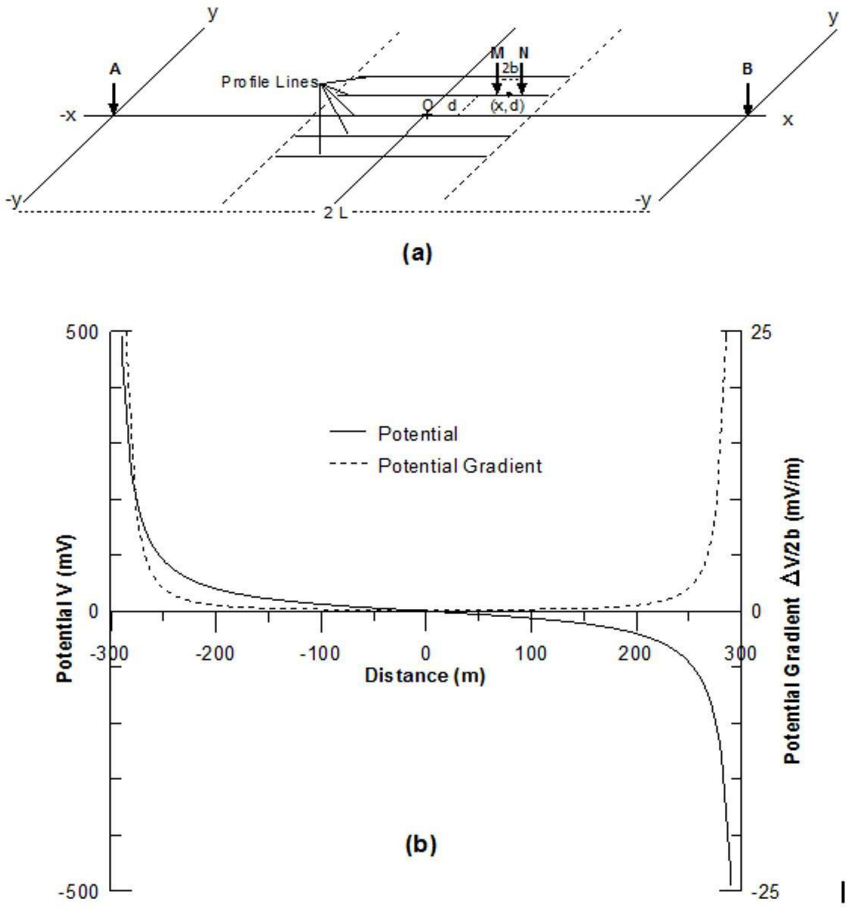

Figure 2: (a) General lay-out of gradient measurement of the potential field where AB = current electrodes and MN = potential electrodes, and (b) distribution of potential and gradient of potential along the line at the surface of homogeneous earth for d=0, I=1000 mA, and ρ = 31.4 ohm-m

RESULTS AND DISCUSSIONS

Gradient Profiling

Initially, a total of 4 Gradient profiles (GP) were carried out using a fixed current electrodes separation of 600 m with the help of deep resistivity meter (ABEM Terrameter LS). The potential electrodes separation was taken as 10 m with an observation interval of 5 m along a profile to cover 200 m (-100 m to 100 m) of length in the central region i.e., 1/3rd of the profile. The computation of apparent resistivity was carried out for each gradient profile using Eqn. (1). The plotting of data has been done on a linear scale.

Fig. (3a) shows the apparent resistivity variation along with the profile GP-1 for potential electrodes separation MN=10 m covering profile length of 100 m each side from the center of the profile. Qualitatively, the prominent low having apparent resistivity value of 148 ohm-m on the curve indicates a low resistive body (probably fractured rocks) at a distance of 50 m towards the northwest from the center of the profile. However, the quantitative interpretation of anomaly obtained through gradient measurement is very difficult because the shape of the body does not influence the gradient measurements very much due to the equivalence problem (Schluz, 1985).

Theoretically, the response across these bodies or a dipping conductive vein or saturated dipping fracture zone is obtained in the form of asymmetrical resistivity i.e. a 'low' with 'high' shoulders on either side coming back to background resistivity.

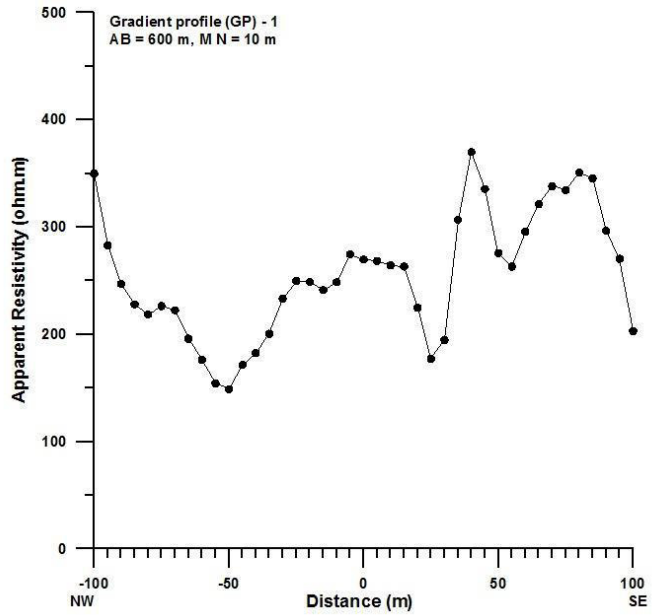

Figure 3a: Response of gradient profiling GP - 1 (P11-P12)

Fig. (3b) shows the variation of apparent resistivity along GP-2 conducted 25m distance towards southwest and parallel to GP-1, covering a total length of 100 m towards NW from the center. The fluctuation in the apparent resistivity curve indicates the presence of inhomogeneity at different positions. There is a prominent low on this profile, with the lowest value of apparent resistivity as 80 ohm-m and at a distance of 50 m towards the left side from the center of the profile. The low obtained along this profile is considered to be more prospective than the previous profile GP-1, and this was selected for conducting vertical electrical soundings to find a quantitative evaluation of layer parameters. This point is marked at the bottom of the figure as VES-1.

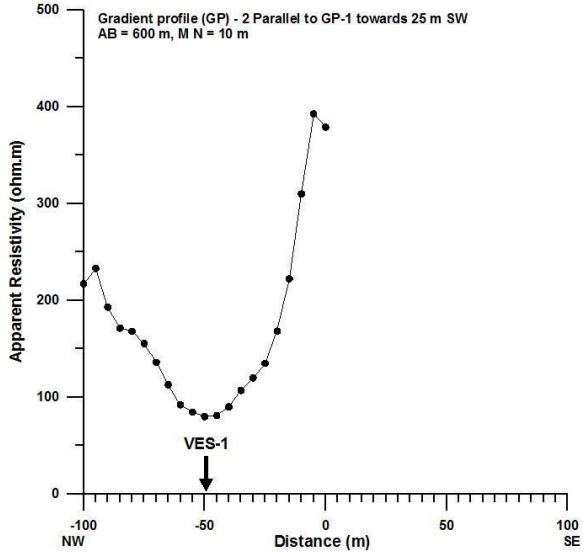

Figure 3b: Response of gradient profiling GP-2 (P21-P22) along with the position of VES- 1

The figure (3c) shows the variation of apparent resistivity along GP-3 for the potential electrode separation MN = 10 m. The prominent low obtained along this profile having the value of apparent resistivity as 127 ohm-m at 45 m towards left from the center of the profile. The low obtained along this profile was selected for conducting vertical electrical soundings to find out the quantitative evaluation of the layer parameters. This point is marked at the bottom of the figure as VES-2.

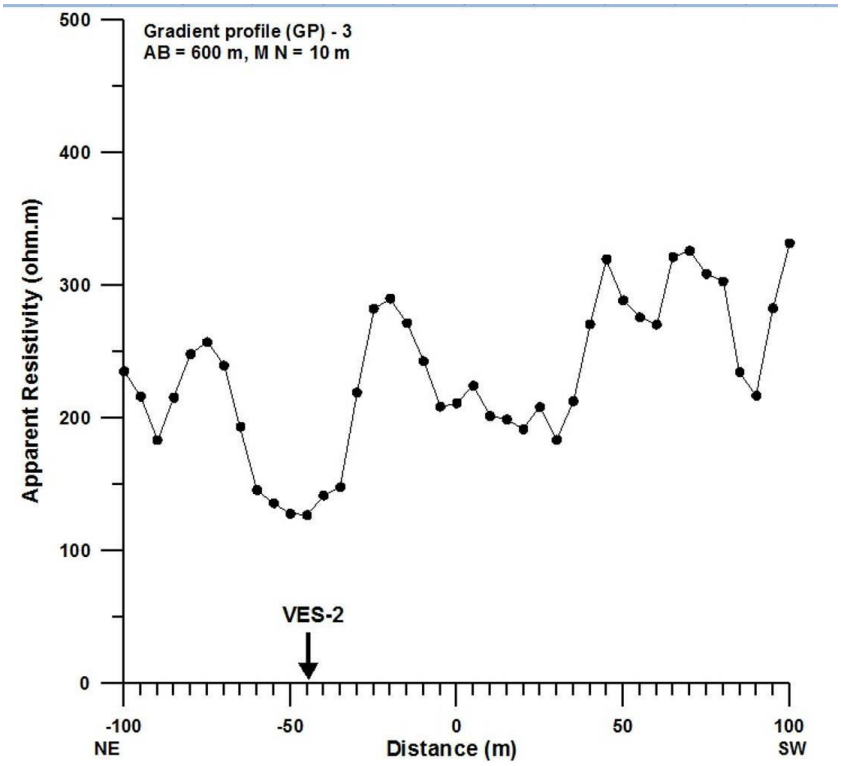

Figure 3c: Response of gradient profiling GP-3 (P31-P32) along with the position of VES- 2

Figure (3d) shows the variation of apparent resistivity along GP-4 for the same potential electrode separation MN = 10 m. The prominent low along this profile having a value of apparent resistivity as 204 ohm-m at 5 m towards left from the center of the profile has been observed. However, the prominent high along this profile having values of apparent resistivity as 381 ohm-m at 20 m towards right from the center of the profile has been obtained. The high obtained along this profile was selected for conducting vertical electrical sounding to find out a quantitative evaluation of the layer parameters as well as for comparison purposes with VES-1 and VES-2. This point is marked at the profile as VES-3.

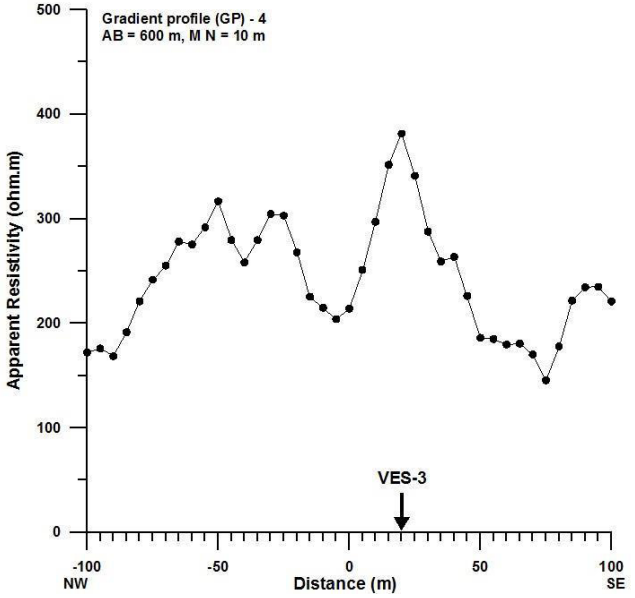

Figure 3d: Response of gradient profiling GP-3 (P41-P42) along with the position of VES- 3

The apparent resistivity values of all gradient profiles have been utilized and prepared as the apparent resistivity contour map. To know the lateral variation of subsurface resistivity in the study area (Fig. 3e). The contour map of apparent resistivity revealed that the orientation of subsurface fractures/weaker zones ('low resistive zones') are in the northeast-southwest direction. The prominent 'low apparent resistivity' zones on GP-2 and GP-3 have been identified from the contour map and selected for VES. The qualitative interpretation of Gradient profile data exhibits that the technique is quite effective in the hard rock areas. It did indicate the presence of fractured rocks (a low resistive formation within the hard rocks).

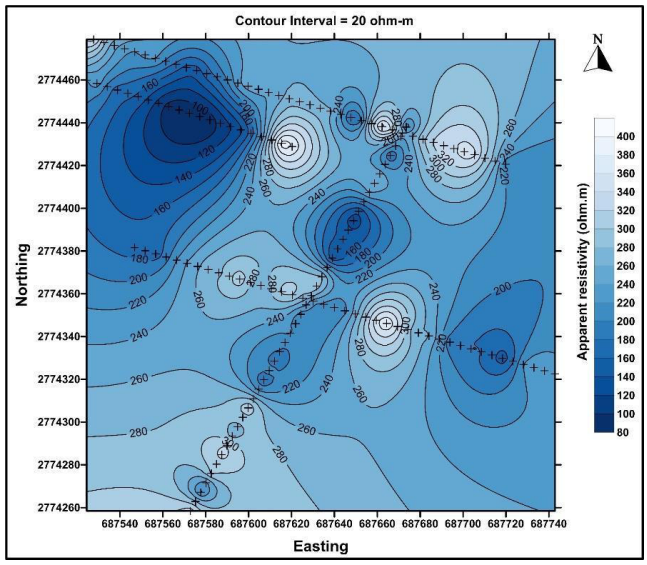

Figure 3e: Apparent resistivity contour map based on gradient profiling GP-1, 2, 3 & 4

Vertical Electrical Sounding

Three vertical electrical soundings (VES) using Schlumberger configuration were carried out for a maximum current electrode spacing of 400 to 600 m with the help of the same deep resistivity meter (ABEM Terrameter LS) unit along with the Gradient profiles as per availability of the space. The data obtained in the field at each sounding location comprised records of current and potential electrode spacing values. Each data set was processed and plotted for AB/2 versus apparent resistivity on a bi-logarithmic scale. Further, the results interpreted in terms of layer parameters, i.e., thickness and resistivity of individual layers. The layer parameters were initially obtained using partial curve matching technique (Keller and Frischknecht, 1966; Bhattacharya and Patra, 1968; and Koefoed, 1979) with the help of three-layer master curves (Rijkswaterstaat, 1969) and auxiliary point charts (Ebert, 1943). These parameters were used as an initial model for computer-assisted interpretation software program IX1D.

Thus the interpretation of the vertical electrical sounding curve is accomplished in terms of the layer parameters. However, the problem arises about their interpretation in terms of lithological units. At this stage, it is necessary to have the correct idea about the actual resistivity values of various formations to reach at the best possible interpretation of geophysical results in terms of different lithological units in the existing geological setups. The interpreted result at the VES-1 location shows the presence of six layers (Fig. 3f). The upper layer having resistivity 15 ohm-m indicates the presence of surface clay of moist nature whose thickness is about 2.0 m. The resistivity of the second layer increases rapidly up to 114 ohm-m, attributed to the presence of semi-weathered sandstone with a thickness of about 3.4 m. The resistivity of the third layer reduces to 12 ohm-m, which indicates the presence of highly weathered sandstone saturated with water whose thickness is about 9 m. The resistivity of the fourth layer increase to 286 ohm-m the presence of semi-fractured sandstone whose thickness is about 40 m. The resistivity of the fifth layer reduces to 28 ohm-m indicates the presence of highly fractured sandstone whose thickness is about 88 m. Such a suitable thickness of fractured sandstone may form a prolific groundwater source that can be used through shallow tube-well. The resistivity of the sixth layer increases to 925 ohm-m, which indicates the presence of semi-compact sandstone.

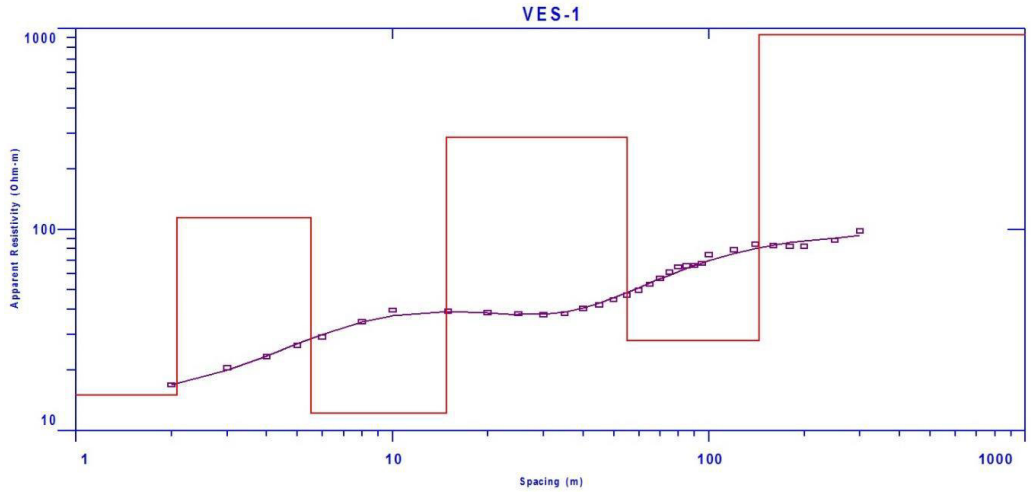

Figure 3f: Apparent resistivity curve and layer resistivity model at VES-1

Fig.: (3g) shows the interpreted result at the VES-2 having five layers. The first layer having resistivity 10 ohm-m indicates the presence of surface clay of moist nature whose thickness is about 0.5 m. The resistivity of the second layer increases up to 29 ohm-m, attributed to the presence of weathered sandstone with a thickness of about 3.0 m. The resistivity of the third layer rapidly increases to 957 ohm-m, which indicates the presence of semi-compact sandstone whose thickness is about 22 m. The resistivity of the fourth layer reduces to 53 ohm-m the presence of highly-fractured sandstone whose thickness is about 49 m. An appropriate thickness of fractured sandstone may form a prolific groundwater source that can be used through shallow tube-well. The resistivity of the fifth layer increase to 8844 ohm-m indicates the presence of compact sandstone.

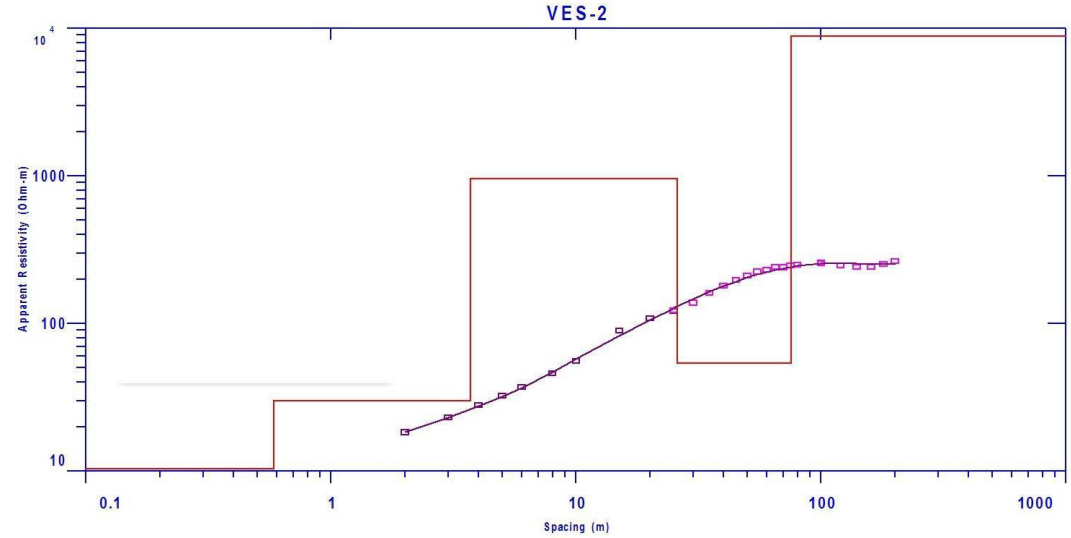

Figure 3g: Apparent resistivity curve and layer resistivity model at VES-2

A 'high' resistivity zone on GP-4 at distance of 20 m from centre of profile towards right side was also selected for VES-3 to know the variation of resistivity with depth as well as comparison to results of VES-1 and VES-2 conducted at resistivity 'low'. The result at VES-3 clearly shows drastic change in layer configurations compare to VES-1 and VES-2. The interpreted result at the VES-3 shows the presence of three layers (Fig. 3h). The first layer having resistivity 18 ohm-m indicates the presence of surface clay of moist nature whose thickness is about 3.2 m. The resistivity of the second layer increases up to 334 ohm-m, attributed to the presence of semi-fractured sandstone with a thickness of about 76.0 m. The resistivity of the third layer rapidly increases to 1749 ohm-m, which indicates the presence of compact sandstone.

Based on the interpretation of the all sounding data, a test borehole has been drilled at VES-1 to identify the different lithological units and the presence of ground water-bearing zones. The fracture zones were encountered in test borehole at 111-114 m, 126-129 m and 141-144 m. The thickness derived from the sounding data is well correlated with the borehole's lithology within the limitations of the method (equivalence & suppression problems). The quality of water is good, with a continuous discharge rate of about 10,000 liters/hour through the delivery size of 2" diameter.

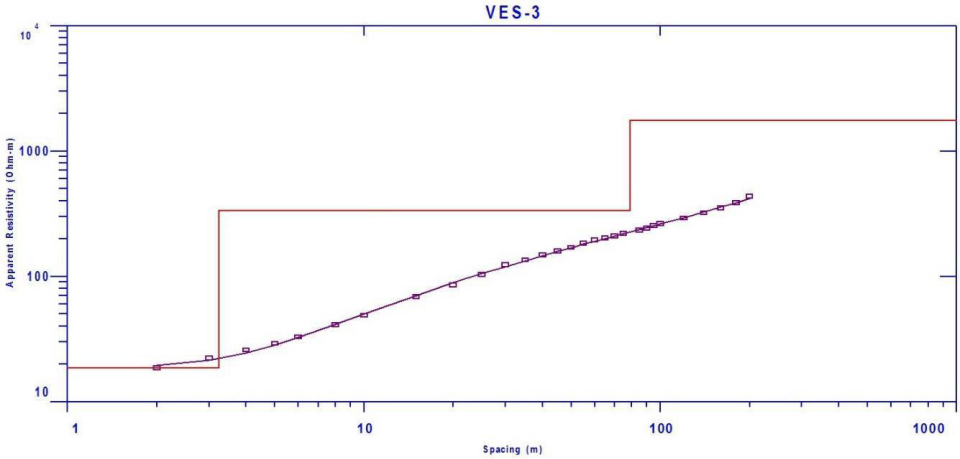

Figure 3h: Apparent resistivity curve and layer resistivity model at VES-3

CONCLUSION

The efficiency of combined Gradient profiling (GP) and Vertical electrical sounding (VES) using Schlumberger configuration is presented here to map the weathered and fractured zones in hard rock areas. The present study indicates that delineation of saturated fractures can be done with proper planning, especially in the hard rock areas. It has been exhibited that the GP survey is more effective and yields much improved results with better resolution. Thus the systematic measurement must be done to see the lateral variation of apparent resistivity using the GP survey. The interesting point ('low' resistive point with sharp gradient) is selected for studying the depth-wise variation of resistivity using the VES survey. It can be inferred that the GP survey is very much useful in deciphering the prospective locations for conducting the VES survey for the exploration of groundwater resources. The unfruitful attempts of conducting a VES survey at several randomly selected locations could be avoided. It can minimize the cost and time of VES surveys to a great extent. It can be finally concluded that the combined approach of resistivity survey (GP followed by VES) for delineation of saturated fractures, especially in hard rock areas, can be gainfully applied.

ACKNOWLEDGEMENT

The authors are grateful to Sri P. K. Tripathi, Head of Office, Central Ground Water Board, NR, Lucknow for his guidance and encouragement during the preparation of this manuscript. The authors are also thankful to Sri Y. B. Kaushik, Ex-Regional Director, Central Ground Water Board, NR, and Lucknow to provide facilities for conducting the investigation work and their support and valuable suggestions.

REFERENCES

Bertin, J., Loeb, J., 1976. Experimental and theoretical aspects of IP. Vol. 1. Presentation and application of the IP method – Case histories. Gebruder Borntraeger, Berlin, 250 p.

Bhattacharya, P. K., Patra, H. P., 1968. Direct current geoelectric sounding, Elsevier, Amstardam.

Ebert, A., 1943. Grundlagen Zur Auswerkung geoelektrischer Tiefenmr-ssulgon. Garlands Beitrage Zur Geopysik, BZ, 10 (1), 1-17.

Keller, G. V., Frischknecht, F. C., 1966. Electrical methods in geophysical prospecting. Pergamon Press, New York, 517 p.

Koefoed, O., 1979. Geosounding principles, 1. Resistivity sounding measurements, methods in geochemistry, and geophysics. Elsevier, Amsterdam, Oxford, New York, 276p.

Karous, M., Mares, S., 1988. Geophysical methods in studying fracture aquifers, Charlse University, Prague, 93 pp. [ER, EMI, SP, SRR, borehole].

Kearey, P., Brooks, M., 1984. An introduction to geophysical exploration. Blackwell Scientific Publications, Oxford, London, 296 p.

Krishnan, M. S., 1982. Geology of India and Burma. 6th Ed. CBS publishers and distributors, New Delhi, 536p.

Kunetz, G., 1966. Principles of direct current resistivity prospecting. Gebruder Borntraeger, Berlin, 250 p.

Rijkswaterstaat, 1969. Standard Graphs for Resistivity Prospecting. EAEG, The Netherlands.

Schluz, R., 1985. Interpretation and depth of investigation of gradient measurements in direct current geoelectrics. Geophysical Prospecting 33, 1240-1253.

Sharma, P.V., 1997. Environmental and Engineering Geophysics. Cambridge University Press, New York, 475 p.

Telford, W. M., Geldart, L. P., Sheriff., 1998. Applied Geophysics (II Ed.), Cambridge University Press, U.K., 536-537p.

Yadav, G.S., Singh, S.K., 2007. Integrated resistivity surveys for delineation of fractures for groundwater exploration in hard rock areas. J Applied Geophysics, Vol. 62, pp. 301–312

Yadav, G.S., Singh, S. K., 2008. Gradient profiling for the investigation of groundwater saturated fractures in hard rocks of Uttar Pradesh, India Hydrogeology Journal, Vol. 16, Issue 2, pp.363-372

Bhujal News, 30(1-4):17-32

Integration of the Advanced Geophysical Methods for Aquifer Mapping-A Case Study from Chandrabhaga Watershed, Maharashtra, India

P. Narendra[1], P K Jain[1], V. Arul Prakasam[2], S D Waghmare[3], Bhushan R Lamsoge[4]

1. Central Ground Water Board, CR, Nagpur, 2. Central Ground Water Board, SER, Chennai, 3. Central Ground Water Board, SUO, Pune 4.RGNGWTRI, Naya Raipur

** Corresponding author-email-narpvla@yahoo.co.in*

ABSTRACT

In India, to establish a methodology for Aquifer Mapping, in addition to hydrogeological and traditional geophysical surveys, advanced geophysical methods comprising the Electrical Resistivity Tomography (ERT), Ground Transient Electromagnetic (TEM) and SkyTEM (Time-domain heli-borne electromagnetic system) methods have been applied first time in basaltic terrain to delineate the aquifer system up to 200 m depth. These advanced techniques clearly brought out the precise mapping of aquifers on 1:50,000 scale. VES results infer that the Basalt thickness is increasing from east to west. The VLF and GRP inferred the location and orientation of the fractures / lineaments. The observed low resistivity breaks within the ERT profile over basaltic terrain could be inferred as weak zone as an indicative of lineament, which are potential groundwater bearing zones. TEM provides significant information of shallow depth up to 50 m bgl. Heliborne Transient Electromagnetic investigation with the integration of ground geophysics and controlled points such as borehole lithologs has been used to derive the basaltic trap thickness. However, ERT, TEM & Sky-TEM failed to identify or demarcate red/grey/green bole layer of significant thickness (5 m and more) beds at a depth > 50 m in Basaltic terrain as well as different litho units of Gondwana.

Key Words: *Aquifer mapping, advanced geophysical methods (ERT, TEM & Sky-TEM), Basaltic Terrain, Maharashtra*

INTRODUCTION:

During the year 2012-14, Central Ground Water Board (CGWB), under 'pilot project on aquifer mapping' (AQMAH) carried out detailed multi-disciplinary hydro-geological survey in Chandrabhaga watershed to decipher the lateral and vertical disposition of the aquifer system prevailing in the area. Intervention of advanced geophysical techniques and establishing the utility, efficacy and suitability of these techniques in different hydrogeological setup was also one of the objectives of the project. Therefore, apart from the traditional hydrogeological and geophysical surveys, the Electrical Resistivity Tomography (ERT), Ground Transient Electromagnetic (TEM) and SkyTEM (Heli-Borne Time-domain electromagnetic) methods have also been applied first time in basaltic terrain to delineate the aquifer system up to 200 m depth (CGWB, 2015a and 2015b). The present research papers deals with the advance geophysical techniques *(ERT, TEM & Sky-TEM),* used for demarcation of aquifer geometry, aquifer mapping in trap covered Gondwana formation with the help of geo-electric layers/data.

In Chandrabhaga watershed, prior to this study, CGWB has carried out 19 VES to decipher the vertical and horizontal extensions of basaltic aquifer. The 2D inverse models of resistivity variation with depth suggest that the potential aquifers mostly occur in weathered/fractured zones within the traps or below it. The interpreted results have been verified by a bore well drilled at a site near Ghogali village. A potential water-bearing aquifer was struck at a depth of 35 m, which was in good agreement with the interpreted results (Ratna Kumari et al, 2012). The Electrical Resistivity Tomography (ERT) survey has proved the occurrence of groundwater potential zones in hard rock (a heterogeneous environment). Resistivity models have ascertain presence or potential groundwater zones at several sites in this top alluvium and weathered mantle which can be explored for groundwater. Similarly, resistivity models have also deciphered groundwater potential zones at deeper level within and below traps in the Lameta/Gondwana formations (Ratna Kumari et al, 2012). The gravity maps prepared by GSI based on gravity survey carried out in parts of study area prior to the pilot project indicate that the positive contours southeast of

Kalmeshwar in the residual Gravity map infer that the high-density granitic basement is shallow and the Gondwanas are absent in this area (T.S. Ramakrishna, et al, 1990).

STUDY AREA

Chandrabhaga Watershed (WGKKC-2), Nagpur district, Maharashtra state is taken up for the micro level aquifer mapping study. Chandrabhaga Watershed (WGKKC-2), occupy an area of 360 sq. km. is situated in the north western part of Nagpur district covering about 60 villages in parts of Nagpur (rural), Kalmeshwar and Katol talukas (Fig. 1). It lies between north latitudes 21°10' and 21°10' and east longitudes 78°42' and 78°59' and falls in parts of Survey of India toposheets 55 K-11, 12, 15 & 16. The watershed is well connected by all season motorable roads (CGWB, 2015a). (Fig. 1).

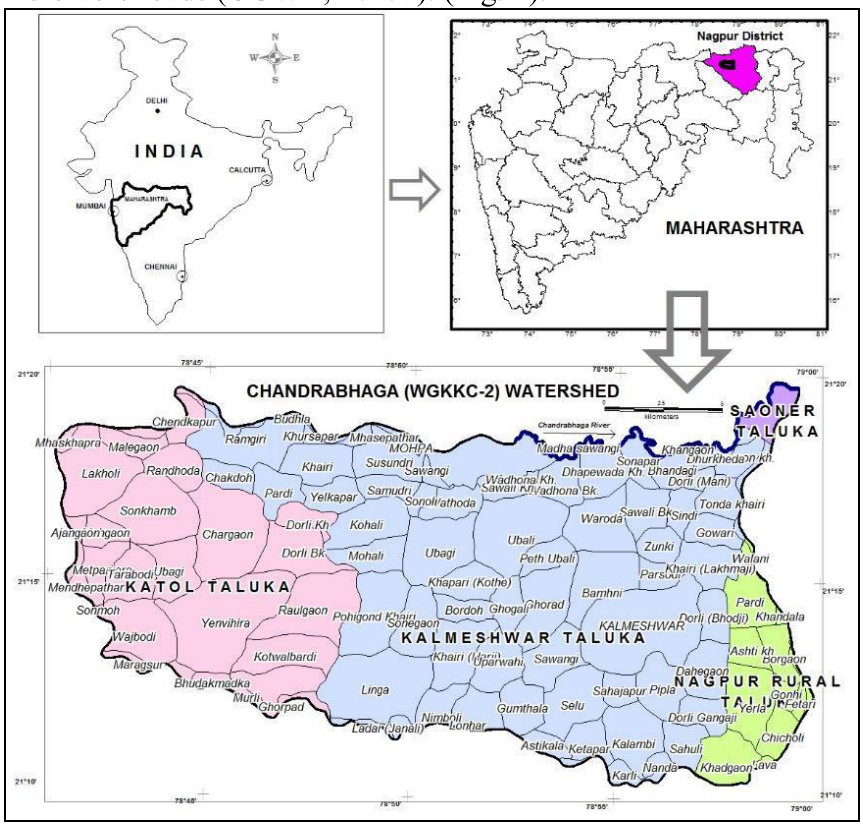

Fig. 1: Location map of Chandrabhaga Watershed (AQMAH pilot area),Nagpur,Maharashtra

Physiographically, Chandrabhaga watershed forms the Moderately Dissected Plateau (MDB) of Deccan trap (basaltic terrain) where four sets of lineaments are interpreted, which trending in NE-SW, NW-SE, N-S and E-W directions (CGWB, 2012 and 2015a). The area has an undulating terrain with highest elevation around 509 m amsl in the north-western part and the lowest about 310 m amsl in the north eastern part**.**

The ephemeral Chandrabhaga River is flowing from a height of 334.333 m amsl at village Wadhona (Bk) to 299.69 m amsl at village Sillori. The area is drained by tributaries of the Chandrabhaga river viz., Saptadhara River, Mortham Nala forming a dendritic pattern. The flow direction of main stream i.e., Chandrabhaga is from west to east and its tributary from south to north, the main stream ultimately joins the Kolar river outside the watershed in the eastern part.

Major part of the area is occupied by Basaltic lava flows of Upper Cretaceous to Eocene age, trap covered Gondwana and Trap covered Gneiss formations (CGWB, 2012, 2013). The Gondwana formation of Permian is mainly exposed in the north-eastern part and also occurs as a small linear patch south of Kotwalbardi and Linga villages along the southern boundary (Fig 2). In Gondwanas, the major litho-unit is Kamthi formation which is followed by Barakars (CGWB, 2012 and 2013).

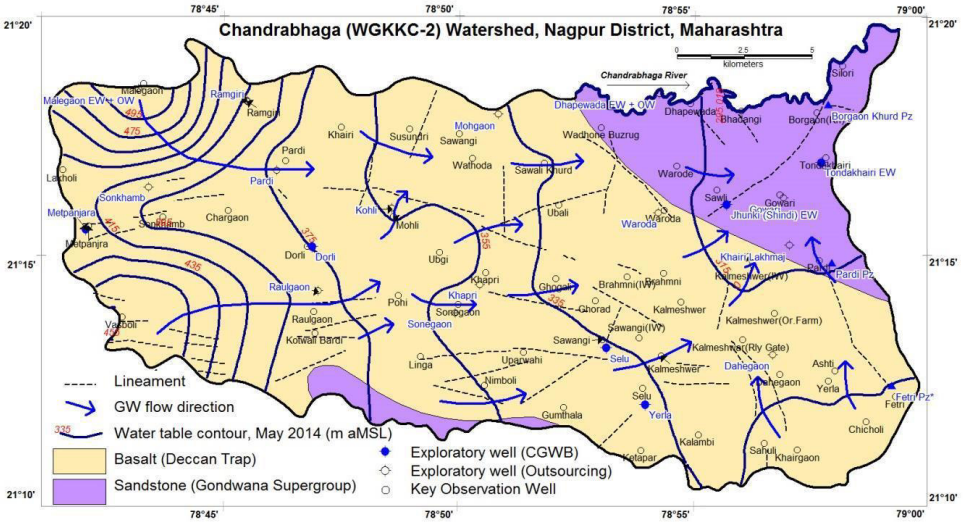

Fig.2: Hydrogeology and lineament, Chandrabhaga Watershed (WGKKC-2)

HYDROGEOLOGY AND SUB SURFACE LITHOLOGICAL INFORMATION

Ground water occurs under phreatic conditions in the exposed lava flows and in semi-confined to confined state in the subsurface flows. Ground water is present in interconnected pore spaces of vesicular unit and in the jointed and fractured portions of massive unit of each flow. However, secondary porosity and permeability that developed on account of weathering, fracturing and joints play a very important role in storage and movement of ground water and constitute the important water bearing formations (aquifer) in hard rock of basalt. Ground water in Gondwana group of formation occurs under both phreatic and confined conditions. The occurrence of sufficient thickness of shale as an impervious unit above and below the sandstone simulate the confining condition in the sandstone aquifer.

CGWB has drilled 10 boreholes in the watershed, depth ranging from 40 to 202m bgl. The water bearing zones were encountered at depths ranging from 7 to15m bgl and 183.5 to 186.5m bgl. The discharge of the wells ranging from negligible to 13.96 lps. The ground water quality is good except nitrate, which is found above permissible limits of 45 mg/L. The borehole data indicate that Gondwana sandstone was encountered at 123 and 111m bgl respectively at Dorli in the western part of the watershed. Whereas, the same was encountered at very shallow depth i.e., 27m bgl in eastern part of the watershed at Jhunki (Shindi), and at Borgaon (Khurd). However, at Pardi, located in the eastern corner, it is exposed at ground level. Thus it inferred that the thickness of Basalt is increasing from east to west. The lithology of EW drilled at Yerla shows that the basalts underlain by Lameta beds which is then followed by Archaean Gneisses below 59 m bgl.

METHODOLOGY

The role of geophysics in groundwater exploration is vital to understand subsurface conditions accurately and adequately. Geophysical investigations help assess the presence of aquifers in geologic formations, estimate weathered zone thickness or bed rock topography and fractures, and assess quality (in terms of salinity) of groundwater. Geophysically, it is possible to precise the three-dimensional geometry and disposition of aquifers.

Application of geophysical methods for aquifer characterization has been in practice in India since the 1930s, mostly through electrical resistivity sounding and profiling and geophysical logging of boreholes.

In view of mapping the entire aquifer systems in India within a short period of time, geophysical methodologies were applied comprising a combination of techniques that give fast coverage and yield the desired information as precisely and adequately as possible. With this objective, Heliborne Time-domain Electromagnetic and magnetic and ground based techniques comprising resistivity sounding, resistivity imaging, time-domain electromagnetic sounding and Very Low Frequency Electromagnetic were applied in the study area.

The aquifer geometry mapping by these geophysical methods and techniques helps identify the aquifers, their lateral extents and vertical grouping through generation of cross-sections and contour maps. The hydrogeological studies in conjunction with geophysical parameters also help identify the areas for artificial recharge or areas requiring aquifer protection.The flow chart below shows the approach adopted for geophysical investigations under the pilot study.

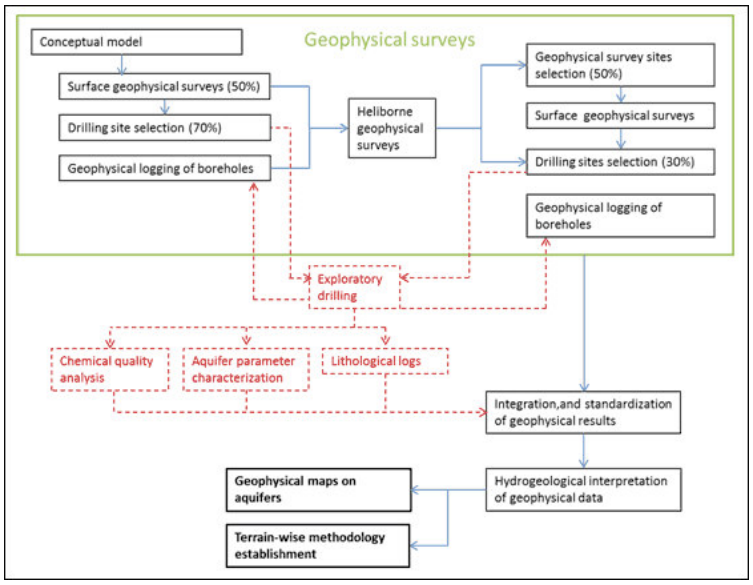

Finally, the geophysical results are integrated, calibrated and standardized with drilling data and hydrogeological studies to produce different geophysical maps on aquifers.

Resistivity imaging technique is a combination of resistivity sounding and profiling, incorporates the effects of lateral variations in resistivity on sounding, and produces a two- or three-dimensional subsurface resistivity image, thus leading to the three-dimensional geometry of the aquifers (Torleif Dahlin, 2001). Ratnakumari, et al, (2012) delineated aquifers concealed within and below the traps in the Deccan traps-covered terrain using 2D ERI. Details about the study area are as follows- In the study area, electrical resistivity imaging is used to substantiate the sounding results across the geologic structures

By the transient electromagnetic method, TEM, the electrical resistivity of the underground layers down to a depth of several hundred meters can be measured. Groundbased measurements as well as airborne surveys (SkyTEM) to cover large areas are possible. The method was originally designed for mineral investigations. Over the last two decades the TEM method has become increasingly popular for hydrogeological purposes as well as general geological mapping. The TEM method applies an ungrounded loop as transmitter coil. The current in the coil is abruptly turned off, and the rate of change of the secondary field due to the induced eddy currents in the ground is measured in the receiver coil, usually an induction coil.

The feasibility of using the transient electromagnetic sounding (TS or TDEM) method for groundwater exploration can be studied by means of numerical models (David V. Fitterman and Mark T. Stewart, 1986). In the study area, Time-Domain Electromagnetic soundings (TEM) are carried out at selected places in addition to the direct current resistivity soundings and imaging to confirm the results and jointly invert the data to reduce the ambiguities. As of now, TEM soundings for aquifer delineation have not been in regular practice in India.In the pilot study for aquifer mapping, geophysical logging of boreholes is carried out to validate the surface and heliborne geophysical data, as well as to precisely delineate the potential aquifers by using Electrical, natural gamma radioactivity probes.

For fast and close-spaced coverage of the pilot areas, Helicopter-borne Time Domain Electromagnetic surveys (Sky –TEM) are carried out. In airborne geophysical surveys, the physical properties of the subsurface are measured from the air (NGRI 2015a, 2015b). The advantages of Heliborne EM surveys are continuous and fast data-acquisition with high accuracy and resolution, and access to any type of terrain. They enable to acquire large

volume of data and are relatively economical as compared to surface surveys in terms of quantum of data obtained in a set time. Recently Heliborne EM surveys, they have been used for aquifer mapping in Europe, USA and Australia. This is the first time that heliborne geophysical surveys are carried out in India for aquifer mapping (CGWB 2015).

RESULT AND DISCUSSION

Electrical Resistivity Survey

A systematic electrical resistivity survey was carried out by employing Schlumberger configuration with maximum current electrode separation (AB) of 600 m depending on the available spread length. A total of 138 VES including 52 VES for exploratory drilling (Fig.3) were carried out to estimate the thickness of the top basaltic formation or depth of Gondwana formations. In addition to this, 300 line meters of Gradient Resistivity Profiling (GRP) and 610 line meters of Very Low Frequency (VLF) electromagnetic profiling were also carried out to locate the fractures/lineaments in Chandrabhaga Watershed. The VES data acquired was interpreted by IPi2Win software and analyzed to infer the subsurface geo-electric layers. The VES results were standardized based on the local Geology, Hydrogeology and existing borehole data (**Table 1**). Each geo-electric layer obtained from the investigations is not exactly the response from the individual litho-units, but it is the equivalent resistivity or the weighted average of the two or more numbers of the subsurface layers.

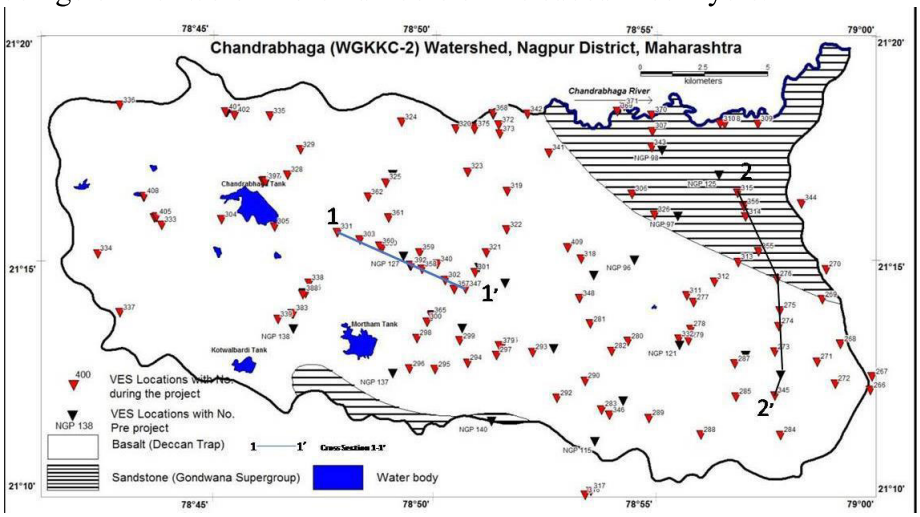

Fig 3: Locations of VES conducted by CGWB Chandrabhaga Watershed (WGKKC-2)

Table 1: Resistivity ranges and inferred lithology, Chandrabhaga Watershed (WGKKC-2)

Resistivity range (Ohm. m)		Probable Lithology	Thickness range (m)	
3.2	181	Top Soil	0.2	2
1	6	Clay	1.1	27.7
1.8	5	Shale	1.1	82.9
6	9	Sandy Clay	3	11.3
11	34	Sand	4.3	11.3
10	14	Sandstone + Shale	2.3	114
16	87	Sandstone	3.5	79.3
152	1343	Compact sandstone	0.9	84
3.5	35	Weathered Basalt	0.6	39.5
30	43	Moderately Weathered Basalt	3.5	8.6
40.5	58	Vesicular Basalt	1.1	125
6.7	40	Fractured Basalt	1.3	144
More than 60		Massive Basalt	1.1	102
1	5	Red/green Bole	0.5	13
5	15	Lameta bed	0.5	5
10	12	Fractured Granitic Gneiss	Bottom most layer	
More than 554		Massive Granitic Gneiss	Bottom most layer	

It is inferred from VES data that the thickness of the basalt is increasing from east to west. It is measured around 60m at village Yerla in the eastern part, around 108 m at village Dorli, and more than 150 m in the western and northern part of the watershed. However, Gondwanas are seen at shallow depths, approximately 30 to 40m depths around village Raulgaon. Occurrence of Gondwana at shallow level could be attributed to reverse faulting at this place or the extension of Gondwana of southern part. All the data generated using various geophysical surveys conducted in the watershed were utilized to generate various 2D, 3D sections and maps of the basins. Fence diagram (Fig. 4) has been prepared based on the VES results for 3D view of the aquifer disposition.

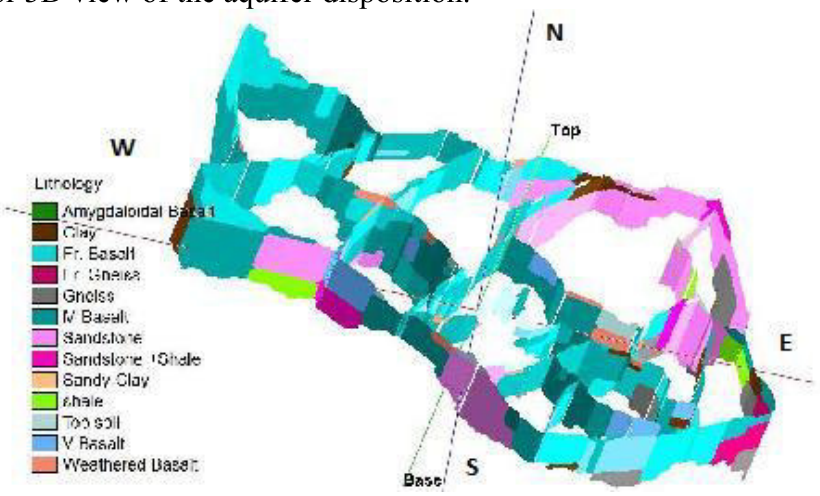

Fig. 4: Generation of Subsurface disposition, geoelectrical layers translated to lithological layers using Rockworks, Chandrabhaga Watershed (WGKKC-2)

The Gondwana formations are extending more than 150m depth in the NE part of the area. The Gondwanas are absent in the SE part of the area and it was confirmed from the existing borehole data at Yerla. In this area, the Archaeans are encountered below basaltic formation at depths around 60 mbgl. In the northern and western parts of the area, the thickness of the top basaltic formation is more than 150m but in the SW part of the area around Raulgaon, the Gondwana formation occur at shallow depths. The various contour maps, 2D and 3D figures were generated based on VES results and geophysical logs.

Gradient Resistivity Profiling (GRP)

Three parallel GRPs – Line 1 (100 lm), Line 2 and Line 3 (85 m each) were carried out in S 70° E – N 70° W direction at Ghorad village for exploratory drilling. Apparent resistivity contours were generated (Fig. 5) using SURFER software based on the GRP data. The results of analysis indicates that in the SE Side, the apparent resistivity values are moderate, ranging from 40-60 Ωm, in the central part, the apparent resistivity values are high, ranging from 60-80 Ωm and in the NW part, the apparent resistivity values are low, less than 40 Ωm. In the NW part of the profile, the low apparent resistivities may indicate fracture zone (Fig. 5).

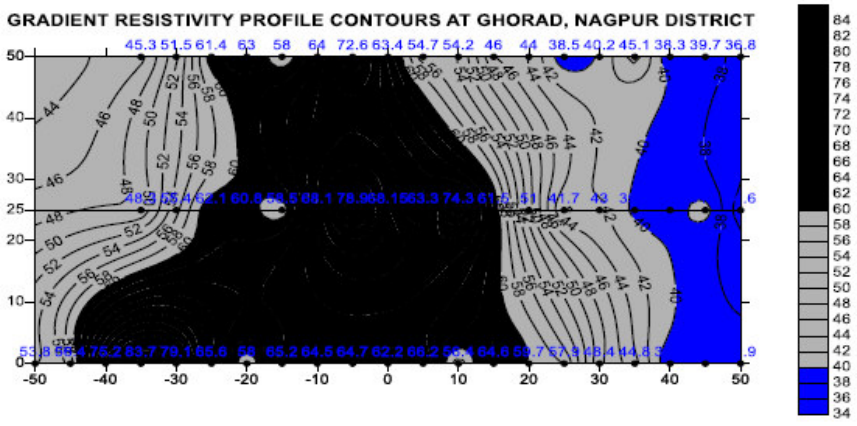

<----S 70° E N 70° W---->

Fig.5: Gradient Resistivity Profiles and contours at Ghorad, Chandrabhaga watershed (WGKKC-2)

The VES results of earlier surveys in the same site (CGWB, 2015a) indicate that the top geo-electric layer of 70 Ωm resistivity and 0.9 m thickness represents top soil. The second geo-electric layer of 24 Ωm resistivity and 1.0 m thickness represents weathered basalt, the third and fourth geo-electric layers of 13 and 6 Ωm resistivities up to 8.8 m depth represents fractured basalt, the fifth layer with 46 Ωm resistivity up to 40 m depth may represent moderately fractured or vesicular basalt. The bottom most layer with 216 Ωm resistivity represents massive basalt. The results of exploratory drilling by CGWB at this site support the inferences from GRP.

Very Low Frequency (VLF) Electromagnetic Profiling

Five parallel VLF profiles, Line 1, Line 2, Line 3, Line 4 and Line 5 were carried out in N85°E-S85°W direction at village Ghorad for exploratory drilling. Line 1 is of 110 m length, Line 2, 4 and 5 are of 125 m length and line 3 is of 120 m length had been taken. The data on Tilt and ellipticity were plotted on linear scale against distance from the starting point of the profile. On the tilt angle profile, a maximum followed by a minimum separated by an inflection point located above the top of the conductive body. The tilt and ellipticity are highly fluctuating, may be due to noise. In order to give an easier correlation between the anomaly and the structure, Fraser derivatives of tilt angles were used. The expression for the Fraser Derivative is (a+b) - (c+d) where a, b, c, and d, are the rough values of the tilt angle measured at four successive stations separated by the same spacing. The values of the Fraser Derivatives are plotted at the middle of the stations b and c. In the case of a fracture, the maximum of this Fraser curve is located just above the position of the fracture. Contour maps were also generated for Tilt, Ellipticity, and Fraser Derivatives (Fig. 6). The maximum of this Fraser curve is located just above the position of the fracture and these points are joined to get the orientation of the fracture. The dotted lines on the fraser derivative contour map represent fractures and they are oriented in approximately N - S direction.

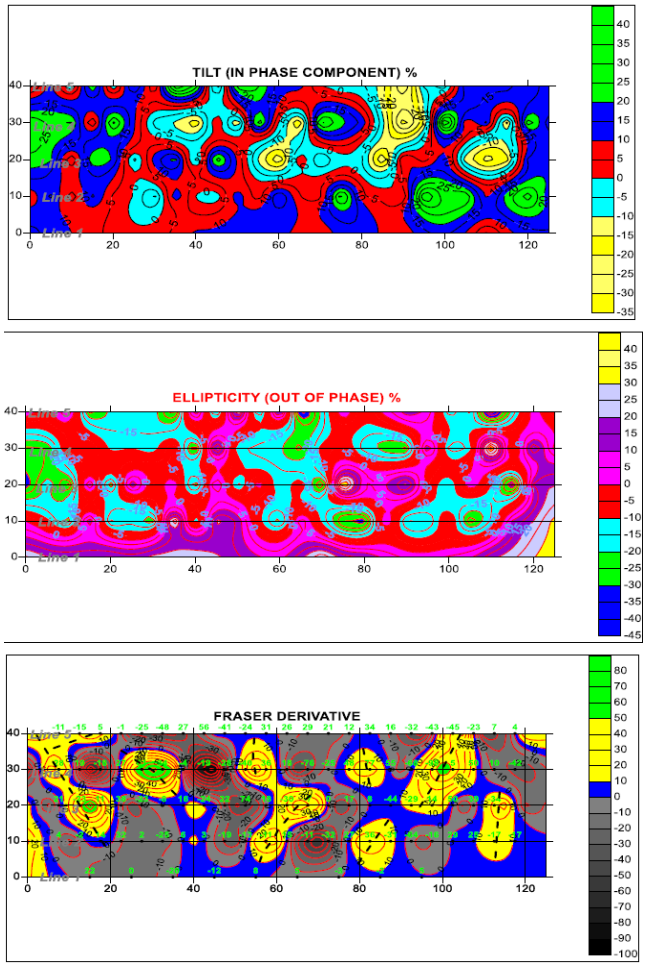

Fig.6: Contour Maps generated based on Parallel VLF Profiles at Ghorad, Chandrabhaga Watershed (WGKKC-2)

The comparative analysis of the GRP and VLF profiles, infer that the fractures in the NW part of the profiles are productive. The low apparent resistivity contours generated from parallel GRP of less than 40 Ωm apparent resistivity and high Fraser derivative values infer potential fracture zone in NW part of the studied area.

Spatial distribution of resistivities at Different elevations (Depth Slicing)

Elevations at the VES locations were recorded through GPS. Depth slicing has been done by generating the contour maps for resistivity values at different elevations based on the VES results. These depth slices are ranging from 400 m amsl to 150 m amsl at every 50 m interval (Fig 7). The western part of the area is highly elevated with 400 to 500 m amsl.

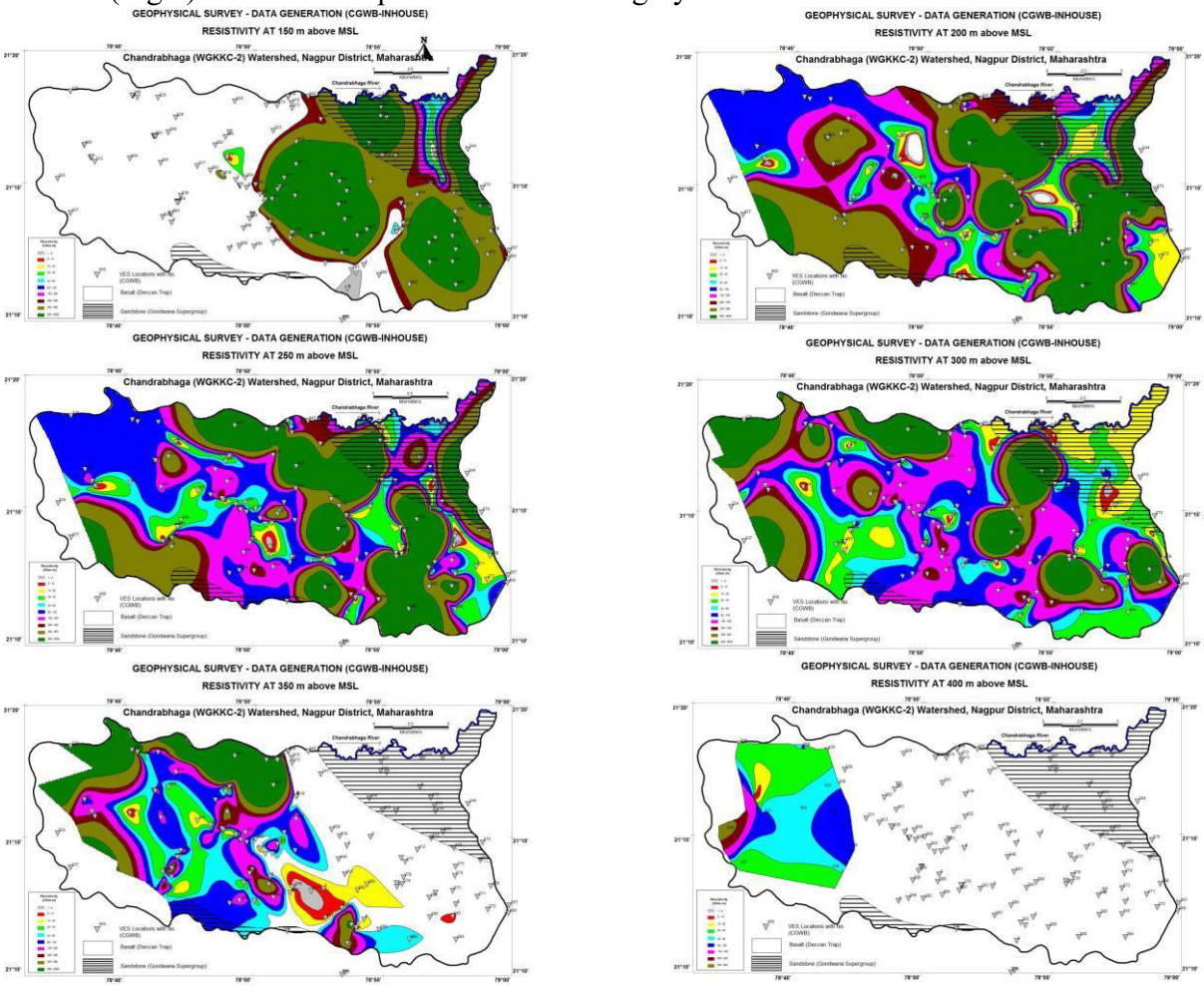

Fig.7: Contour Maps generated based on VES Results, Chandrabhaga Watershed (WGKKC-2)

The elongation of the low resistive contours in north eastern part of the area in N-S direction at 150 mamsl, in the NE-SW direction at 200 and 250 mamsl and in th NW-SE direction in the NE part of the area at 250 mamsl indicates lineaments in respective orientations at respective elevations. The relatively low resistive contours stretching from NW part of the area to the south central part of the area at 200 and 250 mamsl represent basaltic lava flows with different composition. The high resistive contours in the NE part of the area at 150, 200, 250mamsl represent compact or dry Gondwana formation. The low resistive contours in the NE part of the area at 300 mamsl represent unconsolidated / semi consolidated Gondwana formation.

Resistivity cross sections1-1’ and 2-2’ (Fig. 8 and 9) were generated using IPI2Win software. Section 1-1’ of 5.7 Km length was generated (Fig. 8), passing through the villages Kohli, Mohli, (VES No. Ngp 331, 303, 360, 330, 127), Ubgi (NGP390, 358), Khapri (NGP 302, 357, 347). It depicts fractures at VES No. NGP303, 360, 127, 390, 358, 357 and 347. Whereas the low resistivity of 4.6 Ωm at VES no. NGP 330 may correspond to the bole bed below 284 m amsl or 94 m bgl. The Gamma log in the borehole drilled in Khapri village shows relatively a rise in gamma at this depth. The analysis of the samples collected from the borehole at Khapri also support the finding.

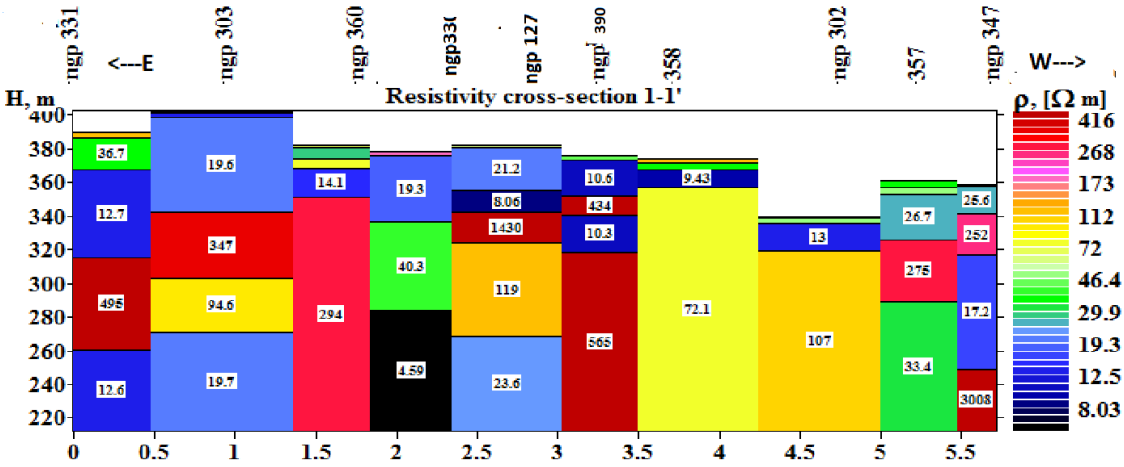

Fig.8: Resistivity Cross Sections along Section 1-1' based on VES Results, Chandrabhaga Watershed (WGKKC-2)

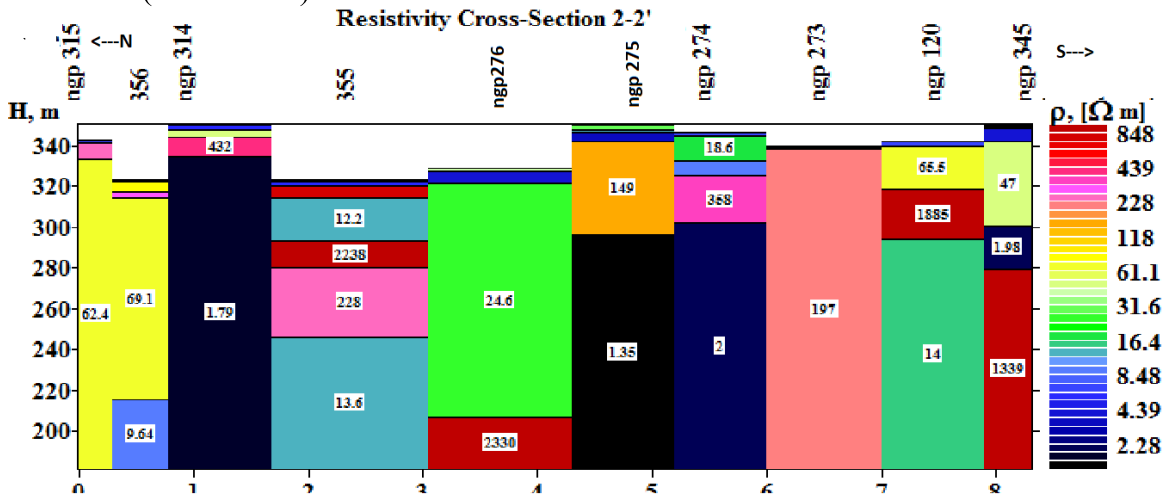

Fig.9: Resistivity Cross Sections along Section 2-2', based on VES Results, Chandrabhaga Watershed (WGKKC-2)

Resistivity cross section 2-2' (Fig. 9) of 8.3 Km length, passing through the villages Gowari (VES No. NGP 315,356,314), Khairi (NGP 355), Pardi (NGP 276), Ashti (NGP 275,274), Yerla (NGP 273,120,345).

In the resistivity cross section 2-2'(Fig. 9) the resistivity ranges between 60 and 70 Ohm m North of Gowari Village (VES 356) correspond to the Sandstone formation. The low resistivity layer of 9.6 Ωm at VES 356 corresponds to the alternate layers of sandstones and shale/clay layers. This has been confirmed with the geophysical log and litholog of the borehole drilled in Gowari village. The resistivity log shows high resistivities up to 80m depth (240m amsl) indicating the sandstones with a thin clay layer between 40 and 45 m depths (280 and 285m amsl). The very low resistive layer South of the Gowari village may correspond to the clay layer. The low resistive layer of 1.8 Ohm m at VES No. NGP 314 may correspond to the clay. At VES 355 near Khairi village, the layer with 12 Ωm from 8.9 to 30 m depth (314 to 293m amsl) and the layer with 13.6 Ωm resistivity below 77 m depth (246 mamsl) to the fractured Sandstone. The low resistive layer of less than 2 Ωm resistivity at NGP 275 and 274 below 55 and 44 m depths respectively near Asta village correspond to the clay / lameta bed which is lying above the Archaean formation and below the Deccan Trap formation. At VES 273 near
Yerla Village the contact of the Basalt and the Archaean formations could not be delineated may be due to the minimal resistivity contrast. However the litholog of the borehole drilled in Yerla village shows basaltic formation up to a depth of 59m bgl followed by lametas and granitic gneisses. The low
resistivity of 14 Ωm below 48 m depth (294m amsl) at NGP 120 corresponds to the fractures gneiss. The high resistivity layers overlying this layer correspond to the compact basaltic formations.

Geophysical Logging

16 exploratory wells were drilled in the study area. These 16 boreholes, were geophysically logged and 16", 64" Normal resistivities, SP, and Gamma were recorded. The logging depth varies from 65 m to 199 m bgl. At couple of places, the geophysical logging has been restricted up to shallow depth due to the collapse of the drilled wells prior to the logging. A few geophysical logs were presented in Fig 10. After studying the geophysical logs consolidated lithologs were prepared for all the boreholes (Fig 11).

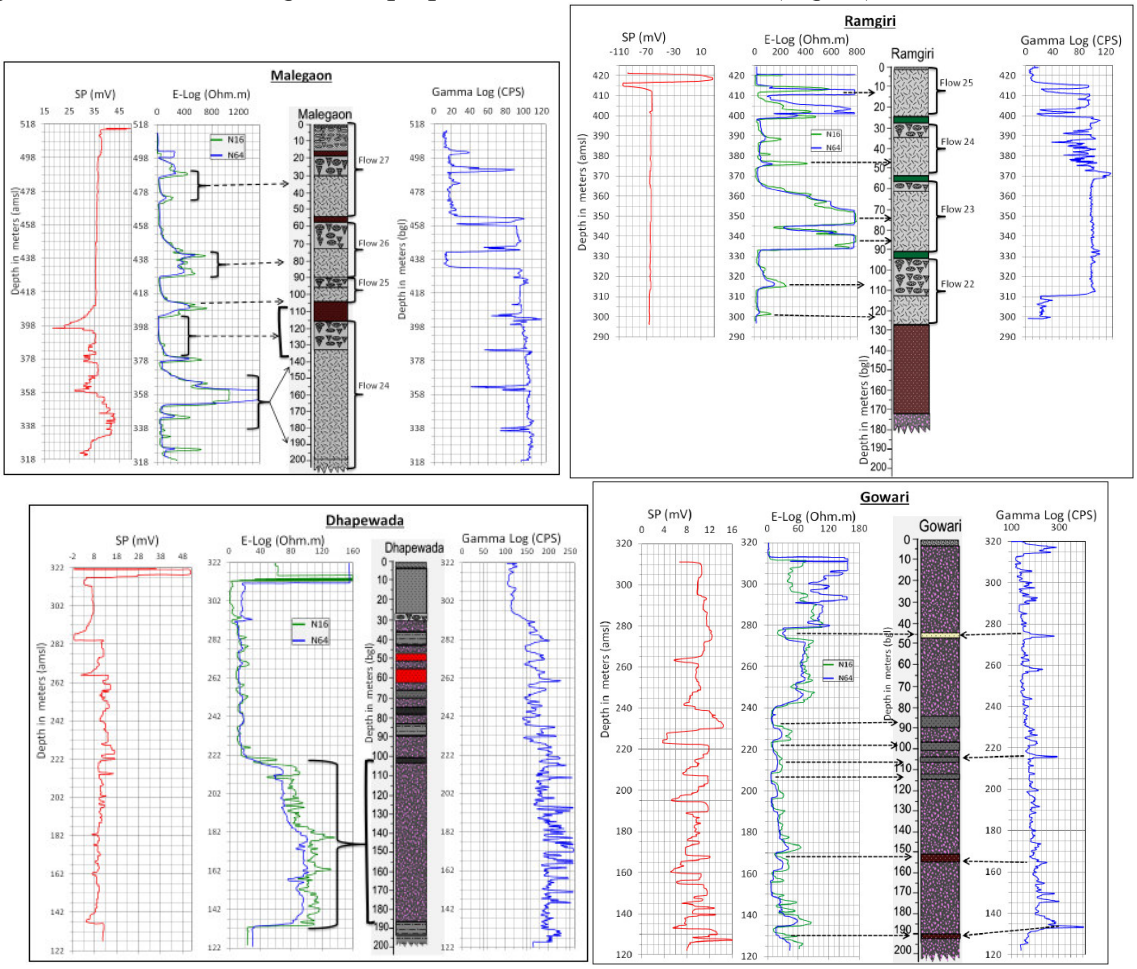

Fig 10: Few Geophysical logs in the pilot project area WGKKC 2

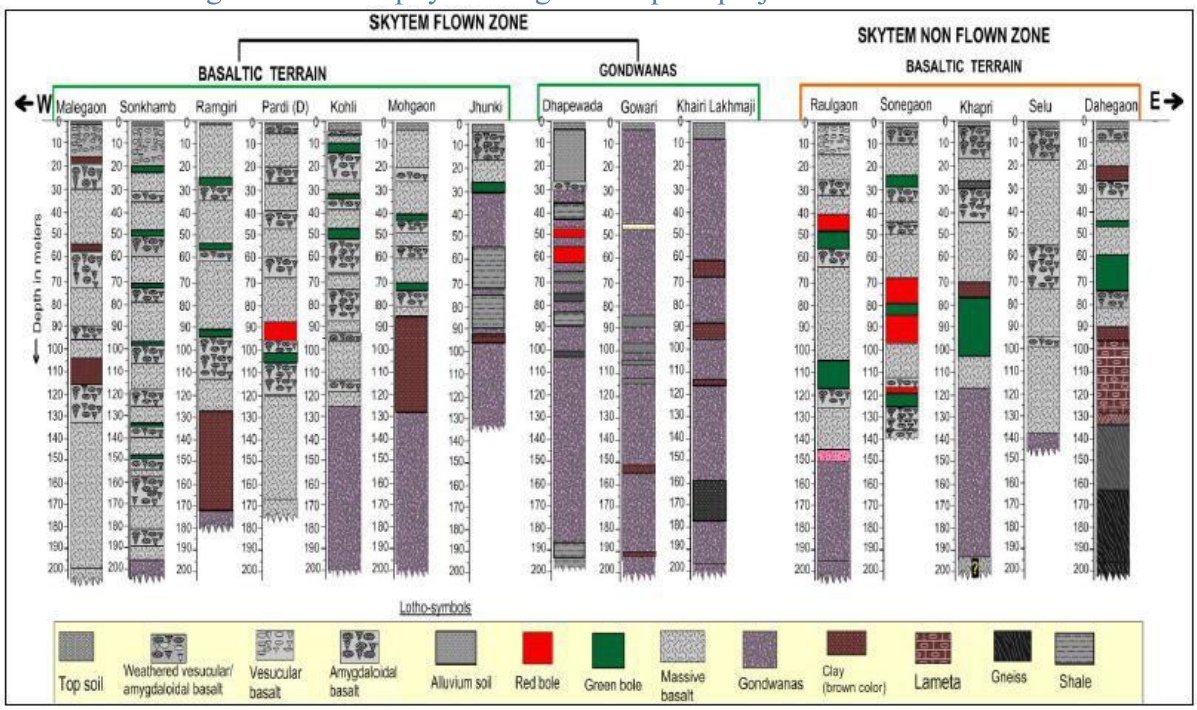

Fig 11: Consolidated lithology of CGWB drilled wells, Chandrabhaga Watershed (WGKCC-2)

Electrical Resistivity Tomography (ERT)

To decipher the disposition of the intertrappeans, and vertical contact of basalts and underlain Gondwana formation, which are thought to be potential aquifer zone, 17 ERT profiles have been carried out to cover the profile A-B of about 15 km line using Wenner Schlumberger configuration with the help of Sysycal Jr Switch 48 Meter. The ERT profiles were performed in N-S orientation where 1st electrode at north and 48th at south is followed (Fig 12). The geo coordinates were noted for each electrode of field lay out.

The ERT ME 3 and 4 (Fig.12) show low resistivity up to 20 Ωm indicating Gondwana sediments that was verified by dug well rock cuttings. Investigated resistivity is found varying in range of 5 to 20 Ωm. However, ME14 that falls on other side of the profile reveals completely different resistivity range varying from 10 to70 Ωm. Such differences are a clear indication of either different mineralogical compositions or different hydrogeological set up. Looking at the megascopic hand specimens it is evident that the northern part of Gondwanas consists of mainly coarse grained Ferruginous sandstone. The low order of resistivity might be the result of Fe elements, water contents, water quality, etc. which needs to be further verified. The Motur Gondwana in south is composed of fine to coarse grained sandstone with inclusion of mudstone as seen in the rock cutting in a dug wells. Higher order of resistivity in this portion still need to be understood by more investigations and would be important from the point of groundwater dynamics. The ERT images, further in south from ERT 5 onward, exhibits basaltic flow pattern as marked by dotted lines lying roughly between 30-80 m depths (ERT 5). Resistivity range, though observed low, indicates increasing trend towards south and reaches up 400 Ωm. theoretically such flow is expected to be continuous. However, observed low resistivity breaks within the ERT profile over basaltic terrain could be inferred as weak zone as an indicative of lineament. Occurrence of such lineaments could be taken as associated potential groundwater bearing zones. The inferred lineaments are marked in the respective ERTs.

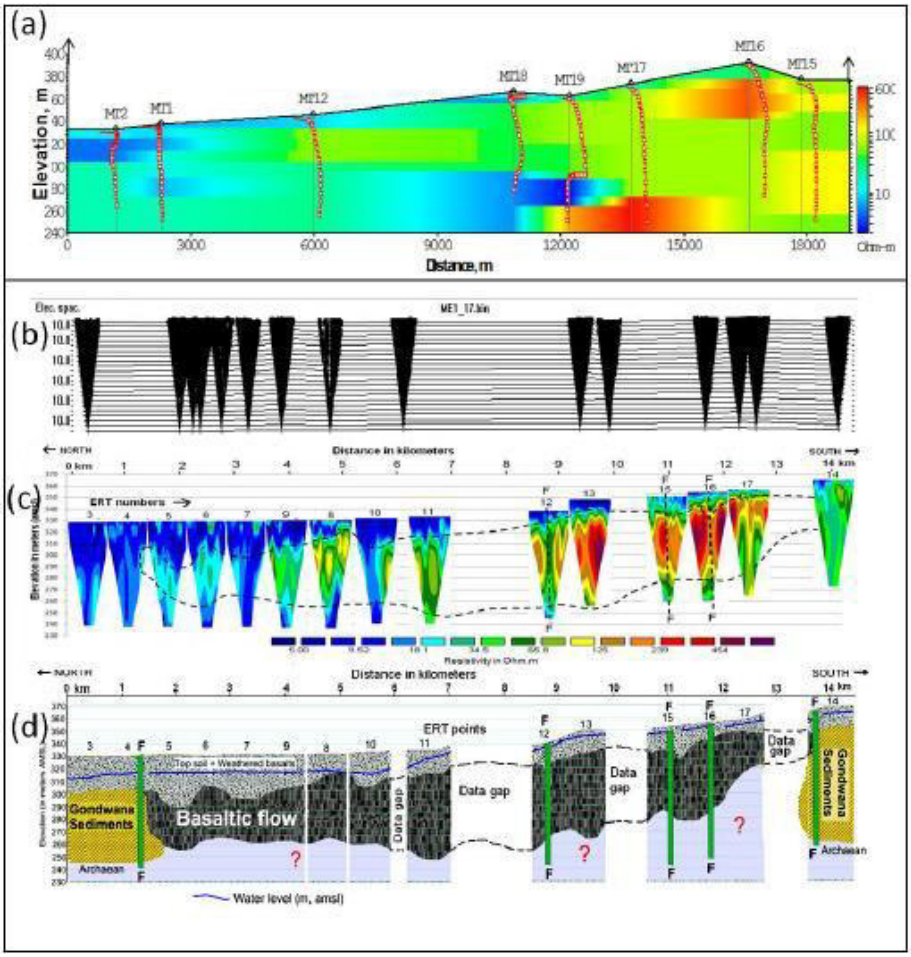

Fig. 12: Resistivity image with altitude from TEM; (b) ERT data pattern; (c) ERT image and (d) derived hydrogeological map from showing basaltic flow of N-S profile along AB line

Ground Transient Electromagnetic (TEM) methods

99 Ground TEM were carried using TEM fast 48 HPC system & TerraTEM with 40m x 40m loop size, 1 and 4 A current.

Hydro-geophysical thematic maps are prepared representing mean resistivity distribution (Fig 13) for depth interval 0-5 m, 10-15 m, 20-25 m and so on upto 80-90 m depths. This shows the change in the resistivity pattern as an effect of lithological / hydrogeological changes. The Gondwana in the NE appears to be of low resistivity compared to Basaltic terrain. Even within the NE zone resistivity varies with depth e.g. resistivity around 25 Ωm at 0-5 m depth changed to around 80 Ωm at 10-15 m depth and reaches back to 25 Ωm at 20-25 m giving a layered model. The above themes are prepared with the sparse data network for Preliminary information only. Its full utilization has been done after SkyTEM survey to clearly demarcate the lithological and hydrogeological interfaces and units etc precisely.

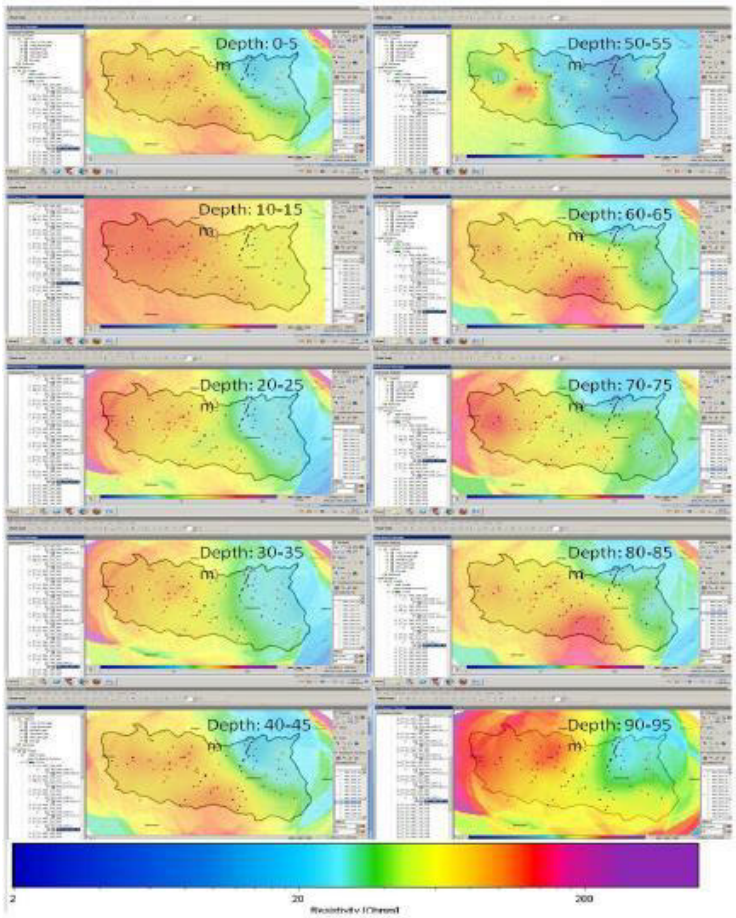

Fig 13: Mean resistivity maps at different depth, Chandrabhaga Watershed (WGKCC-2)

Heliborne Time Domain Electro Magnetic (SkyTEM)

Dual moment ensures high-resolution information from top to deeper level by means of low and high moments. Focus of the survey is to map the principal aquifers within intertrappeans, fractured vesicular/ amygdaloidal basalt and transition zone of Basalt-Gondwanas up to maximum 200 m depth. 189 km^2 (52%) area was covered among total study area of 360 km^2 for which permission was given buy the Nagpur airport, where in total 954-line km of data were acquired (Fig 14). The individual flight lines were closely spaced with only 200 m of separation and the average flight speed of the helicopter was 17 m/s with an average flight altitude (frame height) of 35 m above the ground.

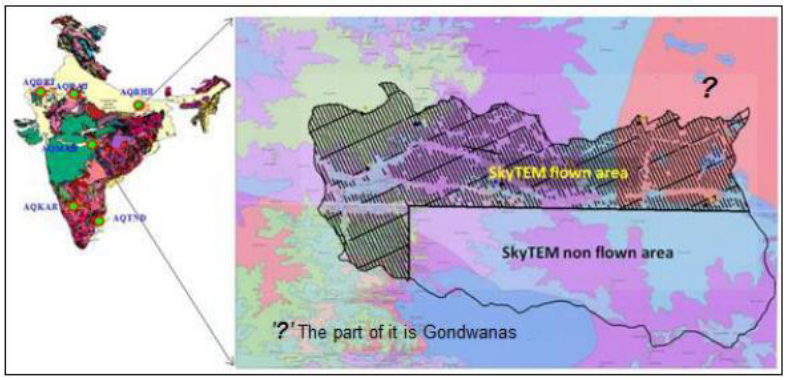

Fig.14: The survey area, the flight lines and tie are shown as black lines (NGRI, 2015)

The collected SkyTEM data were subsequently processed with state of the art processing schemes to remove couplings arising from roads and man-made installations such as iron pipes, buried cables and possibly also closed iron sheep fences. Latter the data were inverted with preliminary inversion to make sure all the coupled and noisy data had been removed, and furthermore to establish a suitable starting model for the entire survey area. The preliminary inversions thus suits as a quality check of the previous processing. Finally the data were inverted with a smooth model using the spatially constrained inversion (SCI) approach (NGRI, 2015).

To translate the geophysical results into the hydrogeological models following protocol was adopted:

a. SkyTEM results are calibrated against the drilling lithologs, ground and borehole geophysical results and then integrated lithological log at each borehole are prepared.
b. Equivalent litho-units of the integrated logs are converted into principal litho-units as proxy of principal aquifer and aquitard.
c. The principal lithologs are imported to the Arhus Workbench and incorporated with the individual sections prepared at each 2 km x 2 km grid line.
d. The principal litho-facies are interpolated and extrapolated along the SkyTEM sections using the calibrated resistivity values.
e. The principle lithological units are finally attributed into principal aquifers, confining layers and Basalt-Gondwana interface.

The integration of HeliTEM data base with ground geophysics and controlled points such as bore hole lithologs has been useful to derive the basaltic trap thickness (Fig 15) and Gondwana topography (Fig 16). To derive these thematic maps the study area have been made into grids of 2 km x 2 km size, then the vertical information available at the node of the grid has been considered for the interpolation. The thickness of lava flows (~400 m) in the NW part and its thinning towards SE of the study area.

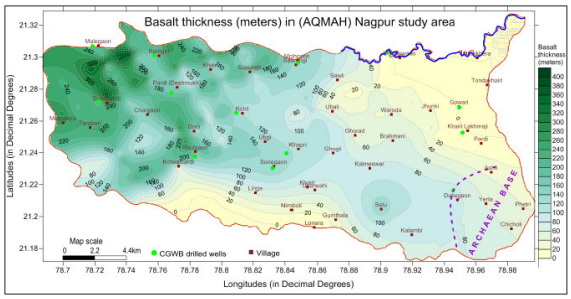

Fig. 15: Estimated basalt thickness derived from the HeliTEM and ground geophysical methods (NGRI, 2015)

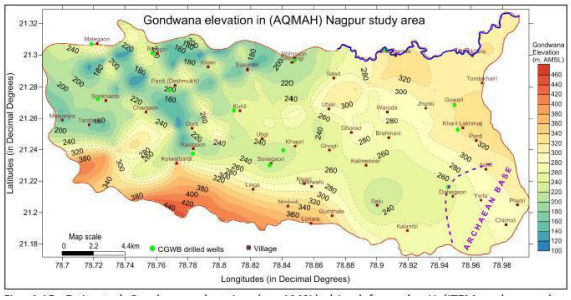

Fig. 16: Estimated Gondwana elevation (m amsl) derived from the HeliTEM and ground geophysical methods (NGRI, 2015)

3D map of Heli TEM sections has been generated (Fig 17) in W_E and SW-NE orientation to understand the basaltic flows directions and their extension on vertical and lateral scale. The W-E section shows individual flows in the west and their extension towards east their ending. Further, on the same section the vertical contact of between Basalt-Gondwana (B-G) has been clearly demarcated with distinct variations in the resistivity. The B-G contact can also be seen its smooth merging with the SW-NE Heli TEM section. The aquifer systems in basalts and Gondwanas and their extensions are also clearly demarcated in the 3D map (Fig. 17)

The performance matrix of various geophysical methods applied Chandrabhaga Watershed (WGKKC-2) is presented in Table 2.

The experiences gained from this study helps to develop a protocol to be adopted for aquifer mapping in the Country.

STEP 1: Acquiring Heli TEM and Heli MAG through Advance geophysical survey

STEP 2: Validation by ground geophysical, hydrogeological studies and exploratory drilling.

STEP 3: Data integration and interpretation for 3D aquifer model and characteristics.

Table 2: Performance Matrix of various geophysical methods applied in Pilot Aquifer mapping (AQMAH) in Chandrabhaga Watershed (WGKKC-2) (NGRI, 2015a)

Sl. No.	Hydrogeological Objective	Geophysical Objective	Performance of Geophysical Method used					
			Surface			Heliborne		Borehole logging
			VES	GRP	TEM	TEM	MAG	
1	Aquifers in weathered zone	Moderately resistive layers	1	NA	1	1	NA	1
2	Aquifers in vesicular and fractured zone	Moderately resistive layer underlying highly resistive (massive basalt) layer	4	NA	3	2	NA	1
3		Geological structures	5	NA	5	3	1	NA
4	Basalt-Gondwana contact	Deeper moderately resistive (Gondwana sandstone) layer	3	NA	4	3	NA	1
5	Mmaximum depth 200m		Depth of investigation depends on subsurface resistivity distribution			NA	NA	NA
Where Index on 5-point Scale is 1: Excellent, 2: Very Good, 3: Good, 4: Fair, 5: Poor, NA: Not Applicable								

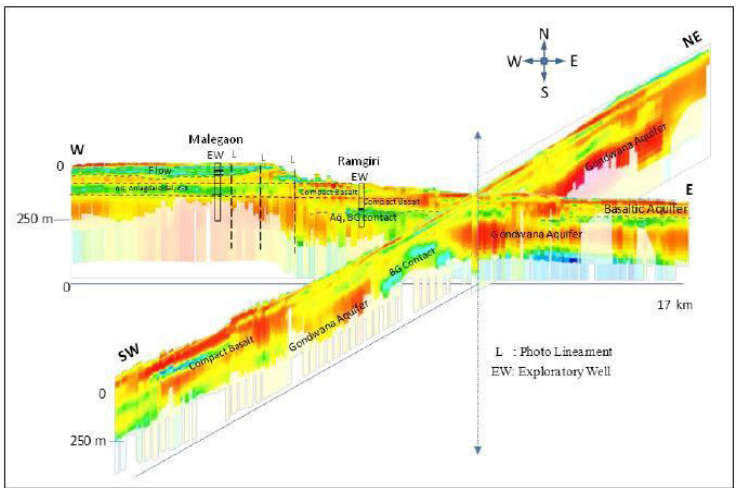

Fig 17: 3D map showing the Heli TEM sections of the AQMAH study area, Nagpur, (NGRI, 2015b).

CONCLUSIONS

Based on the ground water exploration and geophysical surveys the aquifer geometry have been defined, and existing aquifers are categorized into shallow and deeper aquifer in Basaltic formation, Sandstone (Gondwana) formation and in Trap covered Sandstone (Gondwana) [TCG] formation. Besides the traditional geophysical techniques, advanced geophysical techniques viz., Electrical Resistivity Tomography (ERT), Ground Transient Electromagnetic (TEM) and SkyTEM (Time-domain heli-borne electromagnetic system) methods have also been applied to delineate the aquifer system up to 200m depth. These techniques have been used first time in basaltic terrain. These new techniques are rapid, time saving, and found very effective for covering larger and inaccessible area with closed spaced data, but unable to delineate the various basaltic flows occurring below the ground level. North-eastern part of the watershed is extensively covered by rocks of Gondwana Supergroup comprises of Kamthi Sandstone and Shales. The central part is consisting of Trap Covered Gondwana Formation where the thickness of traps ranges from 62.00 m bgl (Waroda) to 195.00 mbgl (Sonkhamb). Towards extreme south-eastern part, Archaean gneisses occur below the traps (Dahegaon), whereas towards the extreme western part of the watershed thickness of the Deccan trap is observed more than 200 mbgl. Based on the VES results, it is inferred that the resistivities ranging from 16 to 87 Ωm represent the aquifer zone in the Gondwana formations, whereas the resistivities ranging from 7 to 40 Ωm represent the aquifer zone in the Deccan Trap formations. However, in the Archaean formations, the fractured Gneiss has been delineated with 12 Ωm resistivity, at only one VES location. The VLF, GRP followed by VES inferred the location and orientation of the fractures/ lineaments in the area while Geophysical logging infers that the thickness of the top basaltic formation is increasing from east (59 m at the village Yerla,) to west (145m at Raulgaon in the SW of the study area and 127 m at Ramgiri in the NW of the study area). The Trap-Gondwana contact and Trap-Gneiss contact were clearly demarcated Very thin layers of clay/bole beds and fractured zones were resolved with high accuracy from Gamma Log. ERT shows significant signatures of structural controls like lineaments and layered nature of flows, but difficult to distinguish between two successive lava flows. The findings from TEM and VES are found complementing each other. Heliborne Transient Electromagnetic investigation has revealed fascinating results on the aquifer systems and its spatial characteristics covering Gondwana, Trap covered Gondwana and Trap covered Gneiss formations in the study area. The integration of Heli-TEM data with ground geophysics and controlled points such as borehole lithologs has been useful to derive the basaltic trap thickness. The integrated interpretation of various geophysical parameters clearly indicates the relative efficacy of Heli-TEM survey with more resolution in demarcating the fractures in amygdaloidal and massive basalts, inter-trappean and Basalt-Gondwana vertical boundary which are the potential aquifers. However, the SkyTEM data fails to identify or demarcate red/grey/green bole layer of significant thickness. The present study helps to develop a protocol of advanced geophysical studies to be adopted for aquifer mapping in the Country.

ACKNOWLEDGEMENTS

This work is a part of 'Pilot Aquifer Mapping' programme of Central Ground Water Board, Central Region Nagpur, Maharashtra, India. Authors are thankful to the Chairman, CGWB, Faridabad and the Regional Director, CGWB, Nagpur for permitting to compile and publish the work. Thanks to all the officers of CGWB, Nagpur and NGRI, Hyderabad for their contribution during the fieldwork. Thanks to all the crew members of drilling rig units, Division-VI, CGWB, Nagpur engaged during the drilling operations.

REFERENCES:

CGWB (2012), Hydrogeology of Maharashtra, Central Ground Water Board, Central Region, Nagpur, Ministry of Water Resources, Govt. of India, Report No.1705/STT/2012, 149p.

CGWB (2013), Hydrogeology and Ground Water Development Prospects of Vidarbha Region, Maharashtra. Central Ground Water Board, Central Region, Nagpur, Ministry of Water Resources, Govt. of India, 1784/OTH/2013, 87p.

CGWB (2015a), Report on Pilot Aquifer Mapping in Chandrabhaga Watershed (WGKKC-2), Nagpur district, Maharashtra, Central Ground Water Board, Central Region, Nagpur, Report No. 1892/NQM/2015. 244Pg.

CGWB (2015b), Consolidated final report on Pilot project on aquifer mapping, Central Ground Water Board, Central Headquarters, Faridabad. July 2015. 200Pg.

David V. Fitterman and Mark T. Stewart (1986), Transient electromagnetic sounding for Ground water, Geophysics, Volume 51, Issue 4, Apr 1, 1986.

NGRI (2013), Aquifer Characterization using Advanced Geophysical Techniques in Representative Geological Terrains of India, 'Interim Report on AQMAH', Sponsored by CGWB-MoWR, Govt. of India under HP-II project funded by Word Bank, CSIR-National Geophysical Research Institute, June 2013, p25.

NGRI (2015a), Aquifer Characterization using Advanced Geophysical Techniques in Representative Geological Terrains of India, 'Heliborne geophysical investigation in India: an innovative accomplishment in 3d aquifer mapping', Sponsored by CGWB-MoWR, Govt. of India under HP-II project funded by Word Bank, CSIR-National Geophysical Research Institute, March 2015, p50.

NGRI (2015b), Aquifer Characterization using Advanced Geophysical Techniques in Representative Geological Terrains of India, 'AQUIM-Final Report, AQMAH, Nagpur District, Maharashtra', Sponsored by CGWB-MoWR, Govt. of India under HP-II project funded by Word Bank, CSIR-National Geophysical Research Institute, March 2015, p50.

Ramakrishna T.S., M S V Rama Rao, K V S Bhaskara Rao, and D V Punekar (1999), Geophysical Study of the Gondwana Basin of Eastern Maharashtra, Geological Survey of India Technical report, Special Publication No. 47, December 1999.

Ratnakumari, Y, Rai, S. N, Thiagarajan, S and Dewashish Kumar(2012), 2D Electrical resistivity imaging for delineation of deeper aquifers in a part of the Chandrabhaga river basin, Nagpur District, Maharashtra, India, Current Science, Vol. 102, No. 1, 10 January 2012.

Torleif Dahlin (2001), The development of DC resistivity imaging techniques Computers & Geosciences Volume 27, Issue 9, 1 November 2001, Pages 1019-1029.

Bhujal News, 30(1-4):33-49

Uranium, heavy metals and fluoride co-occurrence in Groundwater of Kamrup Metropolitan district of Assam, India

Snigdha Dutta[1], Rinkumoni Barman[1], Dakshina Rabha[1], Rishi Raj[2] and Keisham Radhapyari[1*]

[1]Central Ground Water Board, North Eastern Region, Guwahati, Assam,
[2]Central Ground Water Board, North Western Region, Chandigarh, Punjab
[*]Corresponding author- email- k.radhapyari@assam.gov.in

ABSTRACT

Groundwater is very vital to human life. An attempt has been made in the study to investigate the presence of uranium, heavy metals, and fluoride co-occurrence in groundwater of Kamrup Metropolitan district of Assam, India. Groundwater samples were collected from 27 locations and analysed for pH, EC, TH, TA, Turbidity, major cations (Ca2+, Mg2+, Na+, K+), major anions (F-, Cl-, HCO3-, SO42-, NO3-), heavy metals (As, Fe, Cd, Ag, Mn, Cr, Cu, Ni, Pb, Se, Zn, Al) and radioactive uranium using standard procedure. Uranium and heavy metals were quantified using a sophisticated Inductively Coupled Plasma Mass Spectrometer. The concentration of Fe and Mn was found to exceed the permissible limits while the concentration of Al was found to exceed the acceptable limit of BIS drinking water specifications. The concentration of Fe and Mn exceeded the drinking water permissible limit in 33% and 48% GW samples respectively. Uranium concentration was found within the prescribed safe limits of WHO guidelines. Data were also evaluated statistically to find the distribution pattern for each parameter and to establish a correlation of uranium with fluoride and heavy metals. Uranium distribution shows an asymmetric pattern and a positive correlation with fluoride, Cr, Se, and negative correlation with other heavy metals. Low uranium content in the groundwater of Kamrup Metropolitan district may be attributed to the low content of uranium in the aquifer rocks and the absence of industrial and mining activities in the region. Though the drinking water in Kamrup Metropolitan district is safe with regard to uranium occurrence, continuous monitoring is, however, needed for constituents like fluoride, Fe, Mn, As, Al, etc.

Keywords: Uranium, heavy metals, fluoride, co-occurrence, GW, Kamrup metropolitan district.

1. Introduction

In groundwater (GW) studies, water quality is as important as its quantity. When the utility of surface water and GW is compared, GW usage is more popular owing to its easy availability and its natural quality that can be sufficiently used for potable purposes without or little treatment. It has been reported that about 50% people in rural area and 80% in urban area are dependent on GW (Bhattacharya et al., 2017). The assessment of water quality by chemical parameters plays a vital role in classifying water suitability for various purposes. The hydrogeochemical processes occurring in the aquifer system affect the concentrations of the dissolved ions in GW (Kumar et al., 2011). The chemistry of recharging water, water–aquifer matrix interaction, cation exchange processes, and GW residence time within the aquifers are considered as the key dynamic factors for the hydrogeochemical evolution of GW (Drever 1997). Hence, the mechanisms of GW evolution in an aquifer system are explained by the ionic ratios, individual or paired ionic concentrations that are supportive in the calculation of certain indices (like Residual Sodium Carbonate which gives an idea of alkali hazards). Therefore, a detailed study of the chemical composition of GW is essential for assessing the suitability of water for various needs.Besides the major cations and anions, the presence of heavy metals in GW may also affect the water quality. Heavy metals in GW are either of geogenic or anthropogenic in origin. Most of the metals play vital roles in the human body provided they are present within the permissible limits as specified by various agencies. Heavy metals in GW beyond these limits are detrimental and pose a potential long-term toxicological effect on human and ecosystem health (Singh et al., 2010; Marschner 1995; Bruins 2000). The Study of heavy metal contamination in GW is of utmost importance because of

their low biodegradability, accumulation in the food chain and toxic effects (Nurnberg 1982; Ramesh et al., 1995). Distribution of metals in dissolved and particulate phase, gain size sorting of sediments, porosity, conductivity, and other aquifer characteristics are some of the main factors that determine the metal content in GW (Gogoi et al., 2016; Sauvé et al., 2000). In addition to diversified geological processes and complex tectonic formations, anthropogenic activities also play a vital role in ground water contamination, especially in urban areas. Industrial waste, mine waste, waste water, (Gautam et al., 2013) land use/land cover change (Narsimlu et al., 2015; Kumar et al., 2017), atmospheric pollutants, fertilizer applications (Amin et al., 2014; Singh et al., 2017) are the main anthropogenic contributors of metals discharged into water bodies.

Recently radioactive elements like uranium (U) and radon are also being reported in GW of India (Bajwa et al., 2017; Dash et al., 2017; Prakash et al., 2020; Malyan et al., 2019). The first report on the presence of U in GW in India was published in 1995 by Guru Nanak Dev University, Amritsar, Punjab (Times of India, 2010). WHO (2005) and US EPA (September 17, 2013) set the recommended guideline for U in drinking water to be 0.03 mg/L(30 ppb) as the maximum contaminant level (MCL). The three primary U ore minerals are uraninite (UO_2), pitchblende (U_3O_8) and davidite (Fe, Ce, U)$_2$(Ti, Fe, V, Cr)$_5O_{12}$). Leaching of U from sediments to GW is a key process causing geogenic contamination. U enrichment for nuclear fuels and weapons, mining, and milling of U, phosphate fertilizer production from phosphate rocks having U are some of the main anthropogenic sources that cause GW contamination by U (WHO 2012). Dash et al., 2017 reported that redistribution of U and its radionuclide into GW takes place from soil to rocks and governed by several factors like, soil pH, rock matrix, leaching capacity of the soil, water redox state, and concentration of fluoride, phosphate, calcium, carbonate, and potassium. Hakonson-Hayes et al., 2002 stated that radiological hazards and chemotoxic hazards are the twofold human health risks associated with U exposure. A study by Coyte, et al., 2018 has linked higher chronic kidney disease (CKD) in India to presence of U in drinking water.

Overall Assam has suitable drinking water quality considering the major solutes and heavy elements. However, occurrence of fluoride, Fe and As in GW systems were reported in some regions of the Brahmaputra River valley (Das et al., 2003; Singh 2006; Tamuli et al., 2017) GW of the aquifers in Brahmaputra floodplain are arsenic enriched to certain extent (Verma et al., 2015) and this is because much of the sediments of various provenances are reworked, adulterated, mixed and re-deposited that eventually became part of the original aquifers, during higher stage of the Brahmaputra. It is also reported that GW of Assam valleys is highly ferruginous (Aowal 1981). Assam Science Technology and Environmental Council (ASTEC) published a report wherein it is mentioned that the occurrence of Fe along the banks of the Brahmaputra shows high level of concentration in the shallow GW. Testing of water samples done by Central Ground Water Board, NER, surveys conducted by North Eastern Regional Institute of Water and Land Management (NERIWALM, 2004) and State Public Health Engineering Department (PHED) showed that some districts in Assam have higher levels of concentration of As, fluoride and Fe in GW than the permissible limit of BIS. Since there is hardly an aquifer enriched with a single contaminant, co-occurrences of As and fluoride together, or with other metal in GW of the tropical floodplains of the Brahmaputra have recently been discussed (Das et al., 2016 and 2018; Kumar et al., 2016). The drinking water sources of Kamrup, Assam were found to be contaminated with Fe, As, Cd, Mn, and Pb and other heavy metals as reported in many publications (Chakrabarty and Sarma, 2011; Lahkar, and Bhattacharyya, 2019; Radhapyari et al., 2017). The permissible limits, sources, potential health hazards posed by some of the probable contaminants common in groundwater of Kamrup (Metro) are presented in **Table 1** along with their remedial measures. The current study is aimed to provide an insight into the quality and the hydrochemical processes of GW in Kamrup metropolitan (Metro) district, Assam with special reference to the occurrence of radioactive uranium and common heavy metals (As, Fe, Cd, Ag, Mn, Cr, Cu, Ni, Pb, Se, Zn, Al) analysed by Inductively coupled plasma Mass spectrometer (ICP-MS). An attempt is made to evaluate the data statistically to find the distribution pattern for each parameter and to establish a correlation of uranium with fluoride and heavy metals viz. As, Fe, Cd, Ag, Mn, Cr, Cu, Ni, Pb, Se, Zn, Al). This study would give a comprehensive

view and provide baseline data on the GW quality and its suitability for drinking purposes. Additionally, attempts are also made to evaluate possible interrelationships between the occurrence of uranium and major contaminants.

Table 1: Permissible limits, sources, health hazards and remedial methods for some of the potential contaminants of GW of Kamrup (Metro).

Pollutant	BIS Permissible limit (mg/L)/WHO for U (mg/L)	Sources to GW	Potential health hazard	Treatment techniques	References
Fluoride	1.50	Geogenic process, volcanic ash, fertilizers, aluminium smelting, ceramic firing	Acute to chronic dental and skeletal fluorosis, deformities in RBCs, gastrointestinal problems	Adsorbents (activated charcoal, activated alumina, red mud, kaolinite), ion-exchange, reverse osmosis process	Chauhan et al., 2007; Kemer et al. 2009
Iron	0.30	Dissolution of iron-bearing minerals, reduction of iron-oxyhydroxides (FeOOH) in sediments	Haemochromatosis, high serum ferritin, heart disease, cancer, kidney problems	Complete aeration and filtration with pH adjustment, ozonation, chelation, water softner using cation exchanger, zeolite	Rdiagojevich and Whitkar, 1999
Arsenic	0.01	The geogenic process, pesticides, industrial waste, smelting of Cu, Zn ore, geothermal drilling	Arsenicosis, toxicity of the liver and kidney damage which may result in carcinogenicity	Minerals (clays, iron oxides, hydroxylapatite, and struvite, biosorbents (cellulose, chitosan/chitin, alginate, biochar, microalgal, and fungal biomas, tea fungus (zygosaccharomyces sp. and acetobacter sp.) through biosorption, electrocoagulation with Fe electrodes	Asere et al., 2019; Kumar et al., 2004; Murugesan et al., 2006
Manganese	0.30	In river sediments, degradation of algae and other acquatic biota, dissolution of calcite	Intellectual impairment in children, irreversible neurological syndrome like Parkinson's disease, DNA damage and chromosome aberrations	Powdered or granular activated carbon, catalytic oxidative removal, oxidizing and magnetotactic bacteria	Akl et al., 2013; Cheng et al., 2019; Du et al., 2017; Wasserman et al., 2004
Uranium	0.03	From sediments, nuclear power plants, mines	Nephrotoxicity, may cause cancer	Polyethyleneimine modified activated carbon, nano-magnetic iron oxide-urea activated carbon nanolayer sorbent, nanostructure binary iron manganese oxy-hydroxides	Dimiropoulos et al., 2015; Mahmoud et al., 2017; Saleh et al., 2017

2. Materials and methods

2.1 Study Area

Kamrup (Metro), Assam (**Fig. 1**) is situated at the southern bank of the mighty Brahmaputra River. The foothills of Shillong plateau is positioned on the opposite side. It is located between the latitudes of 26º10'20" N and longitude of 91º44'45" E and spread over an area of about 328 km^2. Bharalu River, Deepor Beel, Sola Beel are the major water bodies located here. Kamrup (Metropolitan district) has recorded a population of about 1.0 million at a decadal growth rate of 19% as per 2011 Government of India census. Its altitude varies from 50 to 680m above mean sea level. The major water bearing formation underlying Kamrup (Metro) is alluvial sediment. A large portion is covered by granitic gneisses with lenticular bands of amphibolite, biotite granulite, biotite schist. Isolated occurrences of hornblende-diorite belonging to the Archaean Gneissic Complex are also found. All the rock types are traversed by numerous veins and veinlets of quartz, pegmatite and aplite. It has been described that except for a few city dwellers, every house of Kamrup (Metro) has atleast one tube well or dug well, proving their dependency on GW. About 40% of the people have the facility of municipal supply water but the majority of the population use only GW for domestic as well as industrial purposes (Chakrabarty and Sarma, 2011). The main mode of recharge is rainfall as there is a direct rise of the water table in response to precipitation. Its average rainfall is ~ 1700 mm and the annual rainfall ranges from 1500 mm to 2600 mm (Goswami and Rabha).

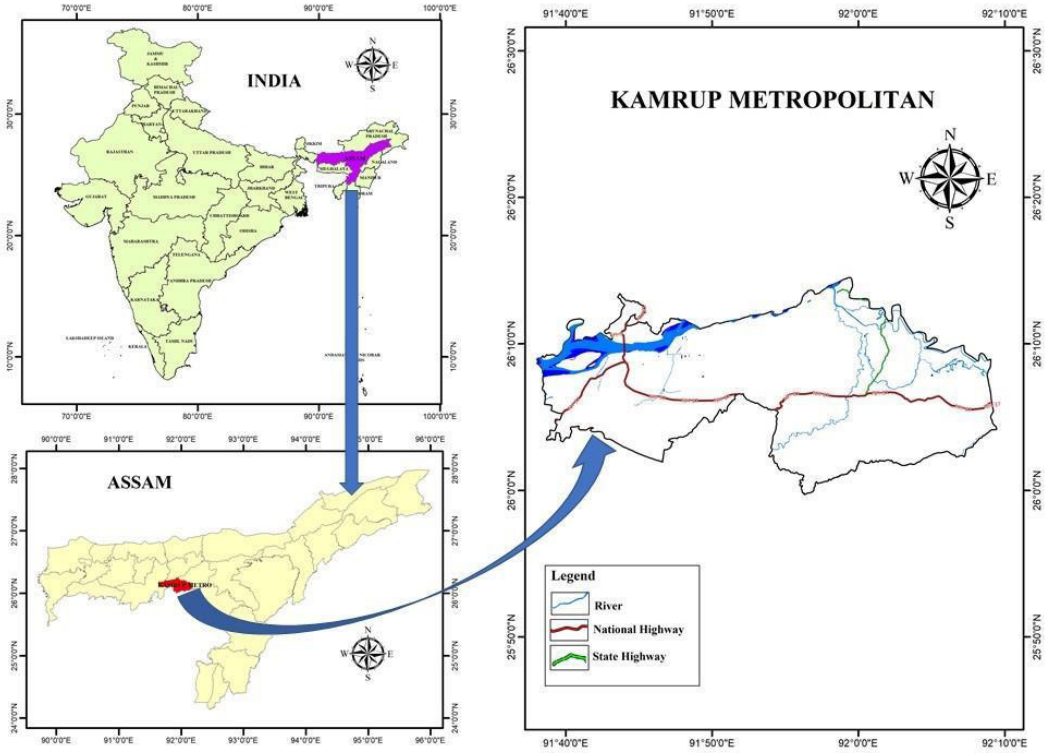

Fig. 1. Map location of Kamrup Metropolitan district, Assam, India

2.2 Sampling

The GW samples were collected from 27 locations across Kamrup (Metro) during the month of January 2020 and listed in **Table 2**. The samples chosen for the study are representative of land use areas viz. residential (Kotabari), industrial (Noonmati, near IOCL), commercial (Lokhra), institutional (Panbazar) and forest (Basistha forest office, Wildlife Sanctuary). American Public Health Association (APHA 2012) guidelines and their standard procedures were strictly followed for sampling, storing, transferring and analysis of all the parameters. Our samples were collected in high density polyethylene bottles (HDPE) for the analysis of major cations and anions in 1000 mL without acidification.

Sampling for U and other heavy metal analysis was done in 60 mL HDPE bottles. Utmost care was taken to avoid interference from air headspace while sampling and storage.U and heavy metal samples were filtered by 0.45 μm membrane on-site before filling into the bottles. A syringe filtration unit technique was used. These samples were acidified by 0.5 mL heavy elemental grade HNO_3 immediately after filtration. They were immediately closed, labeled, stored and transported in ice box with ice pads maintaining a temperature ≤4ºC.

Table 2: List of sampling points in Kamrup (Metro) district with coordinates.

Sl. No.	Location	Latitude	Longitude	Type of sample	Sample code number
1	Adagodown, Sawkuchi	26°08'18"	91°44'29"	Tube Well	C1
2	Basistha Forest Office	26°06'07"	91°47'08"	Tube Well	C2
3	Biswakarma temple Maligaon	26°09'54"	91°43'00"	Dug Well	C3
4	Dhalbama	26°06'16"	91°42'53"	Tube Well	C4
5	Dhirgeshwari near Kali Mandir	26°11'43"	91°45'41"	Tube Well	C5
6	Garchuk	26°06'58"	91°42'59"	Tube Well	C6
7	Ghoramara	26°10'58"	91°42'40"	Tube Well	C7
8	Hazambari	26°13'03"	91°53'29"	Tube Well	C8
9	Khaloibari	26°06'50"	92°03'41"	Tube Well	C9
10	Kharguli	26°11'49"	91°46'06"	Supply Water	C10
11	Kotabari	27°07'48"	91°43'38"	Tube Well	C11
12	Lokhra	26°06'28"	91°44'59"	Tube Well	C12
13	Maligaon Railway Colony	26°09'32"	91°41'52"	Dug Well	C13
14	Nalapara	26°06'49"	91°45'38"	Tube Well	C14
15	Narengi Forest Gate	26°10'42"	91°49'21"	Tube Well	C15
16	Noonmati	26°11'13"	91°48'08"	Tube Well	C16
17	Noonmati (near IOCL)	26°11'26"	91°47'56"	Tube Well	C17
18	Panbazar (Chief Justice)	26°11'25"	91°44'56"	Tube Well	C18
19	Pandu Port	26°10'11"	91°40'52"	Dug Well	C19
20	Panikhaiti	26°12'51"	91°52'48"	Tube Well	C20
21	Patharquery	26°09'58"	91°49'28"	Tube Well	C21
22	Patorkuchi	26°07'02"	91°53'51"	Tube Well	C22
23	Radhagobinda Borah Nagar	26°12'06"	91°47'44"	Tube Well	C23
24	Sawkuchi	26°07'18"	91°44'41"	Tube Well	C24
25	Senabor	26°06'59"	92°05'28"	Tube Well	C25
26	Shiv Mandir (Deepor Beel)	26°06'45"	91°39'37"	Tube Well	C26
27	Wildlife Sanctuary	26°06'46"	91°39'19"	Tube Well	C27

2.3 Instrument

Inductively coupled plasma mass spectrometry (Thermo Scientific, iCAP Q ICP-MS) was employed for the determination of U isotopes and other metals viz. Al, Cr, Mn, Fe, Ni, Cu, Zn, As, Se, Ag, Cd and Pb in GW with a detection limit as low as 0.1 - 1ng. The instrument can complete a single measurement within 60s which includes uptake, data acquisition, and washout. Hence this instrument was validated for use against Revision 5.4 of the US EPA Method 200.8 (Henry and Wills, 2012). The instrument was operated in standard (non-collision cell) mode. The sample introduction system consisted of a Peltier cooled (3ºC), baffled quartz cyclonic spray chamber, PFA-ST nebulizer and quartz torch. Calibration curves for all elements analyzed were constructed by plotting the ratio of the intensity vs. concentration of the analyte (in ppb or mg/L considering the permissible limit), and results showed that the calibration curves are linear with a correlation coefficient (R^2) ~ 0.993-1.000 for U and HM. For NO_3^- and SO_4^{2-} analysis UV-Visible spectrophotometer (Labindia, UV-3200) was used with the quartz cuvette for sample placing. The λ_{max} was set at 220 nm for NO_3^- and 420 nm for SO_4^{2-} analysis and their corresponding standard graphs were plotted. The data were collected and analyzed with Labindia UVwin software. Water quality parameters like pH, electrical conductivity, TDS, turbidity was measured by pH-meter, conductivity meter and nephalo-turbidity meter respectively. Na and K were analyzed using flame photometer (Systronics FP128). Fluoride analysis was done by using ion-meter (Oakton Ion 700) and alkalinity, hardness and chloride were analyzed by titrimetric methods.

2.4 Analysis

The regular ions were analyzed in Regional Chemical Laboratory, CGWB, NER while uranium and other heavy metals were tested at CGWB, NWR, Chandigarh, Punjab. APHA 2012 standard procedures were followed for testing of each analyte. For ensuring precise and reliable results several QA/QC protocols were implemented viz. use of National Institute of Standards and Technology (NIST) certified standard reference materials (152410K for $CaCO_3$, 152405N for Na_2CO_3 and 152406R for NaCl), reagent blank run with each sample batch, carrying out retest and repeat analyses, use of at least five standard solutions for generation of calibration curve for each chemical analyte.

3. Results and Discussion

3.1 General hydrochemical processes

A total of 29 constituents including major cations, anions, heavy metals and radioactive uranium (U) have been investigated. Graphical representation of cations-anions (Fig. 2a**)** and heavy metals (Fig. 2b, Fig.3) shows the distribution of possible contaminants in Kamrup (Metro) districts. BIS drinking water specification, IS 10500-2012 (BIS 2012) and WHO guidelines (WHO, 2012) were referred for the interpretation of the data. pH in GW sample of Dhirgeshwari (near Kali Mandir) (8.57), Ghoramora (8.66) and Nalapara (6.39) were not within the BIS acceptable range 6.5-8.5. Turbidity and TDS value are well within the BIS drinking water guideline. The total alkalinity ranged from 40.03 to 315.25 mg/L while total hardness which is characterized by contents of Ca and Mg salts has ranged between 40 and 280 mg/L. As such Ca^{2+} and Mg^{2+} concentrations are within the prescribed limit. Other ions like Cl^-, SO_4^{2-}, NO_3^-, Na^+ and K^+ are also within the safe limits. Highest fluoride concentration observed was 2.00 mg/L in Dhirgeshwari (near Kali Mandir). This is the only location where the fluoride concentration in GW has exceeded the acceptable limit of 1.0 mg/L, while all other locations have fluoride well below the prescribed limit. This is just a case of fluoride occurrence in an isolated pocket. Fluoride release into GW is mostly favored under drier conditions where GW recharge appears to be low and the rock-water interaction is high (Das et al., 2016) which is further supported by Gibbs plot (Fig. 4) (Gibbs, 1970) revealing the geogenic origin where rock-water interaction is the dominant factor responsible for the GW chemistry.

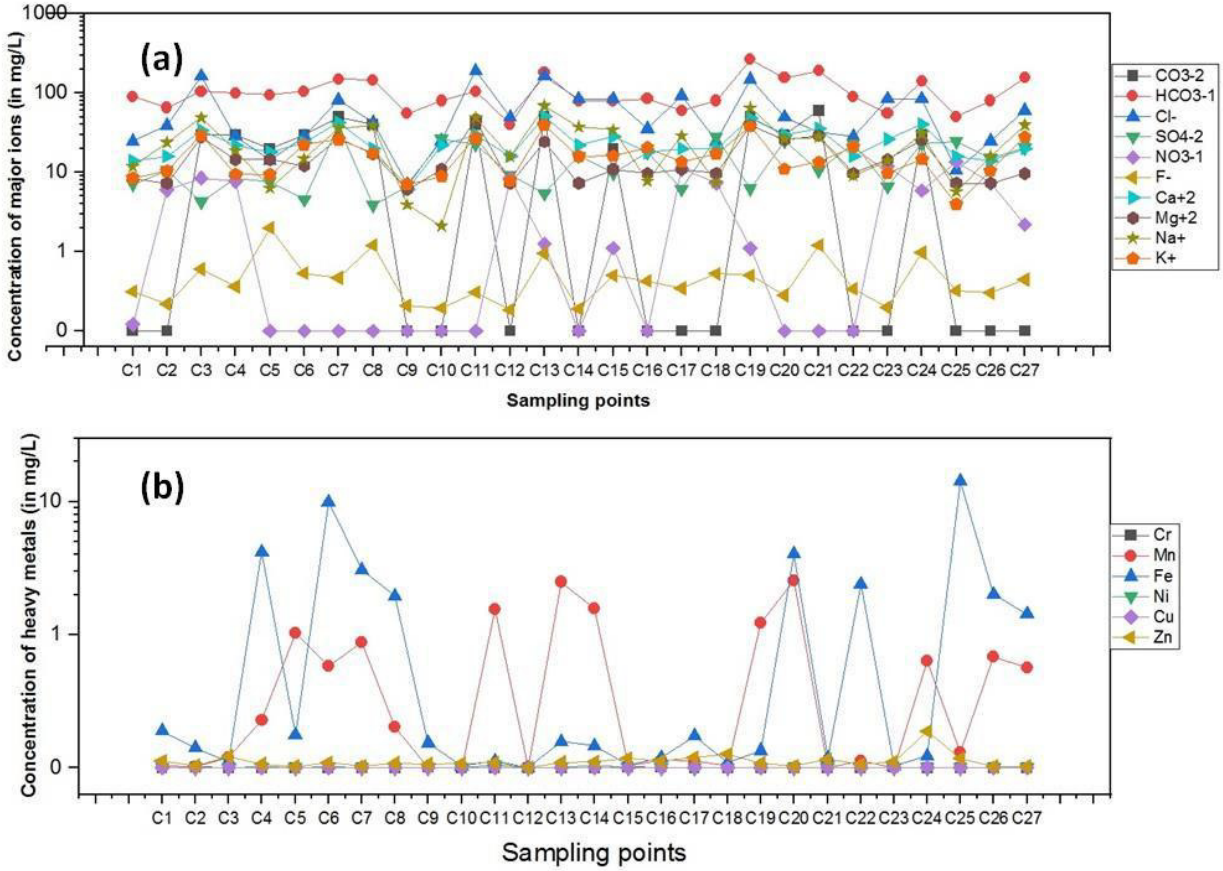

Fig. 2 (a) Graphical representation of cations-anions; (**b)** heavy metals (Cr, Mn, Fe, Ni, Cu, Zn) distribution in GW of Kamrup (Metro), Assam.

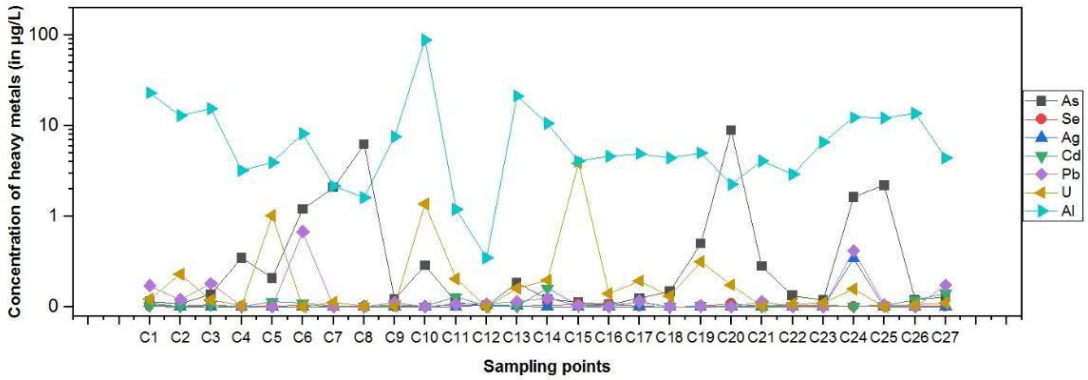

Fig.3 Graphical representation of heavy metals (As, Se, Ag, Cd, Pd, U, Al) distribution in GW of Kamrup (Metro), Assam

The milli-equivalent percentage (meq%) of major cations and anions is plotted using Piper linear plot (Piper 1944) to assess the hydrogeochemical facies and types of water (Fig 5). Piper plot depicts that Ca-Mg-Cl and Ca-HCO_3 type is prominent in the study area which indicates the predominance of geogenic impact in the major ions. The descriptive statistics of concentrations for the studied physicochemical parameters is shown in **Table 3**

Table 3. Descriptive statistics of concentrations for the studied physicochemical parameters

Parameters	Mean	Min	Max	Median	Std. deviation	IQR	Skewness	Kurtosis
pH	7.76	6.39	8.66	7.85	-0.71	1.25	-0.23	-1.59
EC (in µs/cm) @ 25ºC	344.62	85.83	813.10	291.90	-192.22	231.00	1.05	0.18
Turbidity (in NTU)	0.20	0.10	0.40	0.15	-0.12	0.20	0.67	-1.20
TDS (mg/L)	175.38	43.92	416.50	148.20	-98.18	118.60	1.06	0.20
CO_3^{2-} (mg/L)	36.92	20.00	60.00	30.00	-12.51	20.00	0.39	-0.84
HCO_3^- (mg/L)	106.77	40.03	265.25	90.07	-51.27	62.58	1.33	2.10
TA (as $CaCO_3$) (mg/L)	124.54	40.03	315.25	100.08	-68.69	82.57	1.08	0.85
Cl^- (mg/L)	63.15	7.09	191.43	42.54	-51.07	58.49	1.23	0.64
SO_4^{2-} (mg/L)	14.72	3.87	38.75	10.61	-9.86	16.22	0.84	-0.27
NO_3^- (mg/L)	6.21	0.08	13.57	7.29	-4.26	6.71	0.03	-1.04
F^- (mg/L)	0.66	0.27	2.00	0.56	-0.37	0.26	2.01	5.58
Ca^{2+} (mg/L)	24.76	6.00	50.04	22.02	-10.89	13.01	0.87	0.23
Mg^{2+} (mg/L)	16.26	6.07	46.10	10.91	-10.55	15.76	1.35	1.25
TH (as $CaCO_3$) (mg/L)	128.89	40.00	280.00	105.00	-66.96	107.50	0.93	-0.34
Na^+ (mg/L)	25.52	2.11	68.91	23.90	-18.24	26.15	0.80	0.07
K^+ (mg/L)	17.11	3.97	39.84	15.50	-9.38	11.64	1.00	0.43
Cr (mg/L)	0.001	0.0001	0.008	0.001	-0.002	0.001	2.384	5.633
Mn (mg/L)	0.578	0.0001	2.542	0.118	-0.753	0.877	1.422	1.411
Fe (mg/L)	1.678	0.001	14.186	0.187	-3.307	1.923	2.862	8.539
Ni (mg/L)	0.003	0.001	0.018	0.001	-0.006	0.003	2.874	7.634
Cu (mg/L)	0.001	0.001	0.004	0.001	-0.001	0.001	2.865	7.463
Zn (mg/L)	0.049	0.001	0.273	0.037	-0.052	0.036	3.360	14.148
Al (µg/L)	10.424	0.540	88.196	4.928	-16.643	8.653	4.215	19.785
As (µg/L)	0.969	0.011	8.905	0.137	-2.033	0.544	3.149	10.077
Se (µg/L)	0.011	0.001	0.034	0.010	-0.008	0.009	1.192	1.423
Ag (µg/L)	0.123	0.001	0.536	0.022	-0.232	0.038	2.205	4.886
Cd (µg/L)	0.033	0.002	0.202	0.013	-0.049	0.027	2.360	5.427
Pb (µg/L)	0.159	0.008	0.831	0.059	-0.231	0.204	2.189	4.379
U (µg/L)	0.358	0.001	3.877	0.103	-0.786	0.270	3.961	17.228

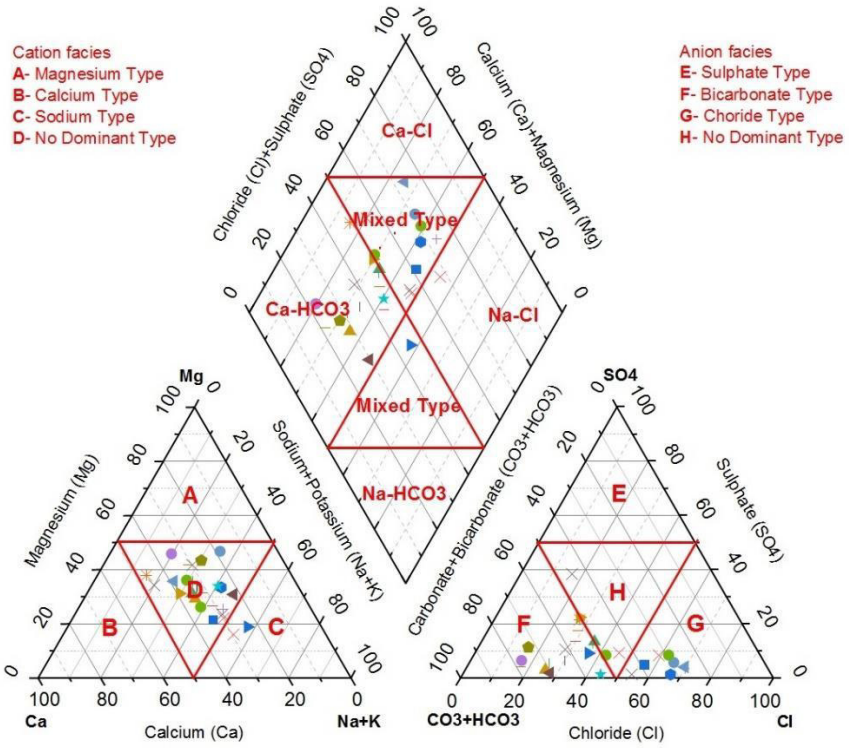

Fig. 4 Piper diagram characterizing the hydrogeochemical facies in ground water of Kamrup (Metro), Assam.

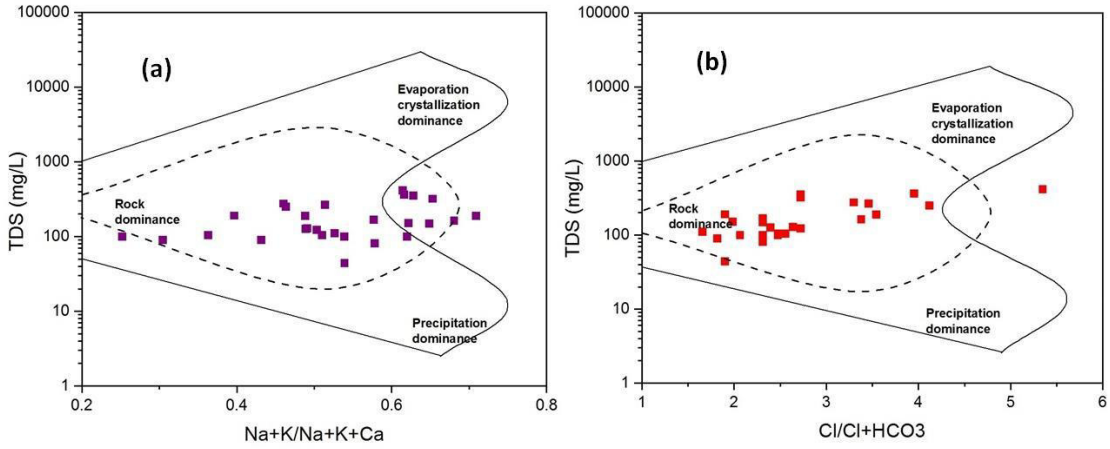

Fig. 5 Gibbs diagram showing the weight ratio of cations as a function of TDS and anions as a function of TDS in samples of ground water of Kamrup (Metro), Assam.

3.2 Uranium, heavy metal and fluoride co-occurrence

Fig. 6a and 6b illustrate the U and Al distribution in the sampling points of Kamrup (Metro) district respectively. The Uranium (U) levels in GW of all locations are within the WHO recommended limit of 0.03 mg/L. The highest U concentration recorded is 0.0038 mg/L in Narengi forest gate. No major mining sites are located in these sampling points, so seepage of acid mine water and surface runoff tailings into shallow aquifers are ruled out. The reducing environment in the flood deposits of Kamrup (Metro) causes an increase in UO_2^+(V) which is unstable and disproportionate. It was reported by Nicolli et al. (1989) that in alkali metal water types there is a higher concentration of U. From the analysis of Na and K the levels of these analytes are very less and the GW of the locations do not fall under the category of alkali metal water, this itself explains the low concentration of U in the GW. Furthermore, the average Al of the study area is 10.424 (ppb) and it varies from a minimum of 0.540 ppb to a maximum of 88.196 ppb, which is recorded at Kharghuli.

The maximum As concentration in GW is 8.9 ppb from the sampling point in Panikhaiti which is below BIS permissible limit of 10 ppb. Since most of the pH was recorded towards the alkaline end, such elevation in pH may exceed the point of zero charge (PZC) for observing desorption of the Fe-oxide/hydroxides, while bicarbonates and other anions compete with As oxyanions for adsorption to positively charged sites on sediment particles as proposed by Smedley and Kinniburgh, 2002. Desorptive co-release of As and fluoride from Fe-oxide/hydroxide is attributed to their co-occurrence. PH-induced desorption can favor co-occurrence in isolated oxidized aquifers which are drier with less recharge.

Mn concentration in 48% of samples are higher than BIS permissible limit of 0.3 mg/L, the highest being 2.54 mg/L. In deeper wells Mn content in GW is significant where rock-water interaction is stronger. Though it is known that the intake of Mn from ingestion of water is very small when compared to oral route intake, (Deveau 2010) there are reports available that confirm the risk of exposure to manganese from potable water.

The As concentration in GW is found to be very less, this also supports the positive relationship between As and fluoride (with each other due to reductive dissolution of Fe-oxide/hydroxides (Das et al., 2017). The highest Fe level in GW reported is 14.18 mg/L in Senabor Assam suggesting the highly ferruginous nature of the sediment and hence the major reason for higher Fe content in GW is geogenic. About 33% of the samples have Fe content above BIS permissible limit of 1.0 mg/L. All other heavy metal levels (Cr, Ni, Cu, Zn, Se, Ag, Cd and Pb) in GW samples are almost negligible or far below their prescribed limits (Table 3). Map showing the distribution of Mn and Fe in GW of Kamrup (Metro) is depicted in Fig. 7 (a & b).

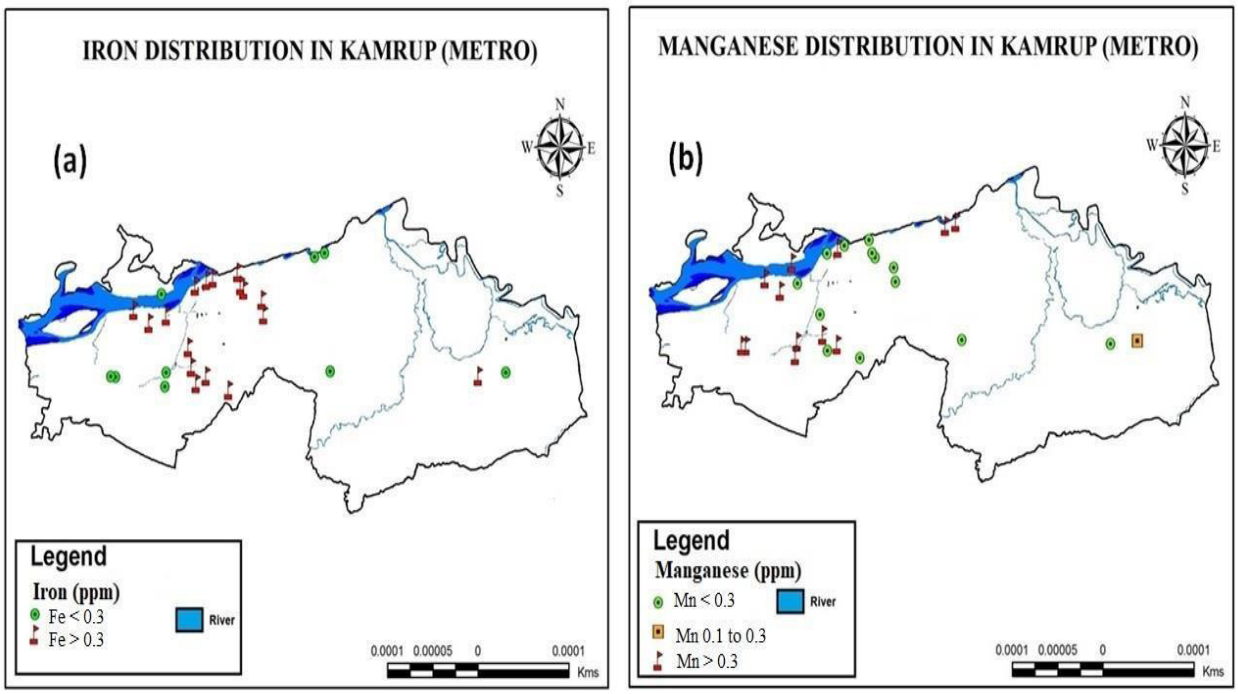

Fig. 6 Map showing **(a)** uranium (**b)** aluminum distribution in GW of Kamrup Metro),Assam.

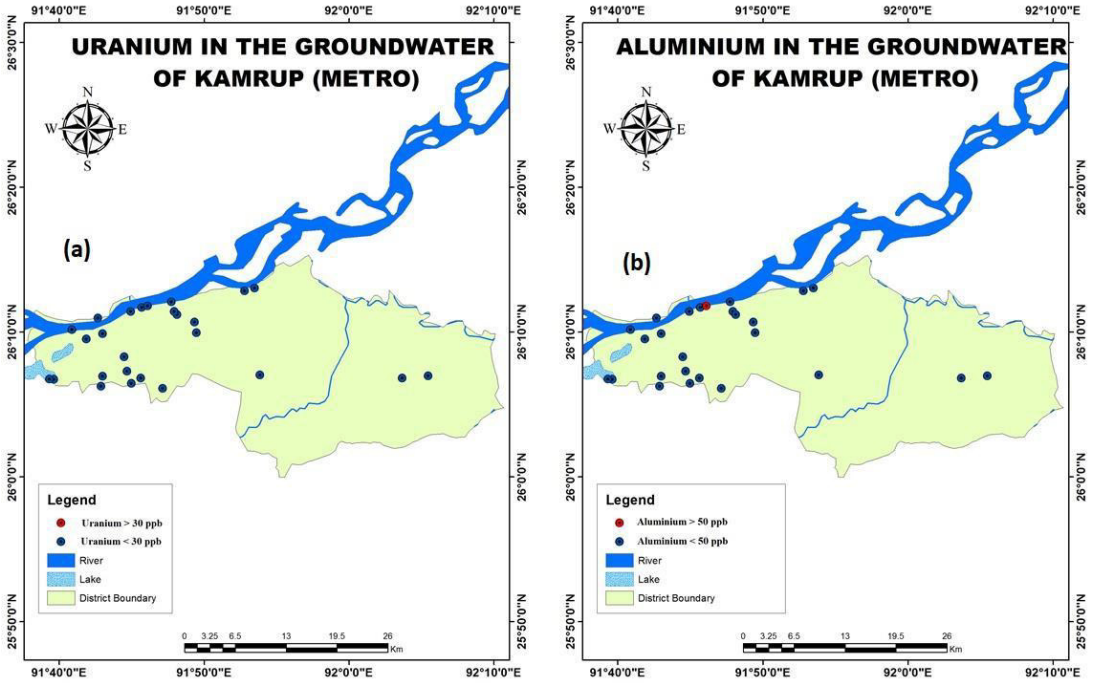

Fig. 7 Map showing **(a)** iron and **(b)** manganese distribution in GW of Kamrup (Metro), Assam.

3.3 Statistical Analysis

Further analyzing the data in terms of statistical parameters, as presented in Table 3, it has found that for the cations and anions skewness and kurtosis values have a combination of positive and negative values. The interquartile ranges (IQR) for each of the ions are large and there is significant difference between mean and median. All these statistical indices indicate that the distributions of ions across Kamrup (M) are asymmetric. However, the trend is not so in case of the heavy metals and U concentration. The skewness and kurtosis values are significantly positive for all of them, the interquartile ranges are less and differences between mean and median are negligible. Hence, it may be reported that there is uniformity (or negligible concentration) in the distribution of heavy metal levels in GW across the study area. U concentration values have the second highest positive skewness (3.96) and kurtosis (17.93), just below Al. This indicates the U distribution to be an asymmetric tail on the right of the median.

Pearson's correlation analysis among these variables with respect to U showing their relationship and strength of the correlation is shown in Table 4 and Table 5. Fig. 8 presents the scatter plots showing the extent of the linear relationship of parameters (F, Fe, Mn, As, Al) with U. From the correlation matrix (Table 4, Table 5) and scattered plots (Fig. 8) shows a positive correlation of U with fluoride (0.105), U with Cr (0.6255) and U with Se (0.316). This actually supports the fact that U, fluoride, Cr and Se may have similar sources of geogenic origin and mobility. Other heavy metals have negative or poor correlation with U. Fe and Mn have a positive correlation and this signifies the presence of ferro-manganese compounds in the aquifers. Furthermore, Table 4 and Table 5 show a positive correlation of Fe with As (0.3271), As with Mn (0.4095), Ni with Cd (0.7734), Cu with Zn (0.7734), Cu with Ag (0.6045), Ag with Pb (0.5344) and Zn with Ag (0.8628). Even though there exists a positive correlation between a number of other heavy metals, it could not reveal any significant inter-metal relationships in the groundwater of Kamrup (Metro). However, in GW having higher Fe content, activities of Fe-reducing bacteria reduce least crystalline Fe-Mn-oxyhydroxide phases that adsorb As which is subsequently released into GW by reductive dissolution (Manning and Goldberg, 1997).

Table 4. Correlation matrix of U, Fe, As, Mn, Al and fluoride constituents of GW of Kamrup (Metro) district.

	U	F-	Fe	As	Mn	Al
U	1					
F-	0.1046	1				
Fe	-0.2031	-0.0649	1			
As	-0.1153	0.1134	0.3271	1		
Mn	-0.0854	0.1524	0.0403	0.4095	1	
Al	-0.0861	-0.2088	-0.0863	-0.1339	-0.1102	1

Table 5. Correlation matrix of U, Cr, Ni, Cu, Zn, Se, Ag, Cd and Pb constituents of GW of Kamrup (Metro) district.

	U	Cr	Ni	Cu	Zn	Se	Ag	Cd	Pb
U	1								
Cr	0.6255	1							
Ni	-0.0481	-0.1588	1						
Cu	0.0985	0.0317	-0.1156	1					
Zn	0.0541	0.0050	-0.1051	0.6927	1				
Se	0.3160	0.1975	0.2305	-0.1173	-0.1796	1			
Ag	-0.0477	-0.0845	-0.0989	0.6045	0.8628	-0.1387	1		
Cd	-0.0398	-0.1497	0.7734	-0.0352	-0.1663	0.1380	-0.1216	1	
Pb	-0.1502	-0.0968	0.1013	0.3806	0.4873	-0.0040	0.5344	0.0874	1

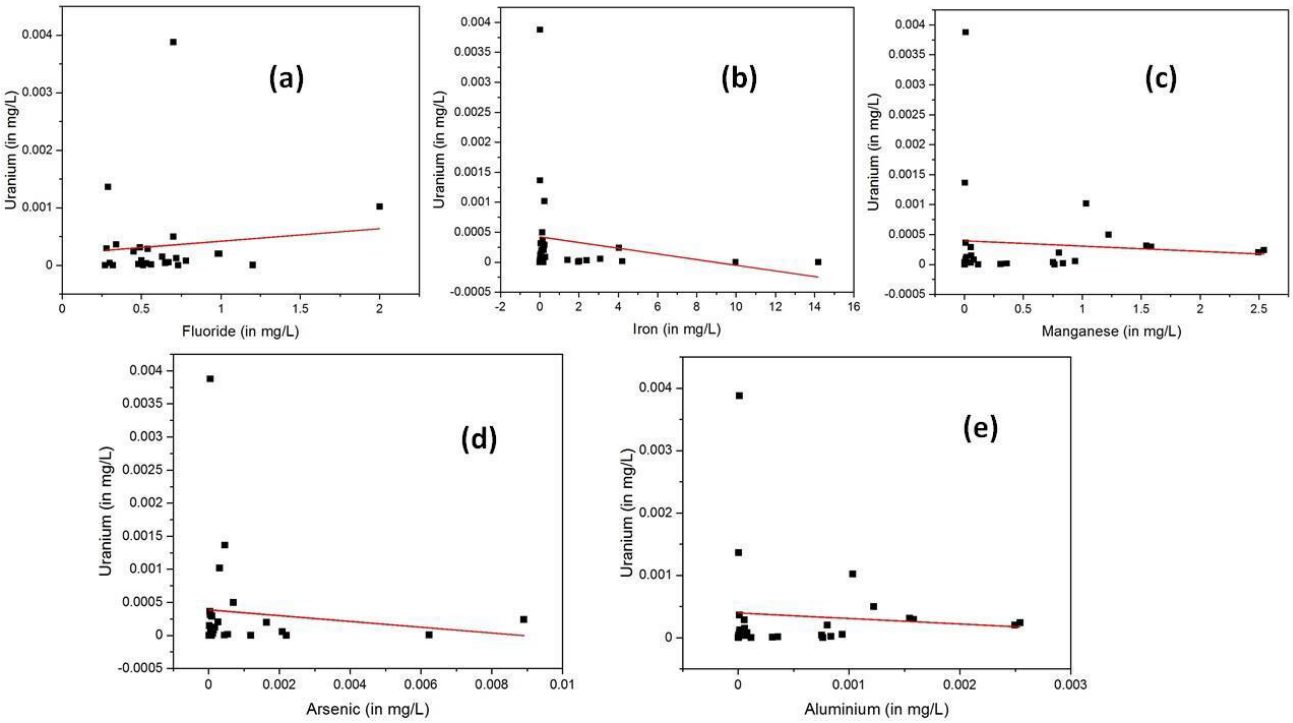

Fig. 8 Scatter plots showing correlation of U with F, Fe, As, Mn and Al.

4. Conclusion

The occurrence of radioactive uranium in the GW of Kamrup (Metro) district is insignificant. In many sampling locations, Fe and Mn were found to be beyond the permissible limit of BIS. And in one location Al concentration exceeded the acceptable limit of BIS. This can be attributed to the humid Brahmaputra flood plains with conditions unsuitable for uranium enrichment. Uranium has shown to have a positive correlation with fluoride, Cr, Se and negative or poor correlation with other heavy metals. A positive correlation of U with fluoride (0.105), U with Cr (0.6255) and U with Se (0.316), Fe with As (0.3271), As with Mn (0.4095), Ni with Cd (0.7734), Cu with Zn (0.7734), Cu with Ag (0.6045), Ag with Pb (0.5344) and Zn with Ag (0.8628) suggested common source of origin. The different statistical estimations for each parameter indicate that their distribution in Kamrup (Metro) district is widely off-normal and has an asymmetric tail on either side of the median. Elevated levels of 33% and 48% of Fe and Mn respectively in the samples were observed. Though the possible source of heavy metals in the samples for this investigation is ascertained to be geogenic in nature (Gibb's plot)), the possibility of anthropogenic sources can, however, be not ruled out. This study can serve as a template to seek out the source of pollution in the sampling points, aid in the design and execution of mitigation strategies, and eventually prevent GW contamination. The source, potential health hazards posed by some of the probable contaminants and their probable remedial measures with reference to groundwater of Kamrup (Metro) are also discussed.

Acknowledgements

The authors thank all the officers of CGWB, NER who collected GW samples from various wells for the present study. The authors are also grateful to the Chairman, Member (East), Member (CGWB), Faridabad and Regional Director, CGWB, NER and Regional Director, CGWB, NWR, Chandigarh for giving permission to analyze the samples at Regional Chemical Laboratory, CGWB, NWR, Chandigarh.

REFERENCES

1. Akl, M.A., Yousef, A.M. and AbdElnasser, S. (2013). Removal of iron and manganese in water samples using activated carbon derived from local agro-residues. Journal of Chemical Engineering & Process Technology, 4(4): 1-10.
2. Amin, A., Fazal, S., Mujtaba, A. and Singh, S.K. (2014). Effects of land transformation on water quality of Dal Lake, Srinagar, India. Journal of the Indian Society of Remote Sensing, 42(1): 119-128.
3. Aowal, A.F.S.A. (1981). Design of an iron eliminator for hand tube wells. Journal of Indian Water Works Association, 13(1): 65-72.
4. APHA–American Public Health Association. (2012). Standard methods for the examination of water and wastewater. American Water Works Association, Water Environment Federation, Washington.
5. Asere, T.G., Stevens, C.V. and Du Laing, G. (2019). Use of (modified) natural adsorbents for arsenic remediation: A review. Science of the Total Environment, 676: 706-720.
6. Bajwa, B.S., Kumar, S., Singh, S., Sahoo, S.K. and Tripathi, R.M. (2017). Uranium and other heavy toxic elements distribution in the drinking water samples of SW-Punjab, India. Journal of Radiation Research and Applied Sciences, 10(1):13-19.
7. Bhattacharya, P., Polya, D. and Jovanovic, D. Eds. (2017). Best practice guide on the control of arsenic in drinking water. IWA Publishing, London, UK.
8. Bruins, M. R., Kapil, S., and Oehme, F. W. (2000). Microbial resistance to metals in the environment. Ecotoxicology and Environmental Safety, 45: 198–207.
9. Buamah, R. Adsorptive removal of Mn, As and Fe from GW, Ph. D. Thesis, Wageningen University. https://repository.tudelft.nl/assets/uuid:666fa78b-8969-4308-b2b1-4b494581cc1f/PHD_THESIS_BUAMAH.pdf (accessed on 30/08/2020).
10. Bureau of Indian Standards, (2012). Drinking water specification IS 10500: 2012. http://cGWb.gov.in/Documents/WQ-standards.pdf (accessed on 25/08/2020).
11. Chakrabarty, S. and Sarma, H.P. (2011). Heavy metal contamination of drinking water in Kamrup district, Assam, India. Environmental Monitoring and Assessment, 179(1-4): 479-486.
12. Chauhan, V.S., Dwivedi, P.K. and Iyengar, L. (2007). Investigations on activated alumina based domestic defluoridation units. Journal of Hazardous Materials, 139(1): 103-107.
13. Cheng, Y., Huang, T., Liu, C. and Zhang, S. (2019). Effects of dissolved oxygen on the start-up of manganese oxides filter for catalytic oxidative removal of manganese from GW. Chemical Engineering Journal, 371: 88-95
14. Coyte, R.M., Jain, R.C., Srivastava, S.K., Sharma, K.C., Khalil, A., Ma, L. and Vengosh, A. (2018). Large-scale uranium contamination of GW resources in India. Environmental Science & Technology Letters, 5(6): 341-347.
15. Das, B., Talukdar, J., Sarma, S., Gohain, B., Dutta, R.K., Das, H.B. and Das, S.C. (2003). Fluoride and other inorganic constituents in GW of Guwahati, Assam, India. Current Science, 85: 657-661.
16. Das, N., Das, A., Sarma, K.P. and Kumar, M. (2018). Provenance, prevalence and health perspective of co-occurrences of arsenic, fluoride and uranium in the aquifers of the Brahmaputra River floodplain. Chemosphere, 194: 755-772.
17. Das, N., Deka, J.P., Shim, J., Patel, A.K., Kumar, A., Sarma, K.P. and Kumar, M. (2016). Effect of river proximity on the arsenic and fluoride distribution in the aquifers of the Brahmaputra floodplains, Assam, northeast India. GW for Sustainable Development, 2: 130-142.
18. Das, N., Sarma, K.P., Patel, A.K., Deka, J.P., Das, A., Kumar, A., Shea, P.J. and Kumar, M. (2017). Seasonal disparity in the co-occurrence of arsenic and fluoride in the aquifers of the Brahmaputra flood plains, Northeast India. Environmental Earth Sciences, 76(4): 183.

19. Dash, R.K., Ramanathan, A.L., Yadav, S.K., Kumar, M., Kuriakose, T. and Gautam, Y.P. (2017). Uranium in GW in India: A review. Journal of Applied Geochemistry, 19(2): 138-144.
20. Deveau, M. (2010). Contribution of drinking water to dietary requirements of essential metals. Journal of Toxicology and Environmental Health, Part A, 73(2-3): 235-241.
21. Dimiropoulos, V., Katsoyiannis, I.A., Zouboulis, A.I., Noli, F., Simeonidis, K. and Mitrakas, M. (2015). Enhanced U (VI) removal from drinking water by nanostructured binary Fe/Mn oxy-hydroxides. Journal of Water Process Engineering, 7: 227-236
22. Drever, J.I. (1997). The Geochemistry of Natural Waters, 3rd ed. Prentice-Hall, Upper Saddle River, NJ, pp. 388.
23. Du, X., Liu, G., Qu, F., Li, K., Shao, S., Li, G. and Liang, H. (2017). Removal of iron, manganese and ammonia from GW using a PAC-MBR system: the anti-pollution ability, microbial population and membrane fouling. Desalination, 403: 97-106.
24. Gautam, S.K., Sharma, D., Tripathi, J.K., Ahirwar, S. and Singh, S.K. (2013). A study of the effectiveness of sewage treatment plants in Delhi region. Applied Water Science, 3(1): 57-65.
25. Gibbs R. J. (1970). Mechanism controlling world water chemistry. Sciences, 170: 795–840
26. Gogoi, A., Chaminda, G.T., An, A.K., Snow, D.D., Li, Y. and Kumar, M. (2016). Influence of ligands on metal speciation, transport and toxicity in a tropical river during wet (monsoon) period. Chemosphere, 163: 322-333.
27. Goswami, M. and Rabha, D., Trend analysis of ground-water levels and rainfall to assess sustainability of GW in Kamrup Metropolitan District of Assam in Northeast India.https://www.iitr.ac.in/rwc2020/pdf/papers/RWC_12_Dolly_R_et_al.pdf (accessed on 29/07/2020)
28. Hakonson-Hayes, A.C., Fresquez, P.R. and Whicker, F.W. (2002). Assessing potential risks from exposure to natural uranium in well water. Journal of Environmental Radioactivity, 59(1): 29-40.
29. Henry, R. and Wills, J., Drinking Water Compliance Monitoring using US EPA Method 200.8 with the Thermo Scientific iCAP Q ICP-MS. https://hosmed.fi/wp-content/uploads/2016/10/AN43132_EPA200_8-Drinking-water.pdf (accessed on 25/08/2020).
30. Karpas, Z., Halicz, L., Roiz, J., Marko, R., Katorza, E., Lorber, A. and Goldbart, Z. (1996). Inductively coupled plasma mass spectrometry as a simple, rapid, and inexpensive method for determination of uranium in urine and fresh water: comparison with LIF. Health Physics, 71(6): 879-885.
31. Kemer, B., Ozdes, D., Gundogdu, A., Bulut, V.N., Duran, C. and Soylak, M. (2009). Removal of fluoride ions from aqueous solution by waste mud. Journal of Hazardous Materials, 168(2-3): 888-894.
32. Kumar, M., Das, N., Goswami, R., Sarma, K.P., Bhattacharya, P. and Ramanathan, A.L. (2016). Coupling fractionation and batch desorption to understand arsenic and fluoride co-contamination in the aquifer system. Chemosphere, 164: 657-667.
33. Kumar, M., Rao, M.S., Kumar, B. and Ramanathan, A. (2011). Identification of aquifer-recharge zones and sources in an urban development area (Delhi, India), by correlating isotopic heavyrs with hydrological features. Hydrogeology Journal, 19(2): 463-474.
34. Kumar, N., Singh, S.K., Srivastava, P.K. and Narsimlu, B. (2017). SWAT Model calibration and uncertainty analysis for streamflow prediction of the Tons River Basin, India, using Sequential Uncertainty Fitting (SUFI-2) algorithm. Modeling Earth Systems and Environment, 3(1): 30.
35. Kumar, P.R., Chaudhari, S., Khilar, K.C. and Mahajan, S.P. (2004). Removal of arsenic from water by electrocoagulation. Chemosphere, 55(9): 1245-1252.
36. Lahkar, M. and Bhattacharyya, K.G. (2019). Heavy metal contamination of GW in Guwahati city, Assam, India. http://www.academia.edu/download/60405721/IRJET-V6I635720190826-56074-xweexi.pdf (accessed on 24/08/2020).

37. Mahmoud, M.E., Khalifa, M.A., El Wakeel, Y.M., Header, M.S. and Abdel-Fattah, T.M. (2017). Engineered nano-magnetic iron oxide-urea-activated carbon nanolayer sorbent for potential removal of uranium (VI) from aqueous solution. Journal of Nuclear Materials, 487: 13-22.
38. Malyan, S.K., Singh, R., Rawat, M., Kumar, M., Pugazhendhi, A., Kumar, A., Kumar, V. and Kumar, S.S. (2019). An overview of carcinogenic pollutants in GW of India. Biocatalysis and Agricultural Biotechnology, 21: 101288.
39. Manning, B.A. and Goldberg, S. (1997). Adsorption and stability of arsenic (III) at the clay mineral− water interface. Environmental Science & Technology, 31(7): 2005-2011.
40. Marschner, H. (1995). Mineral nutrition of higher plants. London: Academic Press.
41. Murugesan, G.S., Sathishkumar, M. and Swaminathan, K. (2006). Arsenic removal from GW by pretreated waste tea fungal biomass. Bioresource Technology, 97(3): 483-487
42. Narsimlu, B., Gosain, A.K., Chahar, B.R., Singh, S.K. and Srivastava, P.K. (2015). SWAT model calibration and uncertainty analysis for streamflow prediction in the Kunwari River Basin, India, using sequential uncertainty fitting. Environmental Processes, 2(1): 79-95.
43. NERIWALM (2004). Pre-seminar proceedings from National Seminar on Arsenic and Fluoride contamination in GW organized by NERIWALM. Tezpur: North Eastern Regional Institute of Water and Land Management, pp.1–10.
44. Nicolli, H.B., Suriano, J.M., Peral, M.A.G., Ferpozzi, L.H. and Baleani, O.A. (1989). GW contamination with arsenic and other heavy elements in an area of the Pampa, Province of Córdoba, Argentina. Environmental Geology and Water Sciences, 14(1): 3-16.
45. Nurnberg, H.W. (1982). Voltammetric heavy analysis in ecological chemistry of toxic metals. Pure and Applied Chemistry, 54(4): 853-878.
46. Piper, A.M. (1944). A graphic procedure in the geochemical interpretation of water analyses. EOS Transactions of the American Geophysical Union, 25: 914–928
47. Prakash, R., Bhartariya, K.G., Singh, S., Singh, K., Rajak, M. and Kaushik, Y.B. (2020). Uranium and its correlation with other geogenic contaminants in ground water of Ganga Yamuna Doab, Fatehpur District, Uttar Pradesh, India. Journal of the Geological Society of India, 95(4): 359-365.
48. Radhapyari, K., Datta, S., Dutta, S. and Gogoi, U. Detection of high level of Arsenic in GW of Assam, India (with reference to Kamrup, Urban), 7th International GW conference at ICAR, New Delhi, 11-13 December, 2017.
49. Ramesh, R., Kumar, K.S., Eswaramoorthi, S. and Purvaja, G.R. (1995). Migration and contamination of major and heavy elements in GW of Madras City, India. Environmental Geology, 25(2): 126-136.
50. Rdiagojevich, R. and Whitkar, E. R. (1999). In Iron in drinking water. Illinois Dept of public health, division of environmental health, 525 Efferson Str., Springfeild, IL 62721.
51. Saleh, T.A., Tuzen, M. and Sarı, A. (2017). Polyethylenimine modified activated carbon as novel magnetic adsorbent for the removal of uranium from aqueous solution. Chemical Engineering Research and Design, 117: .218-227.
52. Sauvé, S., Hendershot, W. and Allen, H.E. (2000). Solid-solution partitioning of metals in contaminated soils: dependence on pH, total metal burden, and organic matter. Environmental Science & Technology, 34(7): 1125-1131.
53. Singh, A., Sharma, R.K., Agrawal, M. and Marshall, F.M. (2010). Health risk assessment of heavy metals via dietary intake of foodstuffs from the wastewater irrigated site of a dry tropical area of India. Food and Chemical Toxicology, 48(2): 611-619.
54. Singh, A.K. (2006). Chemistry of arsenic in GW of Ganges–Brahmaputra river basin. Current Science, 91(10): 599-606.

55. Singh, H., Singh, D., Singh, S.K. and Shukla, D.N. (2017). Assessment of river water quality and ecological diversity through multivariate statistical techniques, and earth observation dataset of rivers Ghaghara and Gandak, India. International Journal of River Basin Management, 15(3): 347-360.
56. Smedley, P.L. and Kinniburgh, D.G. (2002). A review of the source, behaviour and distribution of arsenic in natural waters. Applied Geochemistry, 17(5): 517-568.
57. Tamuli, P., Borgohain, A., Das, B.R. and Talukdar, K. (2017). Prevalence of arsenicosis and its relation to drinking water in Titabor block of Jorhat district, Assam, India. World, 6: 13.
58. US EPA (2013) Basic Information about Radionuclides in Drinking Water, Retrieved from http://water.epa.gov/drink/contaminants/basicinformation/ radionuclides.cfm (accessed on 27/08/2020).
59. Verma, S., Mukherjee, A., Choudhury, R. and Mahanta, C. (2015). Brahmaputra river basin GW: solute distribution, chemical evolution and arsenic occurrences in different geomorphic settings. Journal of Hydrology: Regional Studies, 4: 131-153.
60. Wasserman, G.A., Liu, X., Parvez, F., Ahsan, H., Factor-Litvak, P., van Geen, A., Slavkovich, V., Lolacono, N.J., Cheng, Z., Hussain, I. and Momotaj, H. (2004). Water arsenic exposure and children's intellectual function in Araihazar, Bangladesh. Environmental health perspectives, 112(13): 1329-1333.
61. World Health Organization (2005) Guidelines for drinking-water quality 4th ed p 430. Uranium in Drinking Water. Retrieved from https://www.who.int/water_sanitation_health/dwq/chemicals/uranium290605.pdf (accessed on 27/08/2020)
62. World Health Organization. (2012) Uranium in Drinking-Water—Background Document for Development of WHO Guidelines for Drinking-Water Quality. WHO Press; Geneva, Switzerland.

Bhujal News, 30(1-4):50-62

Assessment of Uranium and Heavy Metals Contamination in Groundwater of Nagaon District, Assam, India

Rinkumoni Barman[1], Snigdha Dutta[1], Biplab Ray[1], Kiran Lale[2], Sudhir Kumar Srivastava[3] and Keisham Radhapyari [1]

[1]Central Ground Water Board, North Eastern Region, Department of Water Resources, River Development and Ganga Rejuvenation, Ministry of Jal Shakti, Guwahati – 781035, Assam, India.
[2]Central Ground Water Board, North Western Region, Department of Water Resources, River Development and Ganga Rejuvenation, Ministry of Jal Shakti, Chandigarh – 160019, India.
[3]Central Ground Water Board, Central Head Quarters, Department of Water Resources, River Development and Ganga Rejuvenation, Ministry of Jal Shakti, Faridabad-121001, Haryana, India.
*Corresponding author: e-mail: k.radhapyari@assam.gov.in; Tel: +91-9957813992

ABSTRACT

It is of utmost importance to study the contamination of groundwater by heavy metals because of their low biodegradability, accumulation in food chain and toxic effects. Detection of uranium in the groundwater of India has become major cause of concern because of its radioactive nature, exposure to which may result in chronic lung diseases and nephrotoxic damage. In this study attempt has been made to expound the extent of contamination of the groundwater in the Nagaon district of Assam, with regards to heavy metal and uranium. Groundwater samples from 18 locations were collected and analyzed for fifteen physicochemical parameters, heavy metals such as Pb, Fe, Zn, Mn, Cr, Cu and Cd and radioactive uranium using the Inductively Coupled Plasma Mass Spectrometer**.** Further, the general water chemistry of the study area, using physicochemical parameters and spatial distribution of uranium and heavy metals has been discussed. The result obtained were compared with the drinking water standard set by WHO (for Uranium) and BIS drinking water limits, which reveals that the uranium content of the district is within the permissible limit. Further, evaluation of heavy metal content of the district shows that except for iron and manganese, all other heavy metals are well below the BIS permissible limit.

Keywords: *Assessment, Uranium, Heavy metal, Groundwater, Nagaon, Assam*

1. Introduction

Water is the most precious gift of nature to human being on earth, which imparts blue colour to it due to the profuse amount of water on the surface (Iqbal & Gupta, 2009; Maruyama et al., 2013). However, only a diminutive portion of the water on the earth surface is potable. In the past few decades, there has been an unprecedented amplification in population, industrialization, urbanization and unplanned agricultural activity, further aggravating the already constrained surface water, resulting in shifting of water dependence from surface water to groundwater for drinking, industrial, and agricultural activities (Raju et al., 2011). In India, groundwater is the prime source for domestic, irrigation and industrial activities, it accounts for 80% rural population and 50% of the urban populations water needs (Bhattacharya et al., 2017). Hence, it is the need of the hour to monitor the quality and quantity of the groundwater for sustainable development. The reporting of uranium (U) contamination in groundwater of India (Coyte, et al., 2018, Yadav et al. 2020, Richards et al. 2020, Prakash et al. 2020) has set up an alarm; which in turn strengthening the importance of monitoring the quality of groundwater for any contamination. Uranium contaminated groundwater, if consumed has the potential of causing chronic lung diseases and nephrotoxic damage (Zamora et al., 1998, Kurttio et al., 2002, Guo et al., 2016).

Uranium is a radioactive element occurring naturally in groundwater, soil and sediments (Wu et al., 2014). Naturally occurring uranium is composed of a mixture of three radionuclides (U-234, U-235 and U-238) (Cothern & Lappenbusch, 1983; Lide, 1992–1993), out of which U-238 contributes 99% with U-234 and U-235 contributing 0.72% and 0.0054% respectively (EPA fact sheet). Uranium exists as a free metal ion or in the form of a complex with organic and inorganic ligands (Zhao et al., 2009, Kopylova et al., 2015). The two most common oxidation states of Uranium that exists in natural water are VI and IV. The VI state is the dominating oxidation state under the reducing condition whereas IV is the prominent oxidation state under neutral and oxidizing condition (Guo et al., 2009, Wu et al., 2014, Cumberland et al., 2016).Heavy metals are one of the common pollutants of groundwater. The prime source of most of the heavy metal is the excessive use of agrochemicals i.e., fertilizers, plant nutrients etc. which significantly elevates the heavy metal content in the soil and water (Rattan et al., 2005).Ingestion of water tainted with the heavy metals can bring about varied types of health hazard, as reported by copious researchers around the world (Li et al., 2010, Wongsasuluk et al., 2014, Pranab et al., 2010, Tareen et al., 2014, Singh et al., 2003, Kavcar et al., 2009, Trivedi et al., 1984). Consumption of water with Fe content above the permissible limit may result in a hereditary issue, Haemochromatosis (Bothwell et al., 1979), similarly ingestion of Pb may harm the central nervous system, kidney, sometimes even results in death. Zinc above the permissible limit may cause anemia, diarrhea and may affect the kidney, liver and stomach (WHO, 1996). The present study focuses on assessment of uranium and heavy metal contamination, in addition to hydrochemical processes in the groundwater of Nagaon district, Assam.. Heavy metals viz. Pb, Fe, Zn, Mn, Cr, Cu and Cd and radioactive uranium contaminations have been studied using sophisticated instrument, Inductively Coupled Plasma Mass Spectrometer (ICP-MS). The data generated from the present study will be helpful in understanding the hydrochemistry of the groundwater and will help in managing the groundwater by the local governing body in bringing out the appropriate plans since the groundwater of the study area is extensively being used for drinking and irrigation purpose.

2. Materials and methods

2.1 Study area

Nagaon district is located in a central geographical position in the State of Assam on the south bank of the mighty river Brahmaputra (**Fig. 1a**). It resides between 25°45" and 26°45" North latitudes and 91°50" and 93°20" East longitudes. The district is bordered by river Brahmaputra on the north, Golaghat and parts of Karbi Anglong district on the east and on the south by the Dima Hasao and parts of Karbi Anglong district. The average altitude of the district is 60.6 masl. It extends over an area of 3,973 sq km. (District census handbook, Nagaon, Census of India 2011). The major rivers of the district are Brahmaputra, Sonai, Jamuna, Kalong, Nanoi, Kopili and Barpani. The geology of the district is underlain by the Pre-Cambrian metamorphic rocks. The Pre-Cambrian rocks consisting of quartzites and phyllites are incarcerated in a small area of the district whereas the granitic gneisses are disintegrated along the northern and southern bank of the Brahmaputra basin (Bhagabati et al., 2001; Mahanta et al., 2015). Nagaon district has a subtropical humid climate with a hot and humid pre-monsoon from March to mid-May, prolonged rainy season (southwest monsoon) from mid-May to September, post-monsoon or a retreating monsoon from October to November followed by winter from December to February (CGWB, 2013).

2.2 Sample collection and analysis

Eighteen numbers of groundwater samples (Dug wells) were randomly collected from different location of Nagaon district during November 2019 (**Fig. 1b**). American Public Health Association [APHA, 2012] guidelines and their standard procedures were strictly followed for sampling, storing, transferring and analysis of all the parameters. Samples were collected in high density polyethylene bottles (HDPE). For the analysis of basic cations and anions bottles of capacity 1000 mL were used without acidification. Sampling for uranium and other heavy metals analysis was done in 60 mL HDPE bottles. Utmost care was taken to avoid interference from air headspace while sampling and storage. Uranium and heavy metals samples were filtered by 0.45 μm membrane on-site before filling into the bottles.

A syringe filtration unit technique was used. These samples were acidified by 0.5 mL trace elemental grade HNO_3immediately after filtration. Inductively coupled plasma mass spectrometry (Model: iCAP Q ICP-MS; Make: Thermo Scientific) was employed for determination of uranium isotopes and other heavy metals. Calibration curves for uranium, manganese, arsenic and iron were constructed by plotting the ratio of the intensity vs. concentration and good correlation regression is depicted as in **Fig. 2**. UV-Visible spectrophotometer (model: UV-3200, make: Labindia,) was used for analyzing SO_4^{2-} and NO_3^- at λ_{max} 420nm and 220nm respectively and collected data were analyzed using Lab india UV-win software. Titrimetric methods were adopted for analyzing alkalinity, hardness and chloride; Na and K were analyzed using flame photometer (Model: FP128, Make: Systronics) while fluoride analysis was carried out using ion selective electrode (Model: Ion meter, Ion 700; Make: Oakton).

Fifteen physico-chemical parameters were analyzed in Regional Chemical Laboratory, CGWB, NER while uranium and other heavy metals were tested at CGWB, NWR, Chandigarh, India. APHA 2012 standard procedures were followed for testing of each analyte. For ensuring precise and reliable results several QA/QC protocols were implemented viz. use of National Institute of Standards and Technology (NIST) certified standard reference materials, reagent blank run with each sample batch, carrying out retest and repeat analyses, use of at least five standard solutions for generation of calibration curve for each chemical analyte.

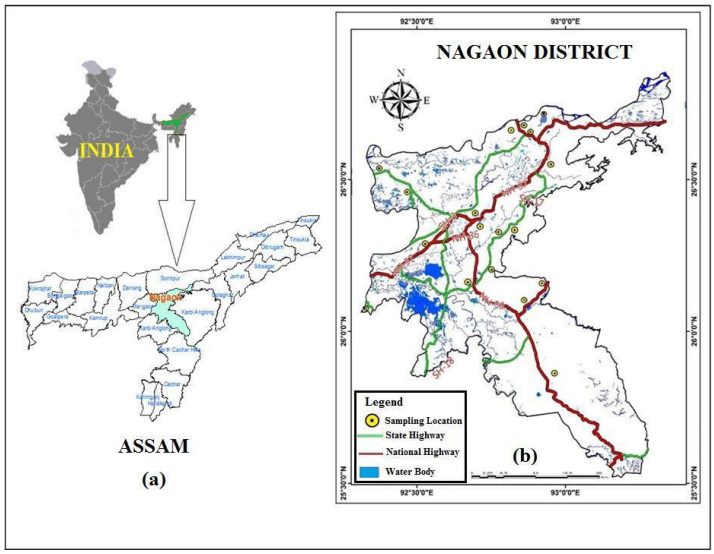

Fig. 1(a) & 1 (b) Location Map of Study Area

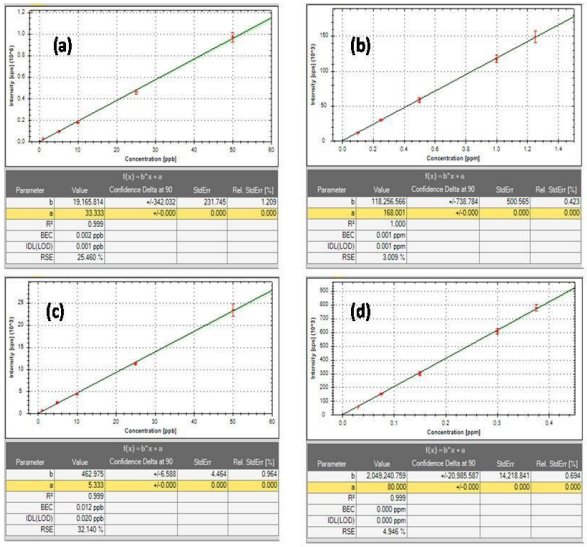

Fig. 2- Calibration curves for uranium, manganese, arsenic and iron were constructed by plotting the ratio of the intensity vs. concentration

Result and discussion

3.1 General water chemistry

The statistical summary of the groundwater samples collected from the study area is shown in **Table 1.** The average pH of the study area is 7.62 and it varies from a minimum of 6.62 to a maximum of 8.45, which is recorded at Jurapukhuri. The conductance of the groundwater in the study area is found to be in the range of 154 µS/cm to 607.8 µS/cm at 25°C. Turbidity varies from 0.01 NTU to 0.4 NTU and TDS from 82.42 mg/L to 354.3 mg/L. The concentration of Carbonate and Bicarbonate range from 16 mg/L to 100 mg/L and 70.06 mg/L to 250.2 mg/L respectively. The concentration of Cl ranges from 17.73 mg/L to 173.71 mg/L and that of Sulphate from 3.1 mg/L to 25.56 mg/L. Contamination of the groundwater by Nitrate is negligible and it ranges from 0.1 mg/L to 3.83 mg/L, which is well below the BIS permissible limit for drinking water. In the study area contamination of the groundwater by fluoride has been detected at two locations namely Dalapani (1.8 mg/L) and Jurapukhri (1.6 mg/L). Both the locations have fluoride content beyond the permissible limit of the BIS drinking water specifications. The average fluoride content in the groundwater of the district is 0.86 mg/L and it ranges from 0.24 mg/L to 1.8 mg/L. Fluoride in the groundwater mainly derived from the dissolution of minerals present in the rocks with which it interacts. Gibbs plot (Fig. 4) of the study area reveals that the rock-water interaction is the dominant factor responsible for the groundwater chemistry and it can be inferred that the fluoride content of the groundwater in the study area may be due to the geogenic sources. Spatial distribution of F^- in the Nagaon district is shown in Fig 3. The concentration of Ca, Mg, Na and K ranges from 12.01 mg/L to 58.05 mg/L, 7.28 mg/L to 42.47 mg/L, 10.94 mg/L to 59.81 mg/L and 0.65 mg/L to 19.85 mg/L respectively.

Table 1. Statistical summary of different constituents of the groundwater samples

Constituent	Min	Max	Average	Std. Dev
pH	6.62	8.45	7.62	0.69
Conductance (µS/cm at 25°C)	154	607.80	438.40	166.62
Turbidity (NTU)	0.01	0.40	0.10	0.15
Total dissolved solids (mg/L)	82.42	354.30	247.04	93.54
Carbonate (CO3) (mg/L)	16	100	28	39.10
Bicarbonate (HCO3) (mg/L)	70.06	250.20	149.64	51.44
Alkalinity as CaCO3 (mgLl)	70.06	285.23	177.64	72.64
Chloride (Cl) (mg/L)	17.73	173.71	74.09	56.39
Sulphate (SO4) (mg/L)	3.10	25.56	14.48	7.58
Nitrate (mg/L)	0.1	3.83	0.80	1.20
Fluoride (F) (mg/L)	0.24	1.80	0.86	0.55
Calcium (Ca) (mg/L)	12.01	58.05	30.62	18.54
Magnesium (Mg) (mg/L)	7.28	42.47	26.44	12.84
Hardness as CaCO3 (mg/L)	60.00	250.00	185.50	60.11
Sodium (Na) (mg/L)	10.94	59.81	36.73	17.46
Potassium (K) (mg/L)	0.65	19.85	9.48	7.38
Cr (mg/L)	0.001	0.002	0.001	0.001
Mn (mg/L)	0.004	3.852	0.699	1.175
Fe (mg/L)	0.078	9.120	0.740	2.111
Cu (mg/L)	0.000	0.002	0.000	0.001
Zn (mg/L)	0.038	0.383	0.105	0.076
Cd (µg/L)	0.003	0.028	0.009	0.007
Pb(µg/L)	0.002	0.757	0.078	0.184
U (µg/L))	0.003	1.129	0.272	0.354

***BDL-** Below detection limit

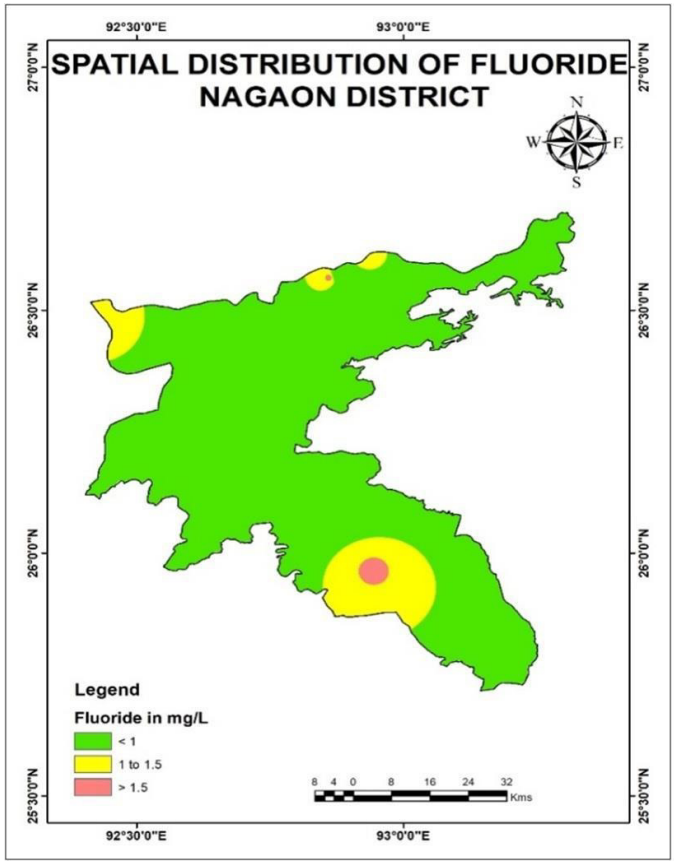

Fig. 3-Spatial distribution of Fluoride in Nagaon district

Gibbs (Gibbs, 1970) recommended two diagrams to comprehend the hydrogeochemical procedures with reference to the atmospheric precipitation, rock–water interaction, and evaporation over the administration of geochemistry of groundwater. The Gibbs plot for the cation and anion of the study area (**Fig. 4a & 4b)** shows that most of the groundwater are from rock dominance and few samples from the precipitation dominance. In alluvial plains, the chemistry of the groundwater is greatly influenced by the rock–water interface (Alam, 2013; Raju et al., 2011). The water type of the study area is evaluated by using Chadha plot and is illustrated in **Fig. 5** (Chadha, 1999). It is apparent from the plot that Ca-Mg-HCO_3 type of water is prominent in the area with 72% of the groundwater sample having Ca-Mg-HCO_3 type and 28% having Na-HCO_3 type of water. From these results, it can be inferred that Ca, Mg are the dominant cation and HCO_3 is the dominating anion and that dissolution of calcite along with evaporation processes are prominent in the study area (Kumar et al., 2016).

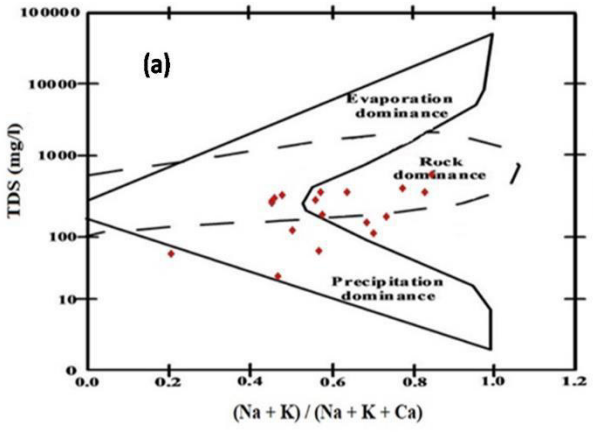

Fig-4(a) The Gibbs plot for the cation

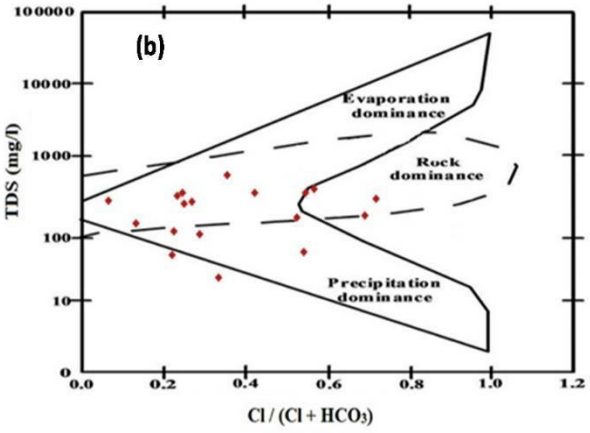

Fig-4(b) Gibbs plot for the anion of the study area

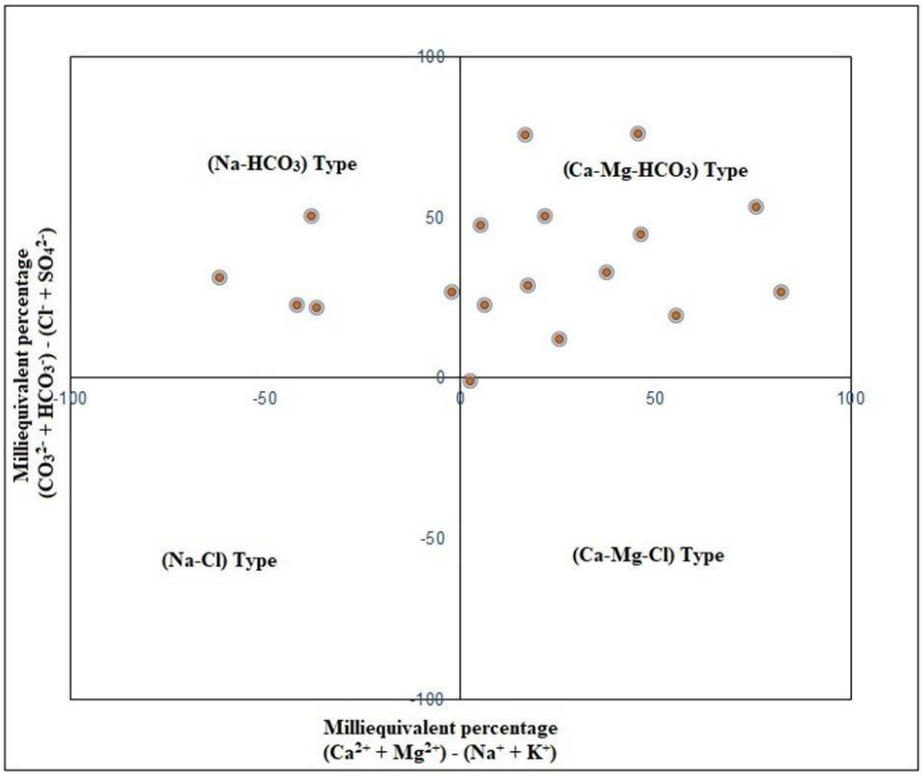

Fig. 5 - The water type of the study area by using Chadha plot

Classification of the analyzed groundwater samples on the basis of TDS and TH (Wanda et al., 2011) shows that all the samples falls in the fresh water category (Fig. 6). It varies from soft-fresh water to hard-fresh water. The hardness of the water in the study area might be due to the interaction of the water with calcium and magnesium rich minerals like calcite and dolomite. The dominance of Ca and Mg ions in the study area has also been confirmed by the Chadha plot (Fig. 5).

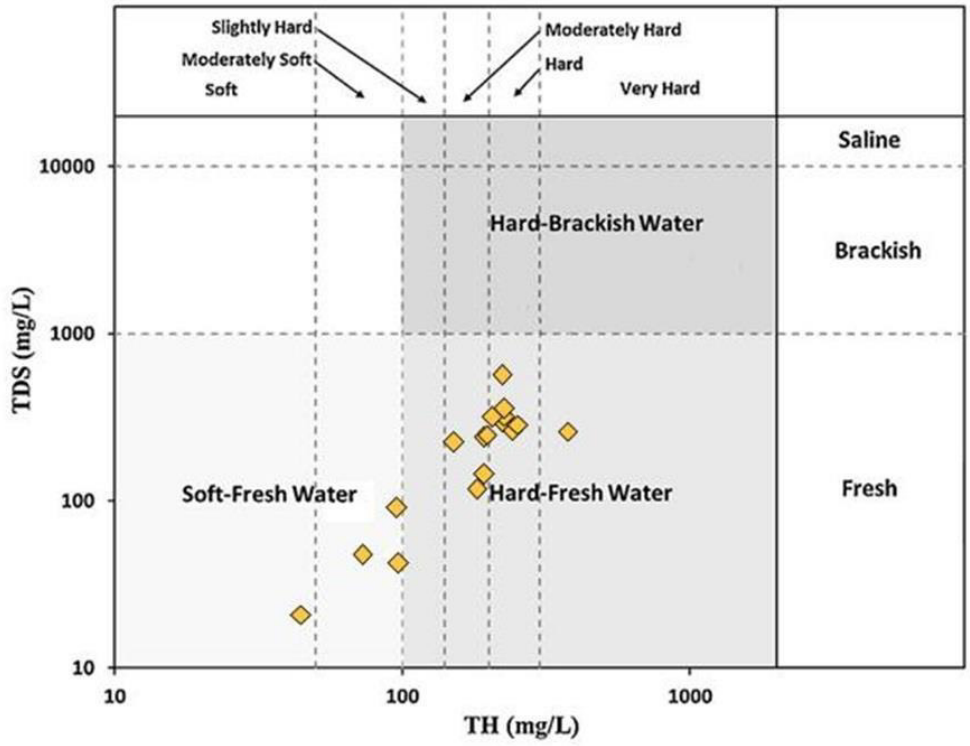

Fig. 6 - Classification of the analyzed groundwater samples on the basis of TDS and TH (Wanda et al., 2011)

3.2 Spatial distribution of Uranium and heavy metal

All the location shows the presence of Uranium (**Table 2**) in the groundwater which varies from 0.003µg/L (Jurapukhuri) to 1.129µg/L (Sulung). However, the concentration is trifling as compared to the provisional health-based Uranium concentration (30 µg/L) guideline in drinking water (Ravenscroft et al., 2009) elucidated by the WHO (WHO, 2011). The low uranium concentration may be due to the less solubility of uranium in the reducing environment of the Brahmaputra flood plain (Prakash et al., 2020). Presence of lead, one of the most toxic elements (Sharma et al., 2015) has been detected in 61% of the collected groundwater samples, maximum being 0.757µg/L detected at Balijuri and a minimum of 0.002µg/L detected at Dalapani, although the concentration is much lower than the BIS permissible limit of 10 µg/L. The reason may be mineral deposition by the river Brahmaputra and its tributaries (Paul 2017) flowing through the district. Iron, the fourth most abundant element in the earth crust, occurring naturally in groundwater in the ferrous soluble form under the reducing condition (Prakash et al. 2020). The area under the study is almost bounded by the reducing condition of the river Brahmaputra and its tributaries resulting in solubility of Fe in almost entire part of the district. The Iron (Fe) content of 16 sampling locations is within the permissible limit of BIS (permissible limit of 0.3 mg/L is denoted by red bar in **Fig. 7a**), however Phulaguri sampling location shows an elevated level of Fe content (9.12 mg/L) (**Fig. 7a,** green bar which shows the actual concentration of Fe present in the sampling locations).

Manganese (Mn) is found in groundwater along with iron geogenically (Kozgar et al., 2012), although there is no correlation between the two elements (Daughney, 2003). The study area shows the presence of Manganese in the range of 0.004 mg/L-3.852 mg/L (**Fig. 7b**). Of the total analysed groundwater samples, 28% of the sample shows Mn content above the BIS permissible limit, which appears to be geogenic in nature as exemplified by the Gibbs plot (Fig 4). The Mn content in the groundwater of the study area is further aggravated by the reducing condition of the Brahmaputra flood plains (Prakash et al., 2020). Analysis of Chromium content in the groundwater samples reveals that 44% of the total samples have chromium content in the range of 0.001 mg/L – 0.002 mg/L, which is way below the BIS permissible limit for Chromium (0.05 mg/L) in drinking water. Zinc, another heavy metal under study, is an essential element for human body, which plays an imperative role in more than 300 zinc mettalo-enzymatic activities (Keith et al., 2000). The zinc content varies from 0.038 mg/L to 0.383 mg/L, which is well within the permissible limit (BIS, 2012). Copper content in drinking water varies widely primarily because of variation in water characteristics like pH, Hardness etc (WHO, 2004). In groundwater, Copper mainly present in the form of complex or as a particulate matter (WHO, 2004). The copper content of groundwater in the study area ranges from 0.001 mg/L to 0.002 mg/L, which is below the BIS permissible limit. Cadmium is a non-essential and poisonous element to the human body and is a very mobile element in the environment (Alloway et al. 1991; Nies, 1999, 2003) both geogenic and anthropogenic sources can elevate Cd concentration in the groundwater (Kubier et al., 2019). In the study area the concentration of Cd varies in the range 0.003µg/L – 0.028µg/L, which is less than the BIS permissible limit of 3µg/L.

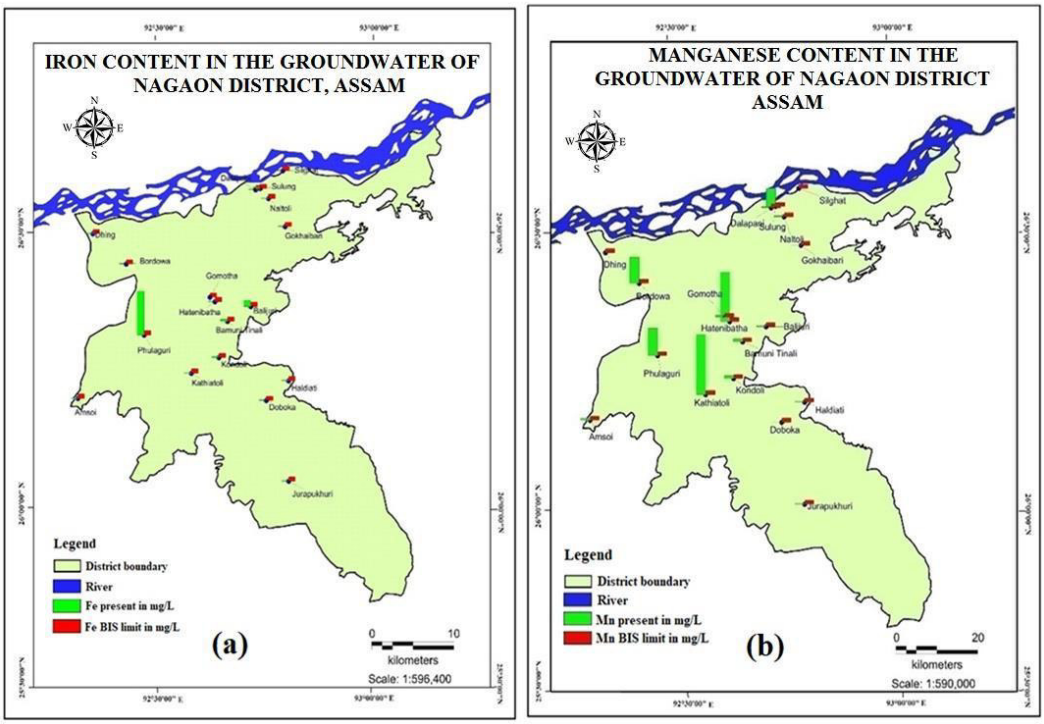

Fig.7 (a)-Iron Content Fig. 7 (b)- Manganese Content in Ground Water of Nagaon in comparison to the BIS permissible limit

Table 2. Uranium and heavy metal concentration in Nagaon district, Assam

Location	Source	Cr (mg/L)	Mn (mg/L)	Fe (mg/L)	Cu (mg/L)	Zn (mg/L)	Cd (µg/L)	Pb (µg/L)	U (µg/L)
Amsoi	Dug Well	BDL	0.122	0.148	BDL	0.121	0.017	BDL	0.016
Balijuri	Dug Well	0.002	0.052	1.303	0.002	0.127	0.018	0.757	0.074
BamuniTinali	Dug Well	0.001	0.221	0.542	BDL	0.060	0.004	0.004	0.018
Bordowa	Dug Well	BDL	1.710	0.125	0.001	0.044	0.028	0.062	0.048
Dalapani	Dug Well	BDL	0.061	0.162	BDL	0.067	0.009	0.002	0.296
Dhing	Dug Well	0.001	0.010	0.156	BDL	0.077	0.005	0.292	0.656
Doboka	Dug Well	BDL	0.020	0.130	0.001	0.142	0.003	0.008	0.039
Gokhaibari	Dug Well	BDL	0.004	0.116	BDL	0.038	0.000	BDL	0.125
Gomotha	Dug Well	0.001	0.114	0.078	BDL	0.114	0.003	BDL	0.426
Haldiati	Dug Well	BDL	0.034	0.111	BDL	0.082	0.010	0.030	0.010
Hatenibatha	Dug Well	0.001	3.193	0.105	BDL	0.110	0.005	BDL	1.080
Jurapukhuri	Dug Well	BDL	0.063	0.175	BDL	0.068	0.010	0.073	0.003
Kathiatoli	Dug Well	0.000	3.852	0.139	BDL	0.114	0.007	BDL	0.124
Kondoli	Dug Well	BDL	0.180	0.349	BDL	0.050	0.009	BDL	0.032
Naltoli	Dug Well	0.001	0.099	0.154	BDL	0.084	0.006	BDL	0.367
Phulaguri	Dug Well	BDL	1.718	9.120	BDL	0.383	0.008	0.091	0.089
Silghat	Dug Well	0.001	0.009	0.126	0.001	0.122	0.010	0.010	0.372
Sulung	Dug Well	0.002	1.111	0.275	BDL	0.092	0.003	0.084	1.129

*BDL- Below detection limit

Computation of the Pearson's correlation matrix, to assess the relationship between the analysed heavy metals in the study area (Table 3) shows a very strong correlation of Zn with Fe (0.913), Pb with Cu (0.824), Cr with Cu (0.519) and Pb (0.641) suggesting common source of origin. Although there exists a positive correlation between a number of other heavy metals as well but it did not divulge any substantial inter-metal relationships in the groundwater of the study area (Manta et al., 2002).

Table 3. Correlation Matrix

	Cr	Mn	Fe	Cu	Zn	Cd	Pb	U
Cr	1							
Mn	-0.059	1						
Fe	-0.143	0.191	1					
Cu	0.519	-0.216	-0.029	1				
Zn	-0.098	0.253	0.913	0.051	1			
Cd	-0.111	0.064	0.013	0.410	-0.044	1		
Pb	0.641	-0.159	0.132	0.824	0.106	0.319	1	
U	0.466	0.300	-0.153	-0.200	-0.049	-0.384	-0.024	1

The concentration of heavy metals in the groundwater is greatly influenced by the nature of rocks with which it interacts, climatic factors, type and extent of mineralization. The pH of the groundwater is one of the factors that drive the extent of mineralization. In general, the mobility of cationic species decreases under high pH condition and increases at low pH conditions (Smith, 2007). The relationship between pH and heavy metal content of the groundwater can be traced by using Ficklin diagram Fig. 8 (Ficklin et al., 1992, Caboi et al., 1999). In the present study Cr, Mn, Fe, Cu, Zn, Cd and Pd were selected as the base metal for plotting the Fickling plot against the pH. The plot classified most of the sample as near-neutral low-metal type and few samples as near-neutral high-metal. The pH range might be due to the carbonate rock and ophiolitic rock which does not allow high amount of base metal in the groundwater (Naseem et al., 2013), which also accounts for the low concentration of heavy metals in the study area.

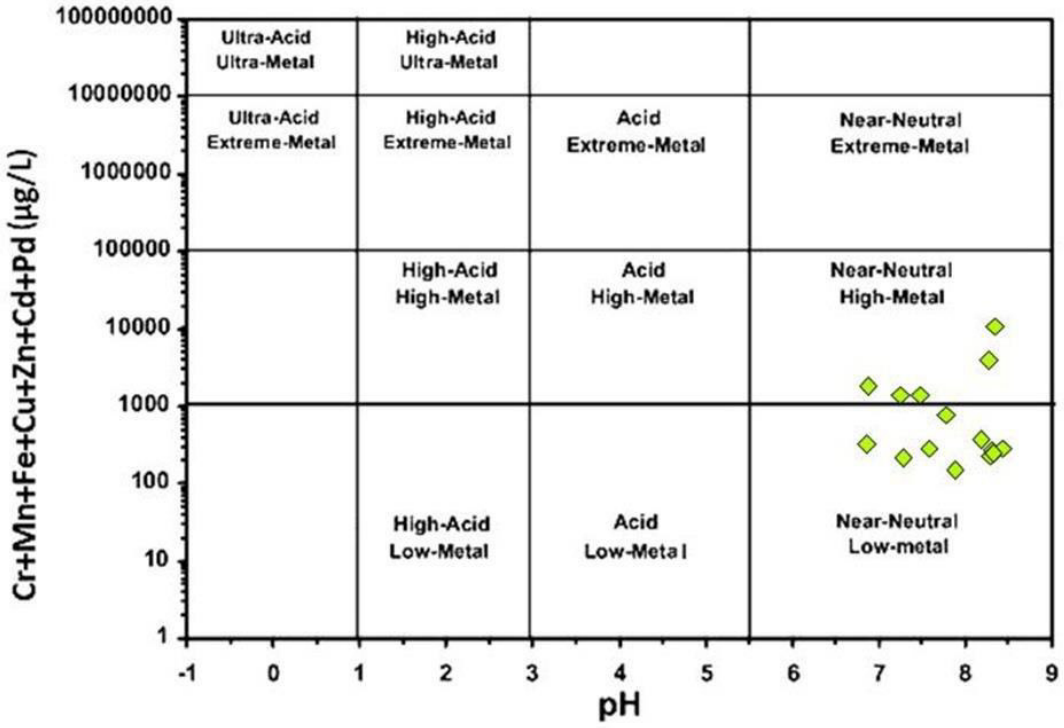

Fig. 8 Plot of metal load and pH of water samples.

4. Conclusion

The assessment of the groundwater quality of the Nagaon district divulges two types of groundwater Ca-Mg-HCO_3 and Na-HCO_3 with Ca and Mg being the dominant cation and HCO_3, the dominant anion. The dominance of Ca and Mg ions resulted in hardness of the water which varies from soft-fresh water to fresh-hard water as classified from the plot of TDS vs TH. The hydrochemistry of the groundwater is mainly due to the rock-water interaction as suggested by the Gibbs plot. Detection of fluoride in the groundwater of the two locations namely Dalapani (1.8 mg/L) and Jurapukhri (1.6 mg/L) may be ascribed to the geogenic sources. Uranium content, which may be attributed due to the geogenic condition of the district (as suggested by the Gibbs plot) is below the WHO permissible limit of 30 µg/L. Low Na and K concentration also facilitated the low concentration of uranium in the study area. Study further reveals that the contamination of the groundwater by the heavy metals has a trivial upshot on the water quality of the district except for Balijuri, Phulaguri, Borodowa, Kathiatoli, Sulung and Hatenibatha. The high Fe and Mn content in these locations may be attributed due to the solubility of the minerals in the reducing environment which exists in active flood plain areas. The existence of positive correlation of Zn with Fe (0.913), Pb with Cu (0.824), Cr with Cu (0.519) and Pb (0.641) suggested common source of origin. The groundwater in the area varies from near-neutral low-metal type to near-neutral high-metal as classified by the Ficklin plot. Despite comparatively low sampling density, the spatial coverage across the district provides a comprehensive and unswerving dataset & good hydrochemical characterization of the Nagaon district. These results have significant insinuations for apposite remedial strategies.

Acknowledgements

The authors thank all the officers of CGWB, NER who collected groundwater samples from various wells for the present study. The authors are also grateful to the Chairman, Member (East), Member (CGWB), Faridabad and Regional Director, CGWB, NER and Regional Director, CGWB, NWR, Chandigarh for giving permission to analyze the samples at Regional Chemical Laboratory, CGWB, NWR, Chandigarh.

References

Alam, F. (2013). Evaluation of hydrogeochemical parameters of groundwater for suitability of domestic and irrigational purposes: a case study from central Ganga Plain, India. Arabian Journal of Geosciences, 7(10), 4121–4131.

Alloway, B. J., & Jackson, A. P. (1991). The behaviour of heavy metals in sewage sludge-amended soils. Science of the Total Environment, 100, 151–176.

APHA, (2017). Standard methods for the examination of water and wastewater. 23rd ed. Washington, DC: APHA.

Bhagabati, A. K., Kar, B. K., & Bora, A. K. (2001). Geography of Assam. New Delhi: Rajesh Publication.

Bhattacharya, P., Polya, D. and Jovanovic, D. eds., (2017). Best practice guide on the control of arsenic in drinking water. IWA Publishing; London, UK.

Bothwell, T. H., Charlton, R. W., Cook, J. D., Finch, C. A. (1979). Iron metabolism in man. Oxford: Blackwell.Blackwell Scientific Publications. Univ. Witwatersrand, Johannesburg, South Africa, pp.xi, 576.

Caboi, R. & Cidu, Rosa & Fanfani, L. & Lattanzi, Pierfranco & Zuddas, P. (1999). Environmental mineralogy and geochemistry of the abandoned Pb-Zn Montevecchio-Ingurtosu mining district, Sardinia, Italy. Chron Rech Miniere. 534. 21-28.

CGWB (2013) Central Ground Water Board, Ministry of Water Resources, Government of India, Nagaon District Ground Water Brochure, http://cgwb.gov.in/District_Profile/Assam/Nagaon.pdf.

Chadha, D.K. (1999) A proposed new diagram for geochemical classification of natural water and interpretation of chemical data. Hydrogeol J 7:431–439.

Cothern, C.R., Lappenbusch, W.L. (1983) Occurrence of uranium in drinking water in the US. Health Physics, 45:89–99.

Coyte, R.M., Jain, R.C., Srivastava, S.K., Sharma, K.C., Khalil, A., Ma, L. and Vengosh, A., 2018. Large-scale uranium contamination of groundwater resources in India. Environmental Science & Technology Letters, 5(6), 341-347.
Cumberland, S.A., Douglas, G., Grice, K., Moreau, J.W. (2016) Uranium mobility in organic matter-rich sediments: a review of geological and geochemical processes. Earth Sci Rev 159:160-185.
Daughney, C.J. (2003), Iron and Manganese in New Zealand's ground water. Jour. Hydrology, v.42(1), 11-26.
District census handbook, Nagaon, Census of India 2011, http://censusindia.gov.in/2011census/dchb/1806_PART_B_DCHB_NAGAON.pdf
EPA fact sheet about uranium, https://semspub.epa.gov/work/HQ/175267.pdf
Ficklin, W.H., Plumlee, G.S., Smith K.S., McHugh, J.B.(1992) Geo-chemical classification of mine drainages and natural drainages in mineralized areas. In: Kharaka YK, Maest AS (eds) Water– rock interaction, vol 7. Balkema, Rotterdam, pp 381–384
Gibbs, R.J. (1970). Mechanism controlling world's water chemistry. Science, 170, 1088–1090.
Guo, H., Jia, Y., Wanty, R.B., Jiang, Y., Zhao, W., Xiu, W., Shen, Z., Li, Y., Cao, Y., Wu, Y., Zhang, D., Wei, C., Zhang, Y., Cao, W., Foster, A. (2016) Contrasting distributions of groundwater arsenic and uranium in the western Hetao basin, Inner Mongolia: implication for origins and fate controls. Sci Total Environ 541:1172–1190
Guo, Z., Li, Y., & Wu, W. (2009). Sorption of U(VI) on goethite: Effects of pH, ionic strength,phosphate, carbonate and fulvic acid. Applied Radiation and Isotopes, 67(6), 996–1000.

Iqbal, M.A., & Gupta, S.G. (2009). Studies on heavy metal ion pollution of ground water sources as an effect of municipal solid waste dumping. African Journal of Basic & Applied Sciences, 1, 117–122

Kavcar, P., Sofuoglu, A., &Sofuoglu, S. (2009). A health risk assessment for exposure to trace metals via drinking wateringestion pathway. International Journal of Hygiene and Environmental Health, 212, 216-227.
Keith, A., McCall Chih-chin Huang Carol Fierke, A. (2000) Function and Mechanism of Zinc Metalloenzymes. Jour. Nutrition, v.130(5), pp.1437–1446.
Kopylova, Y., Guseva, N., Shestakova, A., Khvaschevskaya, A., & Arakchaa, K. (2015). Uranium and thorium behavior in groundwater of the natural spa area "Choygan mineral water" (East Tuva). IOP Conference Series: Earth and Environmental Science, 27, 012034.
Kozgar, M.I., Khan, S., Wani, M.R. (2012) Variability and correlation studies for total iron and manganese content of chickpea high yielding mutants. Amer. Jour. Food Tech., 7(7), 437-444.
Kubier, A., Wilkin, R. T., & Pichler, T. (2019). Cadmium in soils and groundwater: A review. Applied Geochemistry, 108. pp. 104388.

Sajil Kumar, P. J., & James, E. J. (2016). Identification of hydrogeochemical processes in the Coimbatore district, Tamil Nadu, India. Hydrological Sciences Journal, 61(4), 719–731.
Kurttio, P., Auvinen, A., Salonen, L., Saha, H., Pekkanen, J., Mäkeläinen, I., … Komulainen, H. (2002). Renal effects of uranium in drinking water. Environmental Health Perspectives, 110(4), 337–342.
Li, S., & Zhang, Q. (2010). Risk assessment and seasonal variation of dissolved trace elements and heavy metals in the upper Han River, China. Journal of Hazardous Materials, 181, 1051-1058.
Lide, D.R, ed. (1992–1993) Handbook of chemistry and physics. Boca Raton, FL, CRC Press. Mahanta, C., Enmark, G., Nordborg, E., Sracek, O., Nath, B., Nickson, R. T., et al. (2015). Hydrogeochemical controls on mobilization of arsenic in groundwater of a part of Brahmaputra river flood plain, India. Journal of Hydrology: Regional Studies, 4, 154–171.

Manta, D. S., Angelone, M., Bellanca, A., Neri, R., & Sprovieri, M. (2002). Heavy metals in urban soils: a case study from the city of Palermo (Sicily), Italy. Science of The Total Environment, 300(1-3), 229–243.

Maruyama, S., Ikoma, M., Genda, H., Hirose, K., Yokoyama, T., & Santosh, M. (2013). The naked planet Earth: Most essential pre-requisite for the origin and evolution of life. Geoscience Frontiers, 4, 141–165.

Naseem, S., Hamza, S., Nawaz-ul-Huda, S., Bashir, E., & ul-Haq, Q. (2013). Geochemistry of
Cd in groundwater of Winder, Balochistan and suspected health problems. Environmental Earth Sciences, 71(4), 1683–1690.

Nies, D. H. (1999). Microbial heavy-metal resistance. Applied Microbiology and Biotechnology, 51(6), 730–750.

Nies, D. H. (2003). Efflux-mediated heavy metal resistance in prokaryotes. FEMS Microbiology Reviews, 27(2-3), 313–339.

Paul, D. (2017). Research on heavy metal pollution of river Ganga: A review. Annals of Agrarian Science, 15(2), 278–286.

Prakash, R., Bhartariya, K. G., Singh, S., Singh, K., Rajak, M., & Kaushik, Y. B. (2020). Uranium and Its Correlation with other Geogenic Contaminants in Ground Water of Ganga Yamuna Doab, Fatehpur District, Uttar Pradesh, India. Journal of the Geological Society of India, 95(4), 359–365.

Pranab, S., Prasanta, S., &Abam, K. M. (2010). Statistical analysis of heavy metals from samples of Tezpur sub-division in Sonitpur district, Assam, India. International Journal of Applied Biology and Pharmaceutical Technology, 3, 946-951.

Raju, N.J., Shukla, U.K., Ram, P. (2011). Hydrogeochemistry for the assessment of groundwater quality in Varanasi: a fast-urbanizing center in Uttar Pradesh, India. Environmental Monitoring and Assessment, 173, 279-300.

Rattan, R., Datta, S., Chhonkar, P., Suribabu, K., & Singh, A. (2005). Long-term impact of irrigation with sewage ef?uentson heavy metal content in soils, crops and groundwater-A case study. Agriculture, Ecosystems &Environment, 109(3), 310-322.

Ravenscroft, P., Brammer, H., Richards, K. (2009). Arsenic pollution: a global synthesis, vol 28. Wiley, New York.

Richards, L. A., Kumar, A., Shankar, P., Gaurav, A., Ghosh, A., & Polya, D. A. (2020). Distribution and Geochemical Controls of Arsenic and Uranium in Groundwater-Derived Drinking Water in Bihar, India. International Journal of Environmental Research and Public Health, 17(7), 2500.

Sharma Praveen, Chambial Shailja and Shukla Kamla Kant (2015) Lead and Neurotoxicity. Indian Jour. Clin. Biochem., 30(1), 1–2.

Singh, S., Rani, A., Mahajan, R. K., &Walia, T. P. S. (2003). Analysis of uranium and its correlation with some physicochemicalproperties of drinking water samples from Amritsar, Punjab. Journal of Environmental Monitoring, 5,917-921.

Smith, K. S. (2007): Strategies to Predict Metal Mobility in SurficialMining Environments, In:
DeGraff, J. V. (Ed). Understanding andResponding to Hazardous Substances at Mine Sites in the Western United States. Geological Society of America Reviews in Engineering Geology,XVII. 25–45.

Tareen, A. K., Sultan, I. N., Parakulsuksalid, S. M., Khan, A., Khan, M. W., & Hussain, S. (2014). Detection of heavy metals from drinking waters of district Peshin, Balochistan, Pakistan. International Journal of Current Microbiology and Applied Sciences, 3, 299-308.

Trivedi, R. K., Goel, P. K. (1984). Chemical biological methods for water pollution studies. Karad: Environmental publications.

Wanda, E., Monjerezi, M., Mwatseteza, J. F., & Kazembe, L. N. (2011). Hydro-geochemical appraisal of groundwater quality from weathered basement aquifers in Northern Malawi. Physics and Chemistry of the Earth, Parts A/B/C, 36(14-15), 1197–1207.

WHO. (1996). Guidelines for drinking-water quality (2nd ed., Vol. 2). Health criteria and other supporting information, Geneva.
Wongsasuluk, P., Chotpantarat, S., Siriwong, W., & Robson, M. (2014). Heavy metal contamination and human risk assessment in drinking water from shallow groundwater wells in an agricultural area in UbonRatchalhani province, Thailand. Environmental Geochemistry and Health, 36, 169-182.
World Health Organization (2004) Guidelines for drinking-water quality 4th ed p 430.
Uranium in Drinking Water. Retrieved from
http://www.who.int/water_sanitation_health/dwq/chemicals/en/uranium.pdf.
Wu, Y., Wang, Y., & Xie, X. (2014). Occurrence, behavior and distribution of high levels of uranium in shallow groundwater at Datong basin, northern China. Science of The Total Environment, 472, 809–817.
Yadav, S. K., Ramanathan, A. L., Kumar, M., Chidambaram, S., Gautam, Y. P., & Tiwari, C. (2020). Assessment of arsenic and uranium co-occurrences in groundwater of central Gangetic Plain, Uttar Pradesh, India. Environmental Earth Sciences, 79(6).
Kurttio, P., Harmoinen, A., Saha, H., Salonen, L., Karpas, Z., Komulainen, H., & Auvinen, A. (2006). Kidney Toxicity of Ingested Uranium From Drinking Water. American Journal of Kidney Diseases, 47(6), 972–982.
Zhao, J., Fasfous, I., Murimboh, J., Yapici, T., Chakraborty, P., Boca, S., Chakrabarti, C. (2009). Kinetic study of uranium speciation in model solutions and in natural waters using Competitive Ligand Exchange Method. Talanta, 77(3), 1015–1020.

Bhujal News, 30(1-4):63-73

An Integrated Approach to Delineate Groundwater Potential Zones in Parts of Chambal Basin of Sawai Madhopur District, Rajasthan, India

Sayelli Tembhurne*[1], Priya Kanwar[1], S. K. Pareek[1] & K. P. Singh [1]
Central Ground Water Board, Western Region, 6A Jhalana Doongri, Jaipur
*Corresponding author- e-mail- irocksayellitembhurne@gmail.com

ABSTRACT

An integrated approach was applied to delineate groundwater potential zones in parts of Chambal Basin, Sawai Madhopur District, by adopting hydrogeological, geophysical and geospatial techniques. Selection of high yielding groundwater potential sites especially in hard rock terrain is a challenging task, at places, these formations are permeable but lack primary porosity and movement of groundwater in these rocks is controlled by secondary porosity developed due to physical or structural phenomenon. These parameters can be demarcated by topography, drainage, geology, lineaments, thickness of weathered zones etc.. A comprehensive evaluation of all such parameters by preparing various thematic layers using GIS techniques has helped in delineating high yielding groundwater potential zones in the study area. During exploratory drilling, single aquifer system was encountered in the study area, indicating unconfined to semi-confined condition which is substantiated by aquifer test analysis. This study has successfully demarcated the groundwater potential areas, with high discharging wells, falling in the central part of the district extending throughout its north-south length viz. from Bamanwas to Khandar Blocks, yielding in the range of 200 to 700 litres per minute. These potential areas are found in coherence with the structural features as well as drainage pattern in the area.

Keywords: Groundwater, groundwater potential zones, thematic layers, high discharge wells.

INTRODUCTION

Groundwater is a dynamic and important replenishable natural, fresh water resource. In hard-rock terrain the availability of groundwater is limited and is essentially confined to the fractured and weathered zones. The hard rock terrain of the Sawai Madhopur District has poor groundwater zones and faces acute water scarcity both for irrigation and drinking purposes, as most of groundwater contribute to perennial Chambal River. Surface water resources in the area are inadequate to meet the local domestic & irrigation demand, therefore, adequate understanding of geology, hydrogeology and geomorphology is required for proper exploration and exploitation of groundwater resources. Hence, delineation of potential zones for groundwater by integrating the data generated from the field with the GIS data/layer is extremely significant for effective and sustainable management of groundwater systems in this region.

Teeuw (1995) relied only on lineaments for groundwater exploration in Ghana, while others merged different factors apart from lineaments like drainage, geomorphology, geology, slope, land use, rainfall intensity and soil texture (Sander et al. 1996; Sener et al. 2005; Ganapuram et al. 2009). The derived results are found to be satisfactory based on field surveys but it varies from one region to another because of varied geo-environmental conditions. Integrated analysis and study, besides mapping and delineation of potential areas on small and regional scale help in determination of aquifer characteristics, flow pattern and correlation of lithology (Sabale et al.2009).The various earth features such as geology, geomorphology, soil types, land use and land cover, drainage, lineament, exert prime influence on aquifers characteristics and thereby influence the groundwater resources in any region. GIS provides an excellent framework for efficiently handling large and complex spatial data for natural resources management; thus, it has proved to be a useful tool for groundwater studies (Krishnamurthy et al. 1996; Meijerink 1996; Nour 1996; Sander et al. 1996). In past, several researchers have used GIS techniques for the delineation of groundwater potential zones (Chi & Lee 1994; Kamaraju et al. 1995) with successful results. The type and number of thematic layers used for assessing groundwater potential by GIS vary considerably from one study to another.

Integration of hydrogeological and geophysical field studies with GIS for preparing various thematic layers, such as geomorphology, slope, lithology, drainage density, lineament density, soil and land use and land cover in a spatial domain will support the identification of potential groundwater zones. Borehole geophysical loggings are 'continuous depth-profile record of physical properties of the rock matrix and contained fluid, penetrated by the borehole', to exactly delineate the nature of sub-surface lithological formations and is used to demarcate the fractured / weathered zone/s thickness. The present study focuses on the identification of groundwater potential zones in the Sawai Madhopur district, Rajasthan, India, using GIS, geophysical and integrated geological studies for management, planning and sustainable development of groundwater resources. The main objective of this study is to identify groundwater potential zones and to identify high yielding wells in Sawai Madhopur district, India.

Study area

Sawai Madhopur District is located in the eastern part of Rajasthan State and covers an area of 5020.65 Sq. kms. It was named after its founder Sawai Madho Singh-I of Jaipur. It lies between north latitudes 25°44'59" and 26°41'00" and east longitudes 75°59'00" and 77°00'50" and falls in Survey of India's degree sheet no. 54B, 54C and 54N (scale 1:250,000). It is bounded in the north by Dausa and in northeast by Karauli Districts. It is bounded in the east with the State of Madhya Pradesh, south by Kota District while Tonk District constitutes its western boundary. It has six development blocks viz. Sawai Madhopur, Bonli, Khandar, Gangapur, Chauth Ka Barwara and Bamanwas **(Figure.1).**

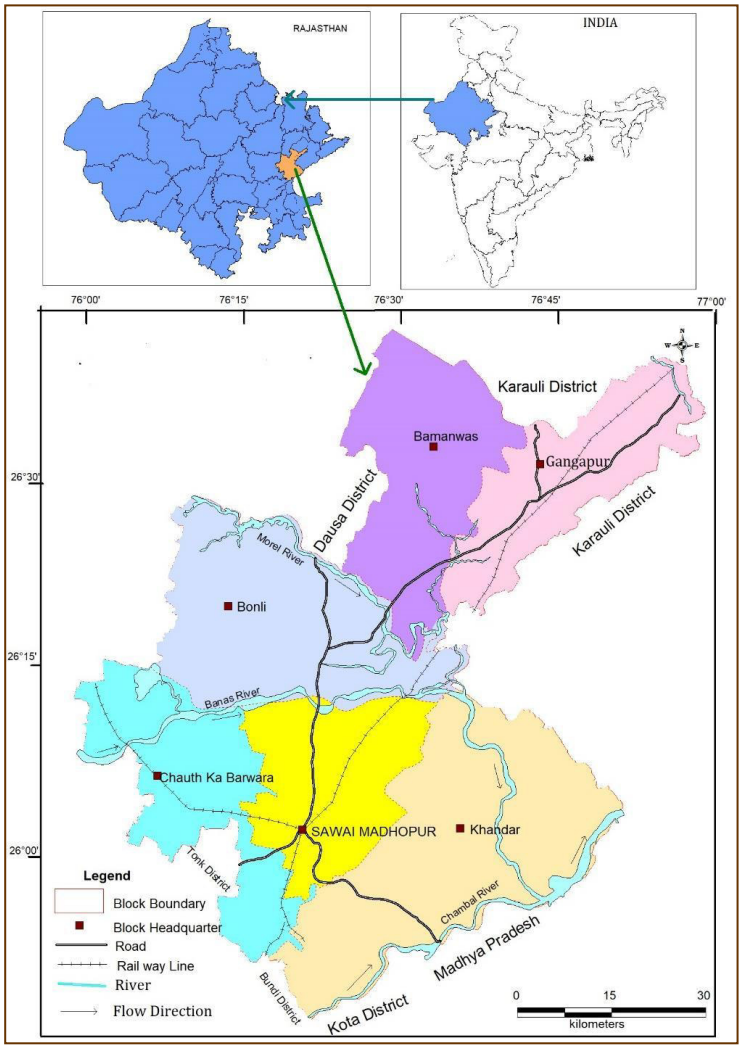

Figure 1. Location Map of Study Area

Agriculture in the area depends mainly on the rainfall from south-west monsoon occurring during June to September months. The average annual rainfall of the district is 701mm. The climate of the district is semi-arid to sub-humid type and is subject to extremes cold and hot at different places. The soil in the study area is basically loamy soil of different textures except in the flood plains of the major rivers.

Chambal is the principal perennial river forming the southern boundary of the study area flows in south-west to north-east direction. It is joined by ephemeral Banas and Morel Rivers and during rainy season many small nallas contribute these rivers. Drainage in the study area forms sub-parallel to dendritic pattern in hilly and plain areas respectively. The geomorphological setting of the study area varies widely from the hills on the south and south-east and low-lying land on northern and north-western parts. It is having ravines on the river banks especially near Chambal River, its flood plains and long narrow linear ridges with structural denudational hills, making it highly perplexing and heterogeneous. The hills are exposed in western parts of Bamanwas, Chauth Ka Barwara Blocks with major hill range of Ranthambore in the Sawai Madhopur and Khandar Blocks. All these hill ranges trend in NE-SW direction following the direction of Great Boundary Fault (GBF) that lies on north-western edge of Ranthambore Hills. The elevation of the area ranges from 180 to 527 m amsl and the general topographic slope is towards south.

Groundwater occurs in unconfined to semi-confined conditions in the study area. The water level scenario deciphered through the measurements of 172 wells during pre-monsoon season of 2020 exhibit that about 30% area has water levels between 2m and 10m below ground level and 70% area has water levels below 10m bgl.

Materials and Methods

Two techniques were used to evaluate the groundwater potential zones. The first technique is geospatial analysis, which is more qualitative and defines the area according to different themes in a two-dimensional overlay viz. topography, geomorphology, drainage etc. The second technique is analysis of data generated in field viz. groundwater exploration, pumping test, geo-electrical borehole logging etc.

The thematic layers of geology, geomorphology, soil was prepared and integrated. To demarcate groundwater potential of the study area the overall drainage pattern was studied along with other structural features like faults and lineaments. Thematic map of specific yield variation with lineaments and drainage were prepared using GIS software in conjunction with available maps. The topographic map was generated from Advanced Space Borne Thermal Emission and Reflection Radiometer Digital Elevation Model (ASTER DEM). Lithological logs from CGWB's exploratory boreholes along with geophysical logging data from geoelectrical logs helped in deciphering the sub-surface lithology and exact thickness of groundwater potential zones in the study area. Thus, by integrating all the information with GIS based maps, finally generated a clear picture of groundwater potential zones in the study area.

RESULTS AND DISCUSSIONS

The occurrence and movement of groundwater in an area is governed by several layers, such as topography, geology, geomorphology, lineaments, land use, land cover, slope, soil, rainfall, drainage density, groundwater depth and interrelationship between these layers (Jaiswal et al.2003). The groundwater Potential area is marked considering all the themes and features in an integrated layer.

GEOMORPHOLOGY

The hydro-geomorphology in the hard rock terrain is highly influenced by the lithology and structures of the underlying formations and is one of the most important features in evaluating the groundwater potential and prospect (Kumar et al. 2008).

Material associated with river/water bodies and active flood plains has higher water retention capability and therefore constitutes best landform for high groundwater potential (Shekhar & Pandey, 2014). The geomorphology of the study area is shown in Fig 2. Flood plain along Banas River across the district receives good recharge and has excellent groundwater prospect. The whole study area was grouped into three major geomorphic groups plains-pediments, hills and ridges. The alluvial plains are developed along the river channels and other drainage lines. They are characterized by highly porous and permeable material and have a good groundwater prospect. Flood plains, palaeo-channels and sandy plains of aeolian origin are the other landscape consists of gravels, sand, silt and clay in the area. Pediments of denudational origin with broad gently sloping debris extend down the foot-hills. Denudational and structural hills, long narrow ridges trending in NE-SW direction are prominent geomorphic structures of the study area.

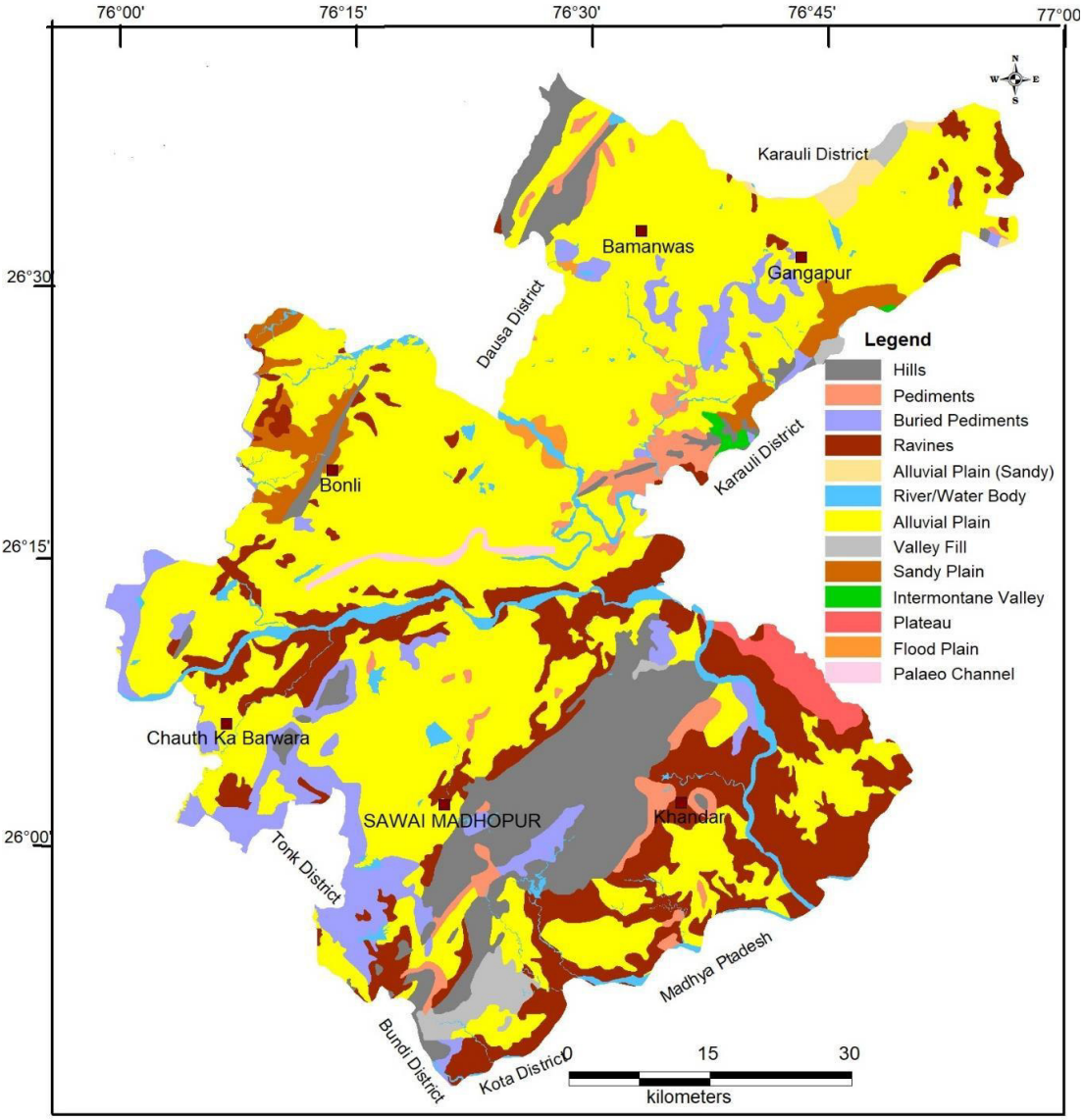

Figure 2: Geomorphology Map of Study Area

TOPOGRAPHY

The topography of any area has its own importance in affecting the run-off, recharge and movement of surface water. Approximately 80% of the study area is flat, that extends from north, north-east to central and some southern parts of the district. Long narrow ridges comprised of quartzite, trending in NE-SW are there in the north-west and west parts of the study area. The major hill forest of Ranthambore is located in the south-central part and lies in Sawai Madhopur and Khandar Blocks. The ground elevation ranges from 180m above mean sea level (amsl) in the south to about 527m amsl in the south-central part. Developments of ravines with bad-land topography along the Chambal River and its tributaries have a conspicuous physiographic region in the district especially covering the southern Khandar block. To assess the groundwater potential, hilly terrain having less than 15% slope was considered.

DRAINAGE DENSITY

The drainage system of the district is well developed due to Chambal, Banas and Morel rivers and their tributaries. The drainage density is the total length of stream channels per unit area. It is an inverse function of permeability and therefore it is an important parameter in evaluating the groundwater zone. The drainage map of the study area is shown in Fig- 3 and is used for obtaining the drainage density map. High drainage density values are favourable for run-off, and hence indicate low groundwater recharge. Drainage in the rocky terrain is sub-parallel type while in plain area, it is dendritic type. The drainage density in the district increases gradually towards south. The drainage density around Bamanwas and Malarna Dungar ranges from 0.30 to 0.50 km/sq.km. In the southern part of the district, it is more than 0.70 km/sq.km. This part is covered by Vindhyan rocks and high density indicates substantial runoff.

LINEAMENTS

Lineaments are natural, linear features like hills, faults, joints and fractures which can be interpreted on the satellite images and aerial maps. Lineaments represent the zones of faulting and fracturing in the bed-rocks resulting in increased secondary porosity and permeability. These factors are hydro-geologically very important as they provide the path ways for groundwater movement and enhanced well yields can be expected (Magesh et al. 2011; Subba Rao et al. 2001). In the study area three major NE-SW trending faults can be located and the hills and ridges follow the same trend (Fig- 3). Most of these lineaments correspond to the hills, ridges and river channels that contribute a significant part of the groundwater recharge and its movement in the study area.

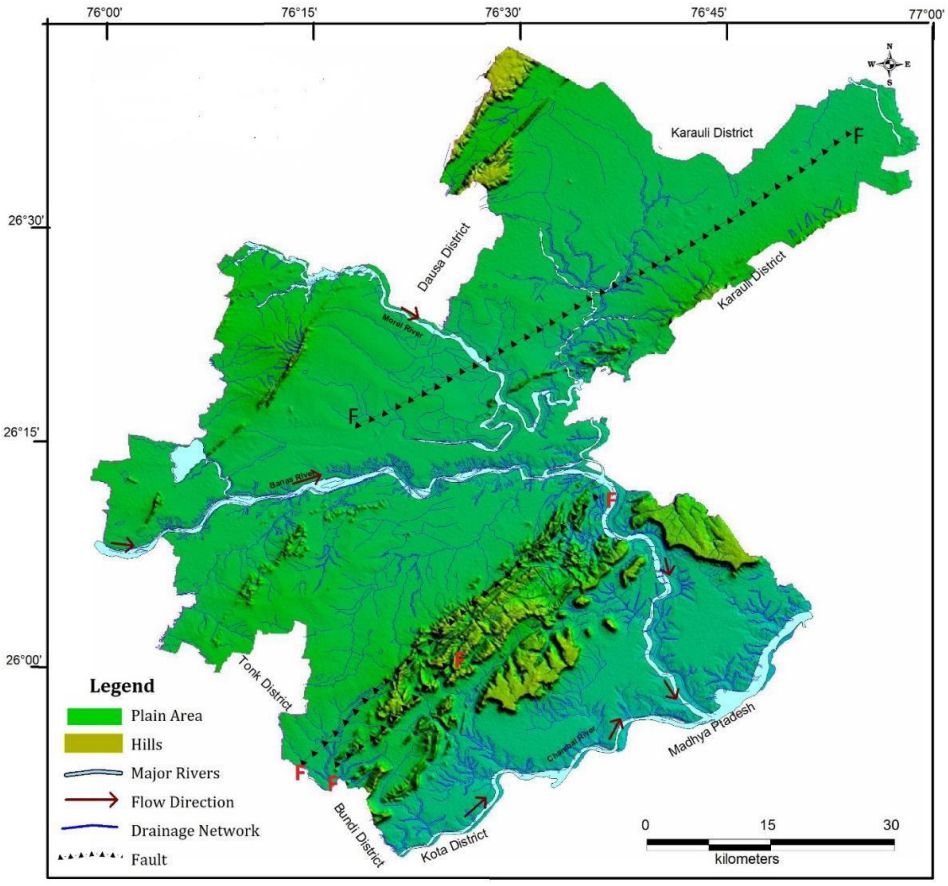

Figure 3. Topography, Drainage and Lineament Map of Study Area

GEOLOGY

Geologically, the area is occupied by rock formations of Bhilwara, Delhi and Vindhyan Supergroup of Archean and Proterozoic age respectively besides Alluvium of Recent age. The rocks of Bhilwara Supergroup comprising mica schists and gneisses are the oldest rocks of Archean age, which are exposed in the district, covering western and central portion of study area. Exposures of these rocks are very few as these are covered by alluvium of varying thickness. Quartzite of Ranthambore belong to this Supergroup, is intruded by dolerite sills and amphibolites at different levels. The Delhi Supergroup rocks overlie the Bhilwara rock formations and are exposed in the northern part of the study area. The Quartzite of Alwar group forms the crest line of hills in this part. The rock formations of Vindhyan Supergroup comprised of limestone and shales are observed in the southern part of study area (Figure 4). In these consolidated sedimentary and meta-sedimentary formations, groundwater occurs in weathered and fractured portions. Alluvium of Recent age comprising of sand, silt, clay and gravel has been considered as good potential area as compared to other rock formations, which covers almost 57% area of the district.

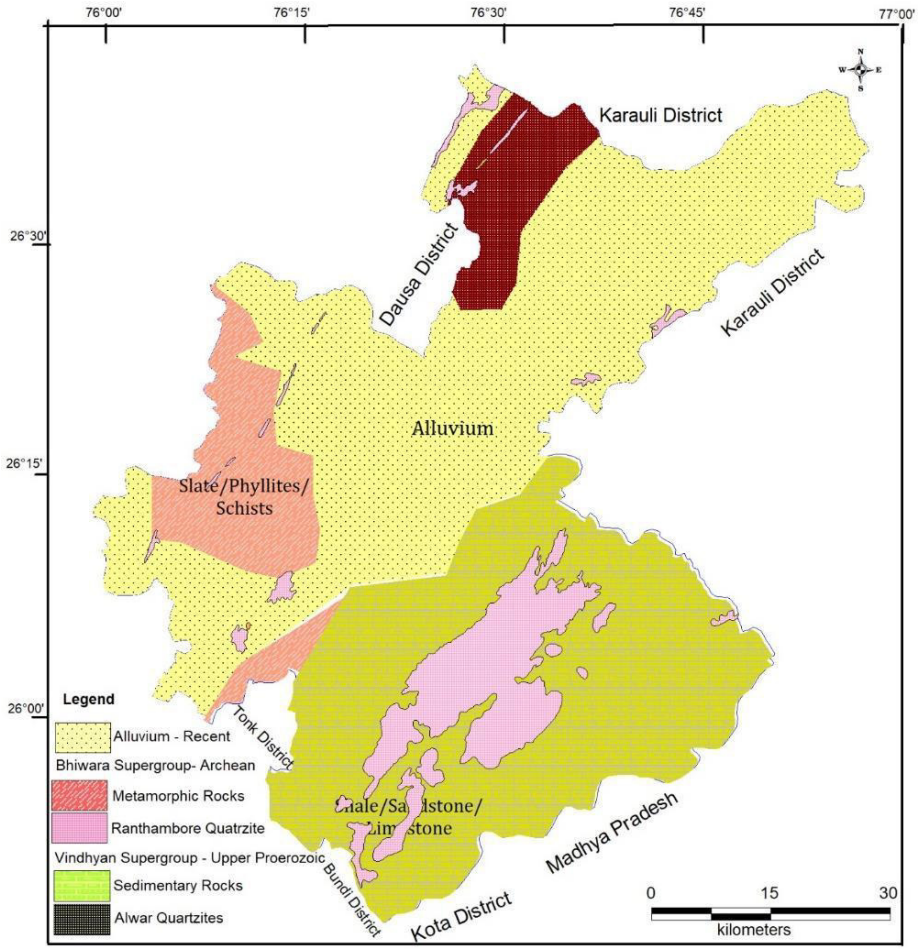

Figure 4. Geological Map of Study Area

HYDROGEOLOGY

Hydrogeology is concerned primarily with mode of occurrence, distribution, movement and chemistry of water occurring in the sub-surface in relation to the geological environment. The principal aquifers in the area are alluvium, sedimentary formations viz. limestone and shales and metamorphic formations viz. phyllites, schists and gneisses. Occurrence and movement of groundwater in alluvial aquifer is directly proportional to the granular zones i.e., the groundwater accumulation will be higher in coarser formation and the formation clear of clayey admixture or intercalation. Whereas, in consolidated formations, the occurrence and movement of groundwater primarily depends on the degree of interconnection of secondary pores/voids developed by fracturing and weathering. The hydrogeological map of area is prepared and presented in Figure. 5.

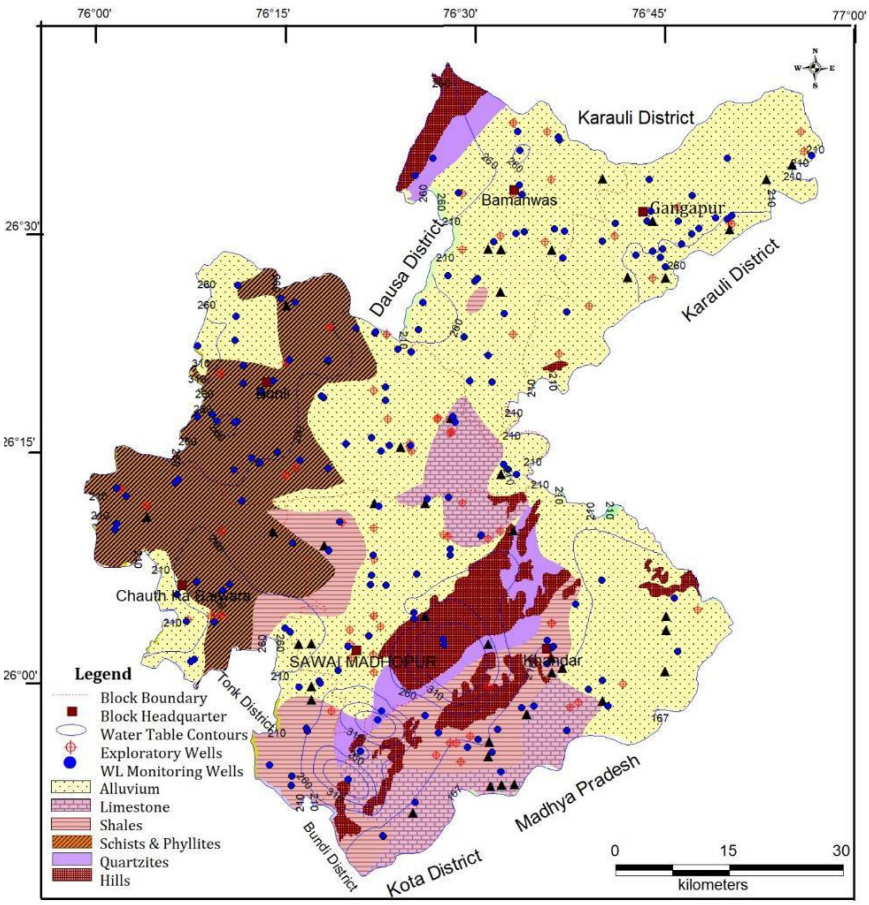

Figure 5. Hydrogeological Map of Study Area

Central Ground Water Board has drilled exploratory wells in the district in various geological terrains to explore the formations lying underneath and to know the aquifer parameters which also gives insight of its weathered thickness. The quantification of discharge/specific yield of aquifers by pumping test analysis is useful for delineating the groundwater potential zones. The block wise details of exploration carried out in the district are Table 1 as below:

Table 1: The block wise details of exploration carried out in the Study area

Blocks	Total Wells Drilled	Depth Range (m bgl)		SWL Range (m bgl)		Discharge Range (litres per minute)	
		From	To	From	To	From	To
Bamanwas	8	41.1	200	3.47	14.68	42	660
Bonli	19	21.78	200	1	36.5	0.6	3000
Chauth ka Barwara	8	105	200.1	11.2	37.47	meagre	200
Gangapur	9	26	200	5.5	45.02	meagre	600
Sawai Madhopur	15	74.55	200	6.94	50	30	1250
Khandar	14	29.45	200	4.87	57.77	100	721
District	73	26	200.1	1	57.77	0.6	3000

WEATHERED ZONE THICKNESS

In Sawai Madhopur district the geo-electrical borehole logs from 16 exploratory wells of CGWB, were interpreted for weathered & fractured zones, groundwater potential zone/s, depth range of saline water zones, change in lithology etc. for designing the well assembly especially in alluvial areas. The information so compiled were integrated to prepare the composite litholog and used as data input for weathered zone thickness and depth to hard rock.

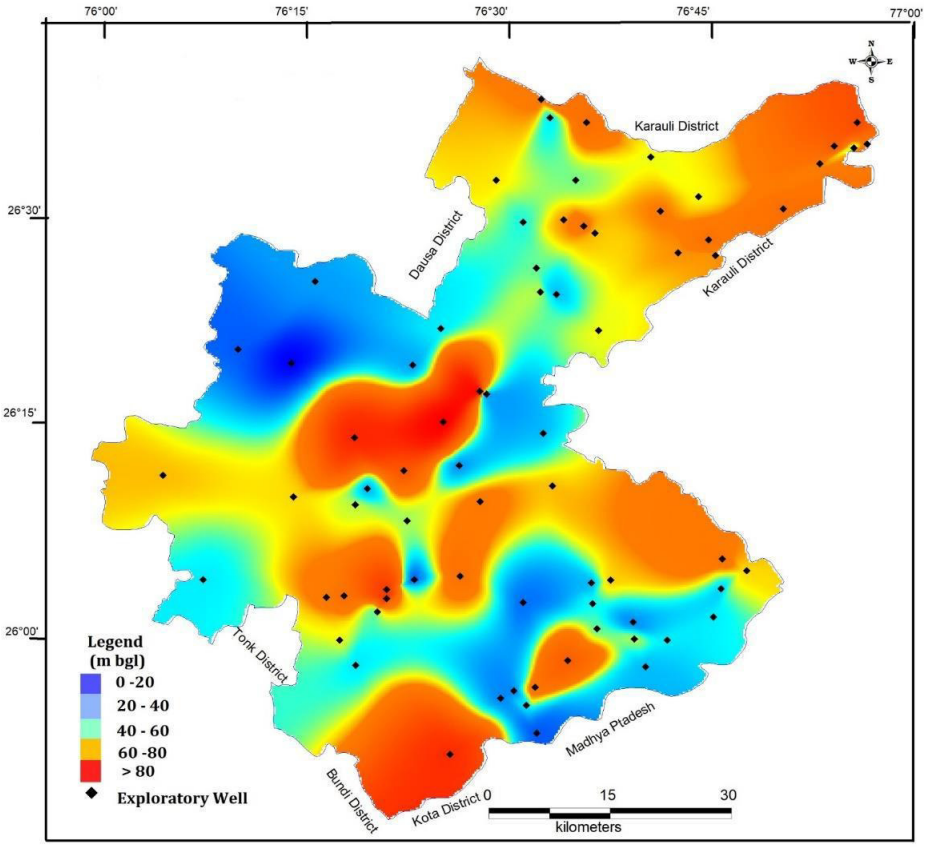

Figure 6. Weathered Zone Map of Study Area

Weathered zone comprises zones of active recharge and exhibit moderate to good groundwater potential in the rocky terrains. In the study area, the thickness of weathered zone is more in the central part viz. 65 to 100m, except for southernmost end of the district, as compared to the peripheral areas where it ranges from 20 to 32m. Thickness of the weathered/fractured zones helps in selecting favourable groundwater potential zones. The regions with greater thickness will yield more water than the thinner weathered zone regions, as groundwater potential is more at the base of weathered zone where the rocks have been broken down into sand size and larger fragments that are not subjected to the extensive weathering process (Amadi et al. 2011).

DELINEATION OF GW POTENTIAL ZONES

Validation of groundwater potential map was done with reference to the well yield data (Central Ground Water Board) (Figure 7). The well yield data from the Rajiv Gandhi National Drinking Water Mission Atlas 2005 was overlaid over the final groundwater prospect zones output map and it was found that excellent to very good groundwater potential zones delineated in present study using RS and GIS tools with integrated technique coincide with the high well yield zones i.e. 200 to 700 lpm (some exceptionally high yield are 3000 lpm at Saesha of Bonli Block), whereas areas delineated under poor to very poor groundwater potential exhibit low well yield (<50 lpm to 50 – 100 lpm). Thus, the findings of this integrated study establish the demarcation of groundwater potential zone which can be useful during groundwater exploration studies.

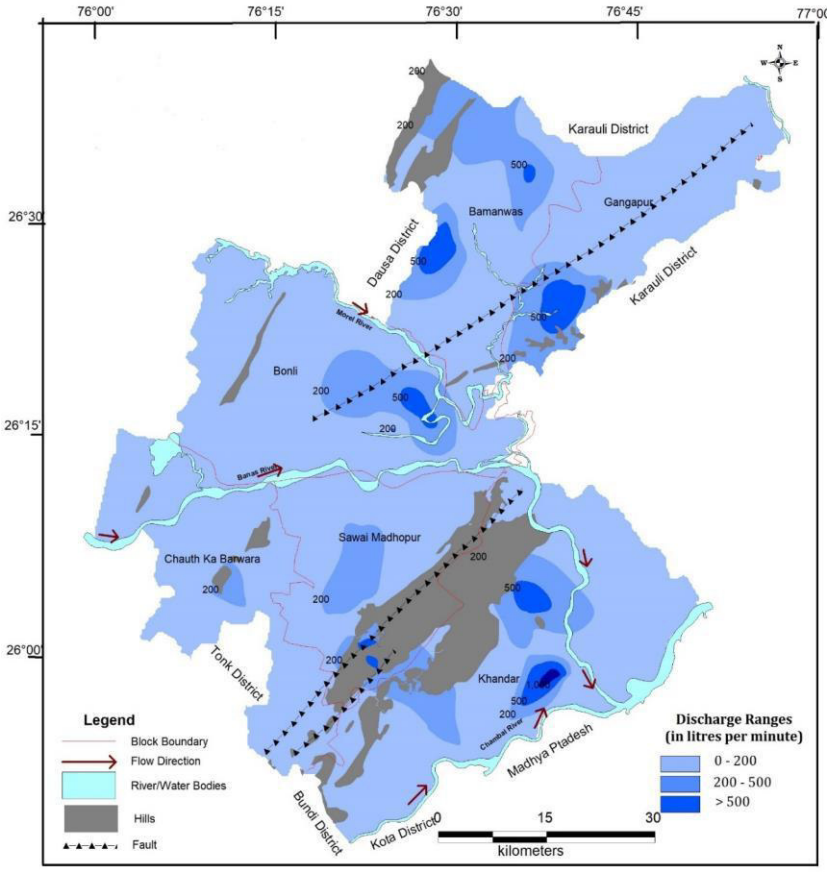

Figure 7: Groundwater Yield Potential Map

CONCLUSIONS

Toposheets and DEM of Sawai Madhopur District provided important terrain information to identify various lithological unit, lineaments and geomorphological units. Majority of these features served as indirect indicators of groundwater occurrence. The lineaments observed may be the result of faulting and fracturing and hence, it is inferred that they are the areas and zones of increased porosity and permeability in hard rock areas. Thus, they have more significance in the groundwater studies. The geological linear features are assumed to be the zone of fractured bed rocks where high groundwater prospect can be expected. Groundwater prospect in the weathered unit are very good in study area due to greater thickness of weathered residuum, dominance of porous sedimentary rocks in the basement and lower topographic gradient which permits retention of groundwater. Presence of hills in the study area which runs NE-SW, in southern part of district, make a vital water divide which creates good groundwater potential areas on both sides of the hilly region and are suitable for groundwater development. Buried channel also form a good prospect of groundwater potential zone in this area.

The integration and analysis of various thematic databases combined with hydrogeological studies viz. groundwater exploration data including borehole geophysical logging data proved useful in the delineation of groundwater potential zones which are substantiated with the high yielding wells encountered during exploration activities carried by Central Ground Water Board, Jaipur. Thus, well yield data validates the correctness of derived groundwater potential zones. The finding of this study can be used for proper management of watersheds and sustainable development for irrigation purposes. Using return flow factor and induced recharge we can use the groundwater before it discharges to Chambal River System. The result of this study will be invaluable for suitable borehole site selection with improved borehole yield.

ACKNOWLEDGEMENT

The authors are highly thankful to Dr S.K. Jain, Regional Director, Central Ground Water Board, WR, Jaipur for his valuable guidance, suggestion and encouragement. We also acknowledge with thanks the valuable suggestion from the anonymous reviewers.

REFERENCES

Amadi A.N, Nwawulu C.D, Unuevho. I, Okoye N.O, Okunlola I.A, Egharevba N.A, Ako T.A, Alkali Y.B. 2011. Evaluation of the groundwater potential in Pompo Village, Gidan Kwano, Minna using vertical electrical resistivity sounding. British J Appl Sci Technol. 1:53–66.

Central Ground Water Board, 2020, Aquifer Mapping and Management Plans of Sawai Madhopur District.
Central Ground Water Board, 2013, District Groundwater Information Booklet.
Chi K.H, Lee B.J. 1994. Extracting potential groundwater area using remotely sensed data and GIS techniques. In: Proceedings of the Regional Seminar on Integrated Application of Remote Sensing and GIS for Land and Water Resource Management; Bangkok; p 64–69.

Ganapuram. S, Kumar G.T.V, Krishna I.V.M, Kahya .E, Demirel M.C. 2009. Mapping of groundwater potential zones in the Musi basin using remote sensing data and GIS. Adv Eng Softw. 40:506–518.

Jaiswal .R, Mukherjee. S, Krishnamurthy. J, Saxena R. 2003. Role of remote sensing and GIS techniques for generation of groundwater prospect zones towards rural development – an approach. Int J Remote Sens. 24:993–1008.

Kamaraju M.V.V, Bhattacharya .A, Reddy G.S, Rao G.C, Murthy G.S, Rao T.C.M. 1995. Groundwater potential evaluation of West Godavari District, Andhra Pradesh State, India – a GIS approach. Groundwater. 34:318–325.

Krishnamurthy. J, Venkatesa Kumar. N, Jayaraman .V, Manivel. M. 1996. An approach to demarcate groundwater potential zones through remote sensing and a geographical information system. Int J Remote Sens. 17:1867–1884.

Magesh N.S, Chandrasekar .N, Soundranayagam .J.P (2011) Morphometric evaluation of Papanasam and Manimuthar watersheds, parts of Western Ghats, Tirunelveli district, Tamil Nadu India: a GIS approach. Environ Earth Sci 64:373–381

Meijerink A.M.J. 1996. Remote sensing applications to hydrology: groundwater. Hydrol Sci J. 41:549–561.

Nour S. 1996. Groundwater potential for irrigation in the East Oweinat area, Western Desert. Egypt Environ Geol. 27:143–154.

Sabale S.M, Ghodake V.R, Narayanpethkar A.B. 2009. Electrical resistivity distribution studies for artificial recharge of groundwater in the Dhubdhubi Basin, Solapur District, Maharashtra, India. J Indian Geophys Union. 13:201–207

Sander. P, Chesley M.M, Minor T.B. 1996. Groundwater assessment using remote sensing and GIS in a rural groundwater project in Ghana: lessons learned. Hydrogeol J. 4:40–49.

Shekhar Shashank & Pandey Arvind Chandra (2015) Delineation of groundwater potential zone in hard rock terrain of India using remote sensing, geographical information system (GIS) and analytic hierarchy process (AHP) techniques, Geocarto International, 30:4, 402-421, DOI: 10.1080/10106049.2014.894584

Subba Rao. N, Chakradhar G.K.J, Srinivas .V (2001). Identification of groundwater potential zones using remote sensing techniques in and around Guntur town, Andhra Pradesh, India. Photo nirvaehak J Indian Soc Remote Sens 29(1, 2):69–78

Sener. E, Davraz. A, Ozcelik .M. 2005. An integration of GIS and remote sensing in groundwater investigations: a case study in Burdur, Turkey. Hydrogeol J. 13:826–834.Teeuw R.M. 1995. Groundwater exploration using

Occurrence of Uranium in shallow groundwater of Uttar Pradesh, India: An overview

K.G.Bhartariya*, S. Rana, Madhavi Rajak and Supriya Singh
Central Ground Water Board, Northern Region, Lucknow
*Corresponding Author: kgbhartariya@yahoo.co.in

ABSTRACT

Uranium is a naturally occurring radioactive metal that occurs in low concentrations in nature in the form of minerals. It is present in ground water as a result of the dissolution of uranium bearing minerals that have been in contact with groundwater for long periods of time. Uranium is a mixture of three isotopes, 238U, 235U and 234U and all three behave the same chemically, but they have different radioactive properties. The predominant forms of uranium are 234U and 238U which occurs naturally in groundwater and surface water. For the present study a large data set was analyzed to predict the occurrence of Uranium in shallow groundwater of Uttar Pradesh. The data set consists of chemical groundwater analyses (Uranium concentrations) on ICP-MS from 824 predefined water quality stations of CGWB, Lucknow spread over entire state of Uttar Pradesh. Uranium concentrations showed a wide range from nil to189 µg/L with an average value of 8.98 µg/L and a standard deviation of 11.94 µg/L. In most groundwater samples (67.48%) ,Uranium concentrations was found in the range of 2 to 30 µg per liter. 4.37% samples exceeded uranium concentration 30µg/L, the maximum contaminant level (MCL) of the USEPA (Environmental Protection Agency) collected from 35 blocks of 22 districts of U.P. The maximum concentration of Uranium (189 µg/L) was found in Mohammadpur block of Bijnor district. It was observed that high uranium concentration locations are found along the river Ganga and Yamuna on the map.

Keywords: Uranium, Shallow aquifer, Uttar Pradesh, Statistical analyses

INTRODUCTION:

Groundwater is a natural resource that sustains the basic needs of all living beings. The chemical quality of water governs its suitability for various activities such as domestic, irrigation and industrial uses. (Wen and chen, 2006). Heavy metals normally present in nature are not harmful to our environment, as they are present in very small amounts. However, if the concentration of these metals is higher than the permissible limit, the roles of these metals change to a negative dimension. Central Ground Water Board, Northern Region, Lucknow first time decided to carry out a study on chemical quality of ground water for Uranium in ground water quality stations of U.P. Uranium is widespread in nature, occurring in granites and various other mineral deposits (Roessler et al., 1979; Lide, 1992–1993). The natural weathering of rocks dissolves the natural uranium, which goes into the groundwater. Once contaminated in the water uranium does not transfer into the air. Natural uranium consists almost entirely of the 238U isotope, with the 235U and 234U isotopes respectively comprising about 0.72% and 0.0054% (Greenwood & Earnshaw, 1984). The state of Uttar Pradesh covers an area of 2, 41,710 Sq Km, occupying Upper and Middle Ganga Plains and is confined between Himalayas in the north, plateau region of Bundelkhand in the South, the river Yamuna forming western limit. The state is surrounded by states of Uttrakhand & Nepal in the north, Madhya Pradesh and Rajasthan in the south, Bihar and Jharkhand in the east, and Haryana and Delhi in the west. Administratively, the State is divided into 18 divisions, 75 districts and 822 blocks. Total numbers of villages is 55,903 (as per census 2011) out of which 52,117 are inhabited. State is also divided into four economic regions i.e. Western Region, Eastern Region, Central Region and Bundelkhand Region. The western region comprises of 30 districts and the eastern region, 28 districts. 10 districts constitute the central region whereas the Bundelkhand region has only 7 districts. Total population of the state (census report, 2011) is 199.58 million, out of which the males are 104.60 million and females are 94.99 million. Ground water samples were collected from pre defined water quality stations by CGWB during pre monsoon period of May, 2019 with the objectives to study ground water quality for Uranium.

HYDROGEOLOGY:

The state consists of both porous and fractured formation. The larger part of the State is underlain by soft rocks of fluvial sediments laid down in the fore deep between Plateau region in south and Himalayas in north during the Quaternary period by the Indus-Ganga system of drainage over the Precambrian existing during geological past. The southern part of the State has entirely different geological conditions being underlain by hard rocks of Precambrian formations under a thin alluvial cover. The Unconsolidated formation covers nearly 85% of the State area. These unconsolidated sediments have been deposited through mighty rivers originating from great Himalayan Mountains. The sediments are an admixture of pebble, gravel, sand, silt, clay and kankar. Sediments are generally coarser in the north and gradually become finer southeastward along downstream of the drainage which is a typical feature of fluvial deposits. This unconsolidated zone is porous and permeable with primary inter-granular porosity and has good ground water potential. Sub-surface correlation of formations in the state has shown presence of several aquifers down to depth of 750 m below the ground. The plateau like terrain of Bundelkhand Massif and Kaimur Range form the Southern Peninsular region is characterized by bare rocky terrain, punctuated by hillocks. The crystalline rocks of Budelkhand Granite Complex (BGC) group occupy Jhansi, Jalaun, Hamirpur, Lalitpur, Mahoba and Banda districts. Groundwater occurs under water table conditions in the weathered residium, as well as within the secondary porosity (joints, fractures, weak plains). The weathered residium may be granular or sandy clay depending upon texture and composition of parent rock.

The upper part of first aquifer down to 50 mbgl is the main source of drinking water through hand pumps and dug wells and is unconfined in nature. The first aquifer as a whole, which is under unconfined to semi-confined conditions, is the most potential aquifer group and is the main source of groundwater in the State. It is extensively exploited through private as well as Government tube wells to meet the drinking water and irrigation needs. The shallow and phreatic aquifers are under heavy stress. The deeper aquifers are confined in nature and have been to a very limited extent.

METHODOLOGY :

A total number of 824 representative ground water samples were collected for Uranium analysis treated with Supra pure HNO_3 from pre defined net work water quality stations, (shallow phreatic aquifer, H/P-IM-II) of U.P during pre-monsoon May 2019. The samples were collected in polyethylene bottles of 125 ml capacity. They were immediately closed, labeled and stored properly for laboratory analysis. The hand pumps were continuously pumped for at least 10 minutes prior to the sampling, to ensure that ground water to be sampled is representative of ground water aquifer. Uranium concentration is determined by inductively coupled plasma mass spectrometry (Thermo iCAP Q) at Regional Chemical Laboratory CGWB, NR, Lucknow as per the standard method. The chemical lab of CGWB, NR, Lucknow is NABL accredited.

Uranium in water :

Uranium occurs naturally in the +2, +3, +4, +5 and +6 valence states, but it is most commonly found in the hexavalent form. In nature, hexavalent uranium is commonly associated with oxygen as the uranyl ion, $(UO_2)^{+2}$. Naturally occurring uranium is a mixture of three radio nuclides (234U, 235U and 238U), all of which decay by both alpha and gamma emissions (Cothern & Lappenbusch, 1983; Lide, 1992–1993). Uranium is used mainly as fuel in nuclear power stations, although some uranium compounds are also used as catalysts and staining pigments (Berlin & Rudell, 1986). The WHO has set a provisional safe drinking water standard of 30 micrograms of Uranium per liter for India, a level that is consistent with US Environmental Protection Agency standards. Uranium is not yet included in the list of contaminants monitored under the Bureau of Indian Standards' Drinking Water Specifications. Uranium can decay into other radioactive substances, such as radium, which can cause cancer with extensive exposure over a long period of time. Nephritis is the primary chemically induced effect of uranium in humans (Hursh & Spoor, 1973).

RESULTS AND DISCUSSIONS:

A total of 824 ground water samples were analyzed to predict the occurrence of Uranium in groundwater of U.P. On perusal of chemical analysis results it was found that Uranium concentrations during the study period showed a wide range from nil to189 µg/L with an average value of 8.98 µg/L and a standard deviation of 11.94 µg/L. The Indian Standards Specifications for drinking water (BIS 2012) does not specify any maximum permissible limit for uranium. Hence, the USEPA (2003) health standard of 30 ppb of uranium in drinking water is considered as the limit for this study. Out of the 824 samples collected and analysed during this study, 28.16 % ground water samples had Uranium concentration less than 2 µg/L. Its concentration was mainly found in the range of 2 to 30 µg / L in nearly 67% ground water samples (Fig.1). The concentration of Uranium in 4.37 % samples was found more than 30 µg /L in ground water samples collected from 35 blocks of 22 districts of U.P (Table-1). Thus concentration of uranium in most ground water samples (Fig.-2) was found below the drinking water health standard. The maximum concentration of Uranium (189 µg/L) was found in Mohammadpur block of Bijnor district. A map (Fig. 3) has been prepared showing locations of sampling known to contain high uranium concentration with river distribution. It was found that high uranium concentration locations were found along the river Ganga and Yamuna on the map. The uranium content in groundwater varies primarily due to leaching or dissolving the uranium from the weathered soil to the groundwater zone. It is important to continuously monitor the groundwater quality in this area to study the impact of uranium mineralization.

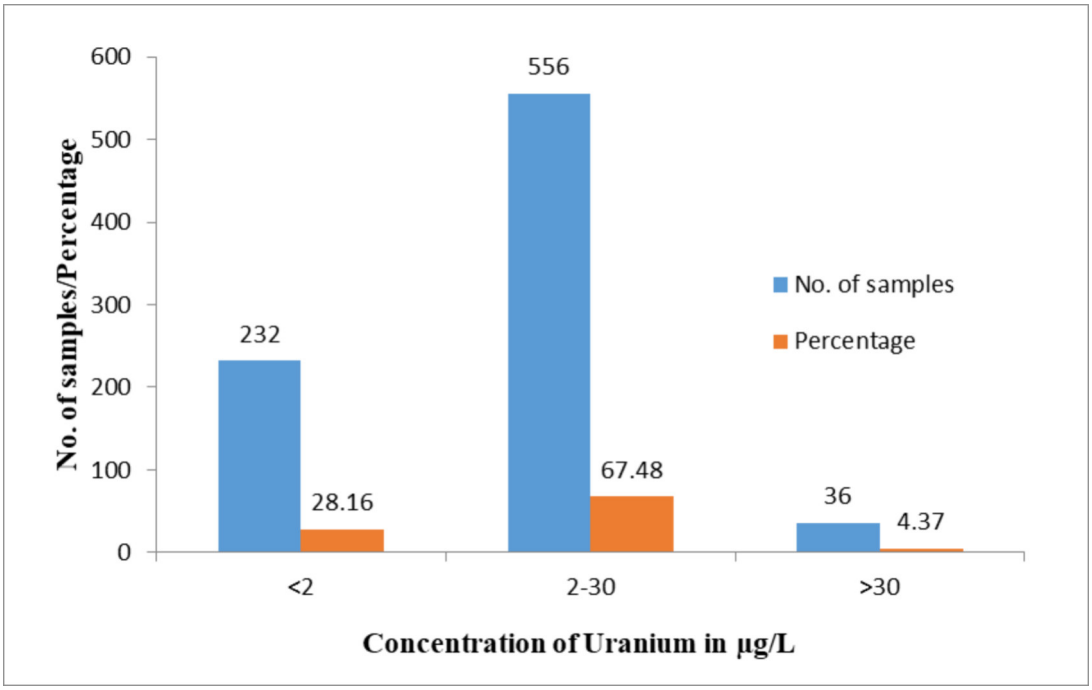

Fig. 1 Frequency distribution of Uranium in ground water of U.P

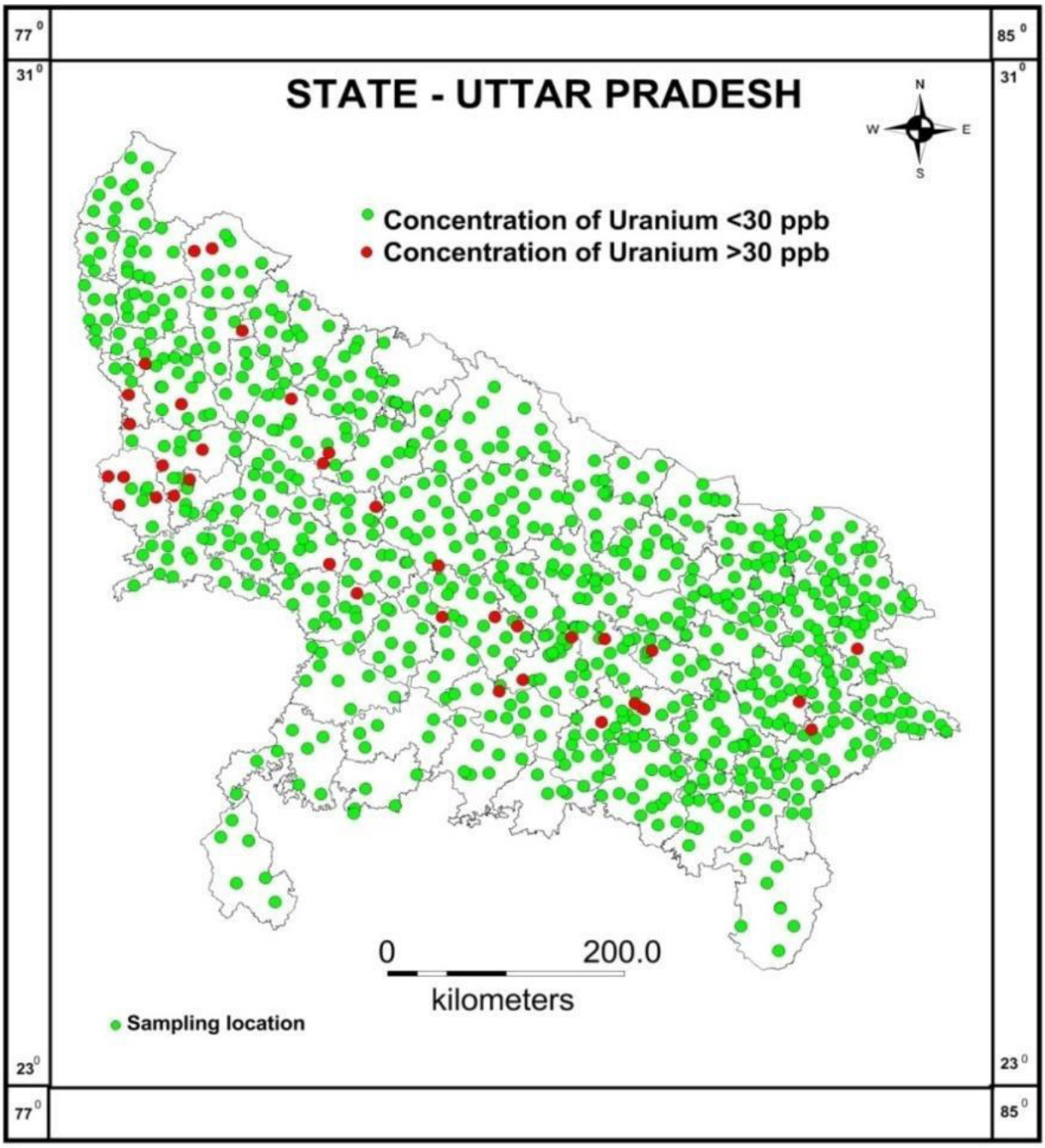

Fig.2 Distribution of Uranium in ground water of Uttar Pradesh

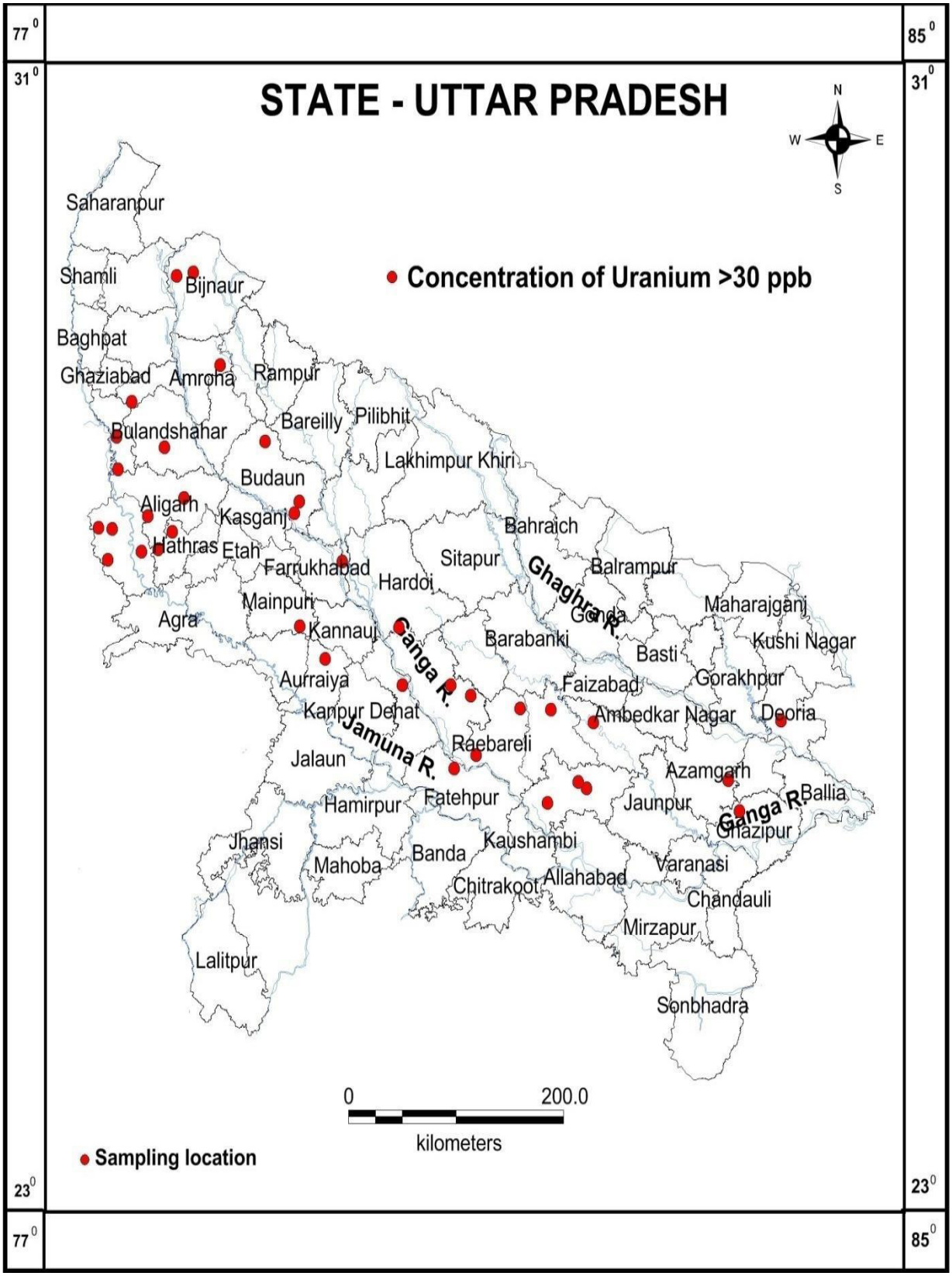

Fig.3 Locations of sampling found to contain high Uranium concentration with rivers

Table-1 Locations of high concentration of Uranium (U) in ground water of Uttar Pradesh

Sl. No.	District	Block	Latitude	Longitude	U in µg/L (>30)
1	Bijnor	Kiratpur	29.4966	78.2696	34
2	Bijnor	Mohammadpur	29.4744	78.1149	189
3	J P Nagar	Joya	28.8512	78.5235	59
4	Hardoi	Mallawan	27.0220	80.1950	33
5	Ghaziabad	Dholana	28.5961	77.6986	42
6	Fatehpur	Malwan	26.0390	80.7100	43
7	Sultanpur	Jagdishpur	26.4483	81.6124	31
8	Sultanpur	P.P Kannaicha	26.3597	82.0117	33
9	Mathura	Chhata	27.7113	77.5143	71
10	Mathura	Nandgaon	27.7158	77.3850	40
11	Mathura	Goverdhan	27.4922	77.4725	31
12	Mathura	Raya	27.5531	77.7886	45
13	Hathras	Mursan	27.5667	77.9408	31
14	Hathras	Sasni	27.6911	78.0744	53
15	Aligarh	Gonda	27.8005	77.8461	53
16	Aligarh	Dhanipur	27.9249	78.1838	41
17	Bulandshahar	Shikarpur	28.2789	78.0042	51
18	Gautam Buddha Nagar	Dankaur	28.3522	77.5556	35
19	Gautam Buddha Nagar	Jewar	28.1244	77.5667	39
20	Rae Bareili	Chhatoh	26.4586	81.3254	55
21	Rae Bareili	Lalganj	26.1305	80.9138	38
22	Unnao	Unchahar	26.5475	80.8654	45
23	Unnao	Nawabganj	26.6208	80.6753	35
24	Ghazipur	jakhaniya	25.7421	83.3724	37
25	Azamgarh	jahanaganj	25.9588	83.2674	32
26	Pratapgarh	Baba Bekhernath	25.8997	81.9442	32
27	Pratapgarh	Babaganj	25.7992	81.5822	32
28	Pratapgarh	Sangaipur	25.9458	81.8665	54
29	Kanpur Nagar	Chaubepur	26.6211	80.2236	32
30	Auraiya	Bidhuna	26.8022	79.5028	30.4
31	Deoria	Bhaluwani	26.3711	83.7608	51
32	Budaun	Bisouli	28.3210	78.9414	48
33	Budaun	Miaon	27.9020	79.2639	62
34	Budaun	Wajirganj	27.8200	79.2145	37
35	Farrukhabad	Rajepur	27.4801	79.6629	34
36	Mainpuri	Kishni	27.0316	79.2664	42

CONCLUSIONS:

Uranium concentration in shallow ground water samples of Uttar Pradesh for the whole of the studied area ranges from nil to 189 µg/L with an average value of 8.98 µg/L and a standard deviation of 11.94 µg/L. The values of uranium concentration in most of the water samples are found less than the recommended value of 30 µg/L. 67% samples have 2 to 30 µg/L uranium concentration so it may not result in any significant risk to health of the residents of the studied area. In only 4.37% of the analysed samples (35 blocks of 22 districts of U.P), the values are found higher than the recommended safe level of 30 µg/L (USEPA, 2003). The maximum concentration of Uranium (189 µg/L) was found in Mohammadpur block of Bijnor district. It was observed that high uranium concentration locations are found along the rivers Ganga and Yamuna on the map. For these samples more detailed investigation needs to be carried out to reach any conclusion.

ACKNOWLEDGEMENTS

The authors express their sincere thanks to Chairman and Member (Water quality), Central Ground Water Board, Faridabad for giving permission to write this paper and Sri P. K. Tripathi, HOO, Central Ground Water Board, Northern Region for providing all logistic supports. Thanks to all field going officers of CGWB, NR for collecting the ground water samples. Guidance and motivation received from Dr. S. K. Srivastava, Sr. Chemist (Scientist-D), CGWB, Faridabad in preparation of paper is highly acknowledged. I am thankful to Dr Shashi Kant Singh, Scientist-B, CGWB, Lucknow for preparing the maps. I am thankful to Sh Tejas.Y.Mankikar, Scientist-B, for providing technical input.

REFERENCES

American Public Health Association (1989) Standard methods for examination of water and waste water, 17th Edition., Washington, DC.

Berlin M, Rudell B (1986) Uranium. In: Friberg L, Nordberg GF, Vouk VB, eds. Handbook on the toxicology of metals, 2nd ed. Amsterdam, Elsevier Science Publishers, pp. 623–637.

BIS (2012), IS: 10500 Indian Standard Drinking Water–Specifications, (Second Revision), Bureau of Indian Standards, New Delhi, India. and amendment (2015).

Cothern CR, Lappenbusch WL (1983) Occurrence of uranium in drinking water in the US. Health Physics, 45:89–99.

Dyck W (1979). Application of hydro geochemistry to the search of uranium. Eco. Geolog. Report. 31: 489.

Greenwood NN, Earnshaw A (1984) Chemistry of the elements. Oxford, Pergamon Press.

Hem, J.D. (1991) Study and interpretation of chemical characteristics of natural waters. Book 2254, 3rd edition. Scientific Publishers, Jodhpur, India.

Hursh, J. B., & Spoor, N. L. (1973). Data on man. In H. C. Hodge, et al. (Eds.), *Handbook of experimental pharmacology* (Vol. 36, pp. 197–240)., Uranium, plutonium, transplutonic elements Berlin: Springer.

Kaushik Y.B, Khan Seeraj, Ranjan Vikas, Haq Saidul (2017), An overview of ground water resources of Uttar Pradesh: Issues and Strategies pp 1-32 Ground water management in U.P:
Issues and Strategies proceedings of Seminar organized by CGWB, NR December 2017.

Lide DR, ed. (1992–1993) Handbook of chemistry and physics. Boca Raton, FL, CRC Press.

Lloyd, J. W. and Heathcote, J. A. (1985), Natural Inorganic Hydrochemistry in relation to Groundwater, An Introduction. Oxford University Press, New York. 294p.

Roessler CE et al. (1979) Uranium and radium-226 in Florida phosphate materials. Health Physics, 37:267–269.

Singh J, Singh L, Singh S (1995). High U-contents observed in some drinking waters of Punjab, India J. Environ. Radioact., 26 (3): 217-222.

Singh S, Malhotra R, Kumar J, Singh B, Singh J (2001). Uranium analysis of geological samples, water and plants from Kulu Area, Himachal Pradesh, India. Rad. Meas., 34(1-6): 427-431

Singh B, Singh G, Sandhu A S and Singh S 1999 Uranium estimation in water samples Collected from some areas of Himachal Pradesh, India; Radiat. Meas.31683–685.

Singh J, Singh L and Singh G 1995 High U-contents observedin some drinking waters of Punjab, India; J. Environ.Radioact.26217–222.

Report on Chemical analysis of Uranium and Trace elements in Ground Water of Uttar Pradesh,CGWB, NR, Lucknow 2020

WHO, Guidelines for drinking water quality. World Health Organization, Geneva.

Wen, F., Chen, X. (2006). Evaluation of the impact of groundwater irrigation on streamflow in Nebraska. J Hydrol327:603-617

Save Water Save Life

Rajiv Gandhi National Ground Water Training and Research Institute
Sector - 23, Atal Nagar, Tuta, Naya Raipur - 492016 (C.G.)
Phone : 91-771-2220701
E-mail : bhujal@nic.in
Web : www.cgwb.gov.in